AD-A187 660 SPATIOTEMPORAL CHARACTERISTICS OF VISUAL LOCALIZATION PHASE 2(U) SRI INTERNATIONAL MENLO PARK CA SENSORY SCIENCES RESEARCH LAB C A BURBECK 30 SEP 87 1/2

UNCLASSIFIED AFOSR-TR-87-1637 F49620-85-K-0022 F/G 6/4 NL

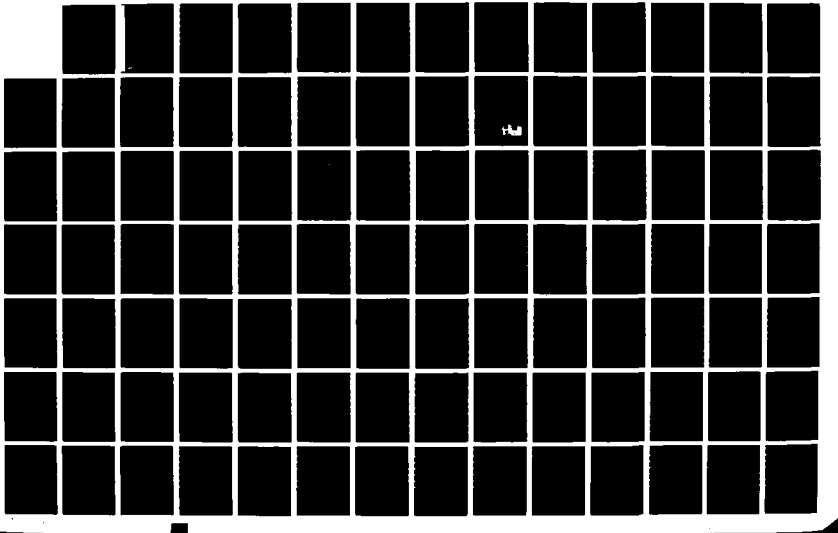

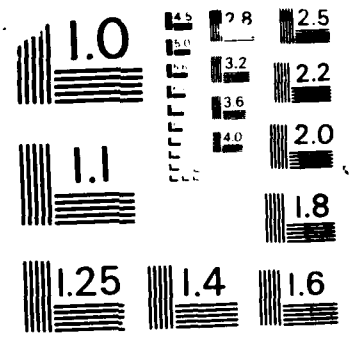

(2)

Report AFOSR-TR- 87-1637

SPATIOTEMPORAL CHARACTERISTICS OF VISUAL LOCALIZATION -- PHASE II

Christina A. Burbeck, Ph.D.
Visual Sciences Program
Sensory Sciences Research Laboratory
SRI International
333 Ravenswood Avenue
Menlo Park, CA 94025

30 September 1987

Annual Report for 1986-1987
Contract F49620-85-0022
-K-

Prepared for

USAF OFFICE OF SCIENTIFIC RESEARCH/NL
Bolling Air Force Base
Washington, D.C. 20332

Attention

Dr. John Tangney
Program Manager
Life Sciences Directorate

SRI International®

REPORT DOCUMENTATION PAGE

1a. REPORT SECURITY CLASSIFICATION: UNCLASSIFIED	1b. RESTRICTIVE MARKINGS: --
2a. SECURITY CLASSIFICATION AUTHORITY	3 DISTRIBUTION/AVAILABILITY OF REPORT: unlimited
2b. DECLASSIFICATION/DOWNGRADING SCHEDULE	
4. PERFORMING ORGANIZATION REPORT NUMBER(S)	5 MONITORING ORGANIZATION REPORT NUMBER(S): AFOSR-TR- 87-1637
6a. NAME OF PERFORMING ORGANIZATION: SRI International; 6b. OFFICE SYMBOL (if applicable)	7a NAME OF MONITORING ORGANIZATION: Air Force Office of Scientific Research
6c. ADDRESS (City, State, and ZIP Code): 333 Ravenswood Avenue, Menlo Park, CA 94025	7b ADDRESS (City, State, and ZIP Code): Building 410, Bolling AFB, DC 20332-6448
8a. NAME OF FUNDING/SPONSORING ORGANIZATION: AFOSR; 8b. OFFICE SYMBOL (if applicable): NL	9. PROCUREMENT INSTRUMENT IDENTIFICATION NUMBER: F49620-85-K-0022
8c. ADDRESS (City, State, and ZIP Code): Bolling AFB, Washington, DC 20332	10. SOURCE OF FUNDING NUMBERS: PROGRAM ELEMENT NO. 61102F; PROJECT NO. 2313; TASK NO. A5; WORK UNIT ACCESSION NO

11. TITLE (Include Security Classification)
Spatiotemporal Characteristics of Visual Localization--Phase II

12. PERSONAL AUTHOR(S)
Christina A. Burbeck, Ph.D.

13a. TYPE OF REPORT	13b. TIME COVERED	14. DATE OF REPORT (Year, Month, Day)	15. PAGE COUNT
Annual	FROM 10/86 TO 10/87	870930	126

16. SUPPLEMENTARY NOTATION

17. COSATI CODES		
FIELD	GROUP	SUB-GROUP
6	4	

18. SUBJECT TERMS (Continue on reverse if necessary and identify by block number)
human vision; visual psychophysics; visual spatial localization.

19. ABSTRACT (Continue on reverse if necessary and identify by block number)

The spatial and temporal characteristics of human visual localization are studied using psychophysical techniques. The primary tasks studied are frequency discrimination and distance judgments in the plane perpendicular to the observer's line of sight. It is found that these tasks cannot be performed directly on the basis of simple transformations of the retinal image, but depend on stimulus context and on judgment of stimulus depth. Experiments are designed to isolate the process underlying these distance and size judgments from more distal visual processes. One prominent finding is that the localization process is remarkably insensitive to those aspects of the stimulus that most affect contrast detection thresholds.

20 DISTRIBUTION/AVAILABILITY OF ABSTRACT: ☒ UNCLASSIFIED/UNLIMITED ☐ SAME AS RPT ☐ DTIC USERS	21 ABSTRACT SECURITY CLASSIFICATION: UNCLASSIFIED
22a NAME OF RESPONSIBLE INDIVIDUAL: Dr John F. Tangney	22b TELEPHONE (Include Area Code): (202) 767-5021; 22c OFFICE SYMBOL: NL

DD FORM 1473, 84 MAR — 83 APR edition may be used until exhausted. All other editions are obsolete.

CONTENTS

ILLUSTRATIONS

I. STATUS OF RESEARCH

A. Introduction

During the past year, large-scale localization has become recognized as a major research topic in vision. Researchers who previously had focused on localization of objects that are separated by only a few minutes of arc -- where the remarkable hyperacuity thresholds are obtained --have recognized that the general ability to localize more widely separated objects with equally high relative precision is just as remarkable and important. The research described here has been at the forefront of this development.

Our research has focused on two general themes:

- Stimulus context plays a larger role in localization (i.e, separation) judgments than it does in contrast detection.

- Localization thresholds can be determined at several sites of processing, and therefore a deliberate effort must be made to elicit the properties of the localization mechanism *per se*.

A description of the research that we have done and are doing on these two themes constitutes the body of this report. Where possible, reference is made to completed manuscripts, which are included as appendices.

B. Effects of Context on Localization Judgments

Unlike contrast detection, localization judgments appear to be intrinsically tied to the context in which they are made. Most strikingly, we have shown that depth judgments are intrinsic in spatial frequency discrimination judgments. Observers cannot ignore the depth to make judgments solely on the basis of the difference in the retinal spatial frequencies of gratings (Appendix A).

We have also found that the addition of flanking stimuli affects large-scale localization in a way that suggests a further context effect. If a pair of parallel bars is added to a pair of target bars as shown in Figure 1, and the positions of the parallels are randomly jittered from trial to trial, then localization accuracy for the targets decreases. Part of this effect is probably due to increased noise, but the effect is larger when the two parallels lie outside the target pair than when they lie between the targets. The outside parallels appear to create a framework for judging the separation between the targets. When that framework changes size randomly from trial to trial, the accuracy of the separation judgment is impaired [1]. The threshold elevations produced by the outside parallels and the inside parallels are shown in Figure 2.

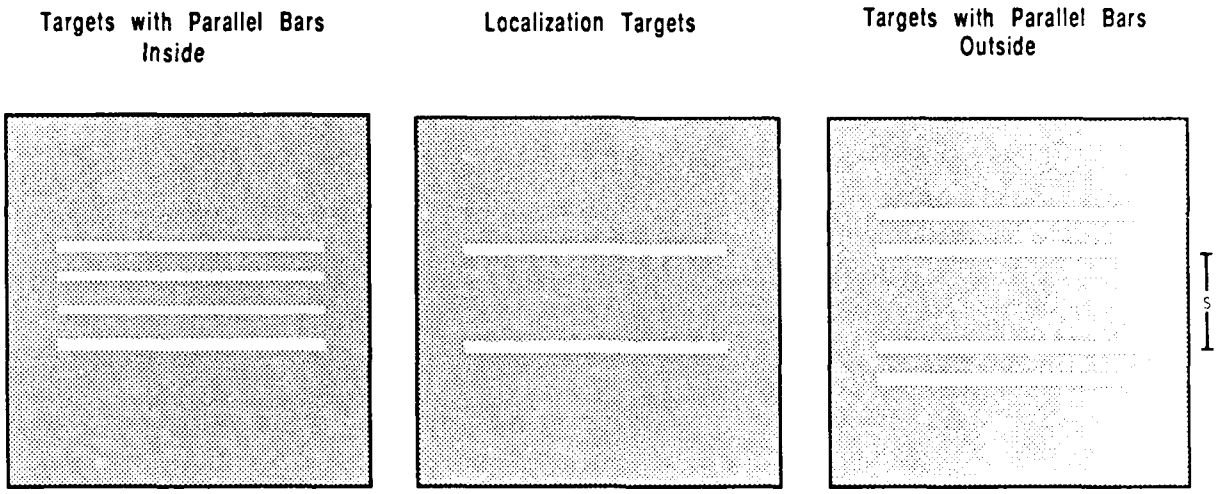

Average distance between targets:	3^{o}
Distance between parallel and nearest target:	$0.45 - 0.9^{o}$
Bar height:	0.3^{o}

Figure 1. *Stimuli used in experiments on the effects of parallels on localization accuracy.*

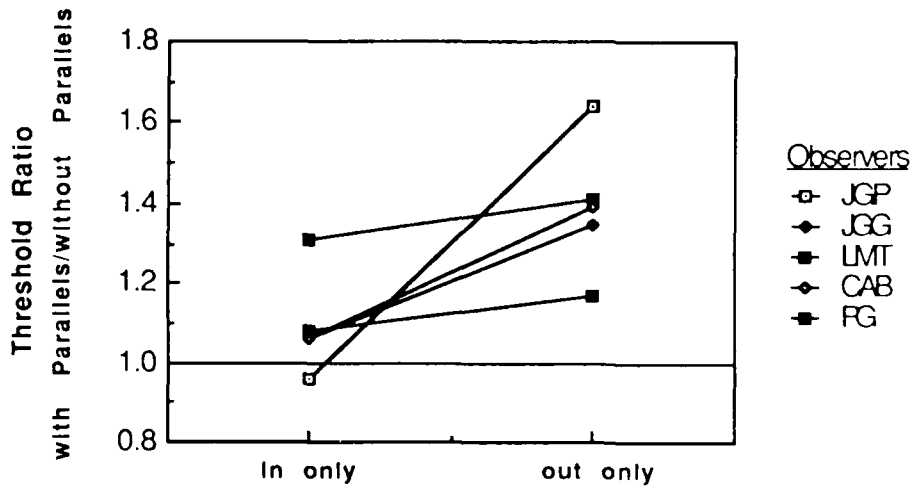

Figure 2. *Change in localization threshold produced by addition of parallels between targets* (in only) *or outside targets* (out only). *Five observers.*

We are currently examining the effect of target size on separation judgments. We have found

in control experiments that, over a large range, target size has no effect on localization accuracy, when the target pair is centered on the fovea. Data for two observers and four target sizes are shown in Figure 3.

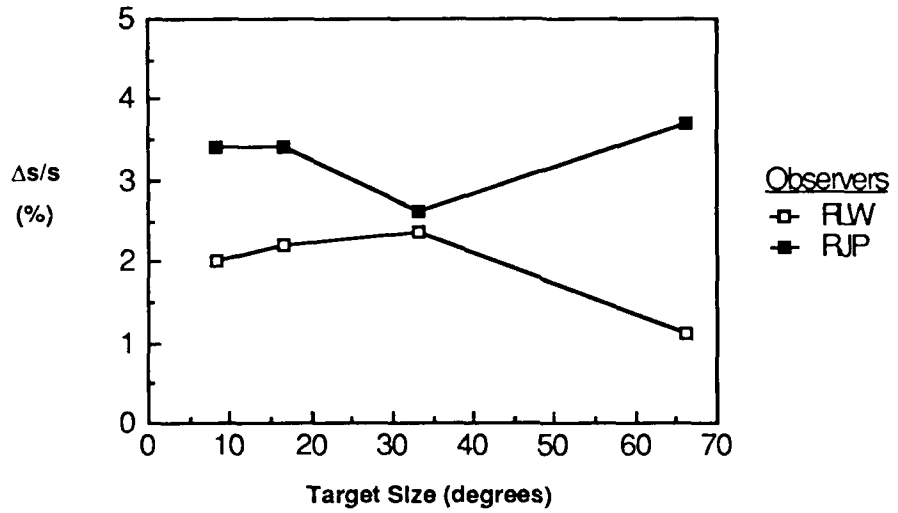

Figure 3. *Localization threshold for a pair of square targets separated by 4 degrees, as a function of the length of the side of the square. Inner edge distances were the same for each target size. Two observers.*

Preliminary data suggest, however, that target size does affect the perceived separation. If comparison is made across target sizes, e.g., if the separation between two large targets is compared to that between two small targets, a bias is evident as shown in Figure 4. In this experiment, the targets were square and differed in size by a factor of four. The large targets were 66 arcmin on a side and the small were 8 arcmin on a side. The observer was asked to compare the distance between the inner edges of the targets. The data indicate that for this observer, at least, the inner edges of the small targets appear to be farther apart than those of the large targets. If the observer were comparing the centers or outer edges of the targets instead of following the instructions, then the larger objects would appear to be farther apart, because those features are farther apart. Instead we find the reverse: the small targets appear to be farther apart, although the

inner edge separation is actually the same.

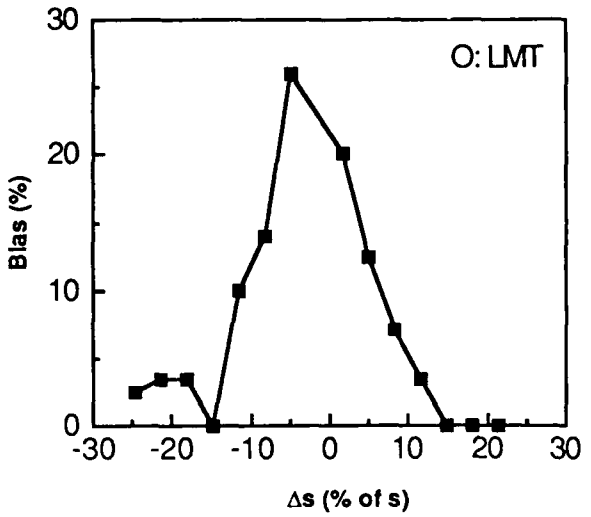

Figure 4. *Bias is the absolute value of the difference between the psychometric functions obtained with a large vs. small comparison and with a large vs. large comparison. The large vs. small comparison was done in both orders, small first then large and vice versa, and the data averaged. Average separation, 4 degrees.*

A plausible explanation for this effect is that the smaller targets appear to be farther away, so the observer, who is trying to estimate the physical properties of the stimulus [1], perceives them as being farther apart. This interpretation allows him to reconcile the fact that the retinal separations are the same with the fact that the (perceived) viewing distances are different.

The perceived spatial frequency shift (PSFS) that occurs when a grating is surrounded by another grating of a different spatial frequency (but the same orientation) is another example of the importance of context in separation judgments. The perceived frequency is altered by the adjacent context, whereas the contrast threshold is not [2]. The importance of context in size judgments has long been recognized: The simultaneous PSFS is simply the contemporary version of the Titchner

figure, in which the perceived size of a disk is altered by surrounding it by smaller or larger disks. However, this context effect does not appear to be intrinsic to the localization mechanism itself. The PSFS depends on the retinal spatial frequencies of the objects, not on their object spatial frequencies. On the other hand, the effect persists even if the test gratings being compared have different retinal spatial frequencies, provided they have the same object spatial frequencies. Thus, the bias is introduced at a stage of processing in which retinal spatial frequencies are represented, but the comparison is made at a stage in which object spatial frequencies are estimated (Appendix F).

This duality has appeared in the results of other localization experiments as well. It is interesting in its own right and relates to the second general issue that we are investigating: the problem of isolating the localization mechanism and understanding its relationship to more distal stages of visual processing.

C. Isolating the Localization Process From More from Distal Stages of Spatial Processing

Localization thresholds cannot, in general, be accounted for by either the retinal or the initial cortical stages of processing that have recently been so extensively studied and modeled. Morgan and Ward [3] have provided evidence that hyperacuity thresholds cannot be accounted for by popular "spatial frequency channels" models. Using a different approach [4], I have shown that large-scale localization also cannot be explained by such models (Appendices B and D). In fact, large-scale localization thresholds are remarkably insensitive to those aspects of the stimulus that are fundamental in a spatial frequency channels representation.

Localization presumably occurs at a higher (more proximal) level of visual processing. However, the properties of this higher level are not readily revealed. It is our working hypothesis that under some circumstances, localization thresholds are determined at stages of processing that precede the site of the separation judgment. The localization threshold is determined wherever the visual system runs up against its limits in performing the task. If the contrast is too low, or the objects too small, the limits may occur at the photoreceptor level. Hirsch and Hylton [5,6] have found conditions in which the limits appear to occur at this or a slightly higher level. If the exposure duration is short and the objects are small, localization thresholds may be determined by the limits of the initial cortical representation. Yap, Levi, and Klein [7] have shown conditions under which this appears to be true. They find that the localization threshold is completely determined by the retinal eccentricity of the objects when cortical magnification is taken into account. On the basis of such results, they theorize that separation judgments are made by a process that acts like a yardstick on the initial cortical representation. This yardstick has a constant error associated with it, independent of the distance being measured.

Our approach is to try to use stimuli that do not push the limits of the earlier stages of processing, in order to determine the limits of the localization process itself. We use relatively large targets, of high contrast and, probably most important, of long duration. Such stimuli yield lower localization thresholds than are obtained with other combinations of parameters (Appendix C). When such stimuli are used, localization thresholds vary only slightly with eccentricity. The targets in the experiments discussed here were 1° squares, with an inner-edge average separation of 4°. The exposure duration was 500 ms. Data obtained on two observers are shown in Figure 5. The increase in localization thresholds with eccentricity predicted by cortical magnification [8] would result in best fitting lines that crossed the x-axis at -0.77. The best fitting lines to our data cross at -22.5 and -26.7, respectively; that is, the "foveal" threshold doubles at about 25 degrees, instead

of 0.77 degrees, as Levi et al. [8] found with small stimuli. In short, the eccentricity effect is much smaller with these stimuli than with those used by Yap et al. [7]. To the extent that the localization thresholds we found are less dependent on eccentricity, I believe that they come closer to showing the limits of the localization process itself.

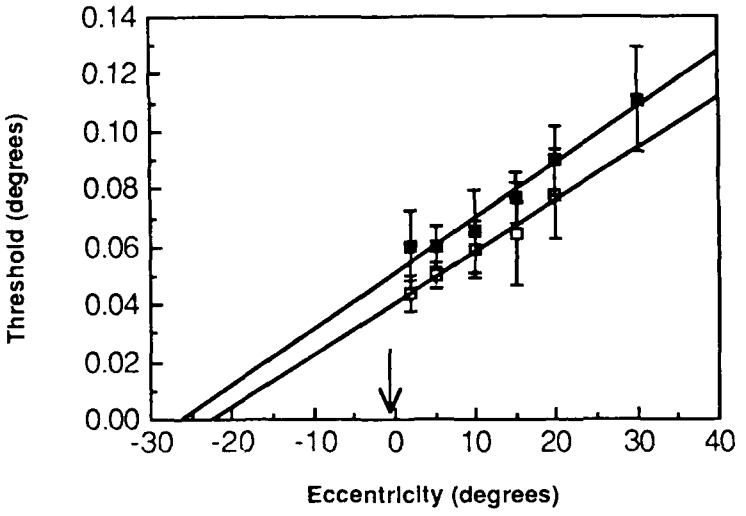

Figure 5. *Localization thresholds measured as a function of retinal eccentricity. Average separation was 4°. The arrow indicates the point of intersection predicted by cortical sampling. Observers RLW and RJP.*

Even with these stimuli, there is still a small effect of eccentricity. We intend to repeat these experiments with image stabilization and no fixation point so that the observer can freely attend to the peripheral targets. This should eliminate any variation in attention with eccentricity. We may also try cuing the observer as to the eccentricity at which the targets will be presented, to further reduce the positional uncertainty associated with peripheral presentation. We would like to be able to eliminate eccentricity effects entirely, if this can be done with stimulus manipulations that are theoretically sound. This goal assumes that the localization mechanism acts independently of

the retinal eccentricity of the objects. Such an assumption seems plausible because of the other classes of independence that we have discovered. Most of these are covered in the Appendices. The response of the localization mechanism is independent of:

- Exposure duration (Appendix C)
- The spatial characteristics of the targets (Appendices B and D)
- The orientation along which separation is judged (Appendix E)
- The relative orientations of the test and reference stimuli [9]
- Retinal image size, that is, response depends on overall object properties, but not on individual properties of the retinal image (Appendix A).

The best example of isolating the localization mechanism is described in a 1986 paper [10] on exposure duration effects (Appendix C). There I showed that the well-known effect of exposure duration on small-scale localization thresholds is not intrinsic to the localization process at all, but instead is another example of the long integration times associated with the processing of high spatial frequencies. This effect had previously been attributed to the localization process and inferences about the nature of the localization process had been drawn from that attribution, whereas the effect actually occurs at an earlier stage of processing.

D. Experimental Issues

Revealing the properties of the localization process is not easy. Localization thresholds can be determined at stages of processing that precede the localization judgment, as we have seen above, and isolating the process from the effects of those prior stages is not trivially done. The effects of context, which seem to be central to the localization mechanism, are particularly difficult to capture. We have found substantial variation across subjects in some of our experiments, and

have seen similar variation in the data from other laboratories doing research in this area. For example, we have measured the effects of randomly jittered parallel bars on localization accuracy in six observers. In five observers the outside parallels had a larger effect than the inside parallels. The sixth observer showed no effects of the parallels at all. Similarly, despite repeated attempts with several observers, we have been unable to replicate Regan and Beverley's [11] effects of pattern adaptation on frequency discrimination thresholds (Appendix F). Our laboratory experience with other paradigms exploring the effect of context suggests that this may not be due to inadequate experimental techniques in one of the laboratories, but instead may be due to some subtle difference in context, or even to inter-subject differences.

Finally, we note that the experimental techniques that have been so successful in revealing some of the properties of the initial stages of cortical processing, e.g. pattern adaptation or masking apparently cannot be used to probe higher levels of processing (Appendix F), although they can shed light on the relationship between the more distal stages and the localization process. To uncover the properties of the localization mechanism, new techniques must be developed. The experiments reported above are first steps in that direction.

II COLLABORATIONS AND SCIENTIFIC VISITS

Dr. Ben Kröse, a postdoctoral fellow at California Institute of Technology under Dr. Bela Julesz and Dr. David van Essen, is working with me on a joint project. He was at SRI for two weeks and we have continued to collaborate since then by phone, letter, and computer disks. Dr. Kröse and I are investigating the effects of spatial interactions on rapid pattern discrimination. We are using the eyetracker to present stimuli at a fixed location in the periphery without having to use a fixation point. The idea is to present the target at a fixed retinal locus to allow the observer to focus his attention and then measure the effect of adding distractors at various distances from the target. We have found two classes of effects of the distractors: one class is quite local and depends on the number of distractors, and one class is more global and is independent of the number of distractors.

Dr. Don Kelly and I completed and published some research on the early stages of spatial vision (Appendix G). This research was an extension of work we had previously done together, it does not bear directly on the localization problem.

III. PUBLICATIONS AND MANUSCRIPTS

A. Published During the Past Year

"Exposure-duration effects in localization judgments," *J.* Opt. Soc. Am. A ***3***, 1983-1988, 1986.

"Position and spatial frequency in large-scale localization judgments," *Vision Res.* **27**, 3, 417-427, 1987.

"Locus of spatial-frequency discrimination," *J Opt. Soc. Am. A* **4**, 1807-1813, 1987.

"Further evidence for a broadband, isotropic mechanism sensitive to high-velocity stimuli," *Vision Res.* **27**, 9, 1527-1537, 1987, with D.H. Kelly.

B. Manuscripts Submitted

"No orientation selectivity in large-scale localization," submitted to *J. Opt. Soc. Am. A.*

"Large-scale localization across spatial frequency channels," submitted to *Vision Res.*

"Serial Stages in Spatial Processing: Evidence from Pattern Adaption Effects," to be submitted to *Vision Res.*

REFERENCES

1. C.A. Burbeck, "Locus of spatial-frequency discrimination," *J Opt. Soc. Am. A* **4**, 1807-1813, 1987.

2. S. Klein, C.F. Stromeyer III, and L. Ganz, "The simultaneous spatial frequency shift: A dissociation between detection and perception of gratings," *Vision Res.* **14**, 1421-1432, 1974.

3. M.J. Morgan and R.M. Ward, "Spatial and spatial-frequency primitives in spatial-interval discrimination," *J. Opt. Soc. Am. A* **2**, 1205-1210, 1985.

4. C.A. Burbeck, "Position and spatial frequency in large-scale localization judgments," *Vision Res.* **27**, 3, 417-427, 1987.

5. J. Hirsch and R. Hylton, "Limits of spatial-frequency discrimination as evidence of neural interpolation," *J. Opt. Soc. Am.* **72**, 1367-1374, 1982.

6. J. Hirsch and R. Hylton, "Spatial-frequency discrimination at low frequencies: evidence for position quantization by receptive fields," *J. Opt. Soc. Am. A* **2**, 128-135, 1985.

7. Y.L. Yap, D.M. Levi, and S.A. Klein, "Peripheral hyperacuity: three-dot bisection scales to a single factor from 0 to 10 degrees," *J. Opt. Soc. Am. A* **4**, 1554-1561, 1987.

8. D.M. Levi, S.A. Klein, and A.P. Aitsebaomo, "Vernier acuity, crowding and cortical magnification," *Vision Res.* **25**, 963-977, 1985.

9. C.A. Burbeck and D. Regan, "Independence of orientation and size in spatial discriminations," *J. Opt. Soc. Am.* **73**, 1691-1694, 1983.

10. C.A. Burbeck, "Exposure-duration effects in localization judgments," *J.* Opt. Soc. Am. A *3*, 1983-1988, 1986.

11. D. Regan and K.I. Beverley, "Spatial-frequency discrimination and detection: comparison of postadaptation thresholds," *J. Opt. Soc. Am.* **73**, 1684-1690, 1983.

Appendix A

Locus of spatial-frequency discrimination

Christina A. Burbeck

Visual Sciences Program, SRI International, Menlo Park, California 94025

Received December 29, 1986; accepted April 2, 1987

In standard frequency-discrimination experiments either the retinal spatial frequencies (cycles per degree) or the object spatial frequencies (real world) could be compared, because the retinal and object frequency differences are the same. Current models of spatial-frequency discrimination assume that observers compare the retinal frequencies. I test this assumption by presenting gratings at different viewing distances (with strong depth cues). The object frequencies of the gratings bear the same relationship that they do in a standard frequency-discrimination experiment, but the retinal frequency of the more distant grating is always markedly higher than that of the near grating. The observer's task is to compare the object spatial frequencies. This change from one depth to two (with no change in the stimulus object) has a negligible effect on the observer's performance, suggesting that observers compare object frequencies even in standard spatial-frequency-discrimination experiments. This conclusion is supported by the findings that (1) observers appear unable to learn to compare retinal frequencies and (2) the interstimulus interval has no effect (over the range 0–1020 msec), implying long-term storage of the visual information. Suggestions are made about why these results are consistent with good system design.

1. INTRODUCTION

In recent years, spatial-frequency discrimination has been gaining popularity as a tool for uncovering properties of early spatial visual processing.[1-6] Its primary use has been in testing and developing models of spatial vision that are based on multiple size-tuned or multiple spatial-frequency-tuned channels. These channels were originally postulated to account for the results of contrast-detection experiments.[7-9] They were subsequently elaborated to account for results of spatial-frequency-discrimination studies[1-6] under the hypothesis that discrimination and detection constitute different decision processes on the same neural representation.[1]

The most well-developed channel models of frequency discrimination are those of Thomas[1] and of Wilson and Gelb.[3] In their models, a grating stimulus is represented by the output of some number of spatial-frequency channels. The discriminability of two gratings is then modeled as a simple function of the differences in the outputs of these channels. Frequency-channel models have successfully accounted for a considerable range of results (see Ref. 10 for a review), but they have not addressed all the relevant and important issues. The research reported here considers one basic issue that has not been discussed in the literature: the relationship between perceived spatial frequency and spatial-frequency discrimination.

Definitions: For brevity, the spatial frequency of a stimulus image on the retina, measured in cycles per degree of visual angle, is referred to as the *retinal* frequency. The spatial frequency of the stimulus, measured in cycles per centimeter in the stimulus plane, is referred to as the *object* frequency. The *perceived* spatial frequency is the observer's estimate of the object frequency. In the experiments reported below, the observer is given strong cues to depth so that, over the range of viewing distances used, the perceived frequency can be considered to be a good estimate of the object frequency.

Perceived frequency varies with perceived stimulus depth in the same way that the perceived size of an object does,[11] resulting in frequency constancy, which is analogous (or identical) to size constancy.[13] However, spatial-frequency discrimination is usually modeled in terms of mechanisms that are insensitive to stimulus depth. Therefore, if current models of discrimination are basically correct, then spatial-frequency discrimination cannot be based on perceived frequency but must, in fact, be dissociated from that percept. Of course, perceived frequencies can also be compared; therefore, if channel models are correct, there must be some other mechanism for that.

Thus a channel-models approach implicitly requires two mechanisms of spatial-frequency discrimination, one that compares retinal frequencies and one that compares perceived frequencies. Because a perceived-frequency comparator requires more information than a retinal-frequency comparator (namely, stimulus depth), we would expect the former to be the less accurate of the two mechanisms because of error in the depth estimate.

In the experiments reported below, I search for evidence of this difference but find none. Instead, I obtain essentially the same psychometric function for spatial-frequency discrimination when perceived frequencies are compared as when, according to channel models, retinal frequencies are compared. Even conservative estimates of the error in the depth judgment suggest that the two functions should differ more markedly. The most parsimonious explanation of the data is that there is only a single frequency-discrimination mechanism and that this mechanism compares (its estimates of) the object frequencies.

2. STANDARD FREQUENCY DISCRIMINATION VERSUS OBJECT-FREQUENCY DISCRIMINATION

Current channel models of spatial-frequency discrimination assume that when two gratings are presented consecutively at a single viewing distance, as they are in standard frequen-

0740-3232/87/091807-07$02.00

cy discrimination tasks, observers compare their retinal frequencies. This assumption can be tested by comparing the psychometric functions for frequency discrimination obtained (1) under standard single-viewing-distance conditions and (2) under conditions in which the observer is required to compare the object frequencies of gratings presented at different viewing distances. Although a mechanism that compares retinal frequencies could theoretically be responsible for performance in the standard single-distance case, it cannot alone account for object-frequency discrimination because that requires depth information. Therefore, if a retinal-frequency comparator is responsible for standard spatial-frequency discrimination, then a different mechanism must be responsible for object-frequency discrimination. If there are two such distinct mechanisms, they should yield different psychometric functions because an object-frequency comparator must contend with noise in the depth estimate whereas a retinal-frequency comparator need not. The following experiments test this implication of channel models of frequency discrimination.

Methods

The author and a naive subject served as observers in this experiment. Other naive observers were used in experiments reported below. All observers had normal or correctable-to-normal vision and ample accommodative range for the experimental conditions.

Stimuli

Horizontal grating stimuli were displayed on two monitors (Conrac 2900 C19 black-and-white monitors with 512 pixels × 512 pixels and a 60-Hz noninterlaced frame rate). The displays were 41 cm × 29 cm, including a 2-cm mean luminance border on all four sides. The stimulus portion of the screens thus subtended approximately 21 deg × 15 deg at 1 m and 11 deg × 8 deg at 2 m. Control experiments were performed in which the angular diameter of the display (as measured at the retina) was the same for the 1- and 2-m conditions. This manipulation had no measurable effect on the observer's performance.

The mean luminance of each monitor was 79 cd/m^2. Microcomputers and associated interface hardware generated the stimuli, randomized the order of presentation, and recorded the data. Gamma correction was performed by an electronic circuit tailored to the display's characteristics. In the contrast range used, luminances were within 2% of the theoretical values.

The contrast of each grating was varied randomly from trial to trial in the range of 40–60% modulation, and the phase of each grating relative to the display surround was also varied randomly from trial to trial in the range 0–90 deg in order to prevent the use of contrast or relative phase as a cue to frequency.

In the standard frequency-discrimination experiments, the gratings were presented on a single screen, located 2 m from the observer. (Some experiments were also conducted with the screen at 1 m. No significant effect of viewing distance was found.) Viewing was monocular, and the room was otherwise dark, to replicate conditions typically used in spatial frequency discrimination experiments. The mean retinal frequency was 8.1 cycles/deg, which corresponds to 7.2 cycles/cm at the 2-m viewing distance.

For the object-frequency comparisons, one display screen was located at 1 m and the other at 2 m from the observer. Viewing was binocular, and the room was dimly lit (~3 cd/m^2) to facilitate acquisition of depth information without significantly reducing the contrast of the stimulus on the display. Figure 1 shows the depth cues available to the observer. (The room illumination was increased to obtain a photograph that would reproduce well.) The pair of object stimuli presented in each trial was identical to that presented in the standard frequency-discrimination experiment. Feedback was also identical. However, in a given trial, one grating was presented on the 1-m screen and the other was presented on the 2-m screen. The gratings were presented sequentially, as in the previous experiment. Because the viewing distances to the two displays differed by a factor of 2, the retinal frequencies of the gratings differed, on average, by a factor of 2. The observer's task was to determine which grating of the pair had the higher object frequency.

Procedure

The method of constant stimuli was used. Each trial consisted of an $(f + n\Delta f/2, f - n\Delta f/2)$ pair, where f is the mean object frequency of the experiment, Δf equals 1% of the mean frequency, and n is an integer from 1 to 8. The two gratings were presented sequentially on each trial. At the observer's initiation, the first grating appeared for 204 msec with abrupt onset and abrupt termination. At 1020 msec after the termination of the first grating, the second grating was presented with the same temporal waveform as the first. The delay between presentations gave the observer time to saccade from one display to the other and to change accommodation appropriately when the displays were at different viewing distances. The effect of the interstimulus interval (ISI) was considered in subsequent experiments.

During each experimental session, each grating pair was presented 10 times in random order. In half of the trials, the higher-frequency grating was presented in the first interval, and in half of the trials it was presented in the second. The subject's task was to indicate during which interval the grat-

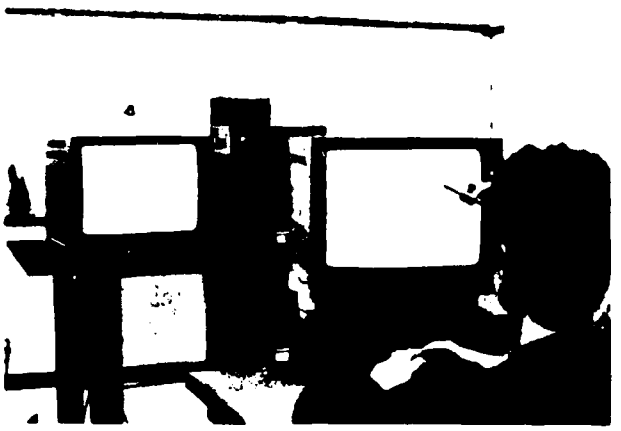

Fig. 1. Photograph of laboratory, showing arrangement of displays and surrounding depth information. The room illumination shown is considerably higher than that used in the object frequency discrimination experiments (see the text), but the photograph accurately represents the visual information available to the observer. For the observer, there was no lateral gap visible between the two displays.

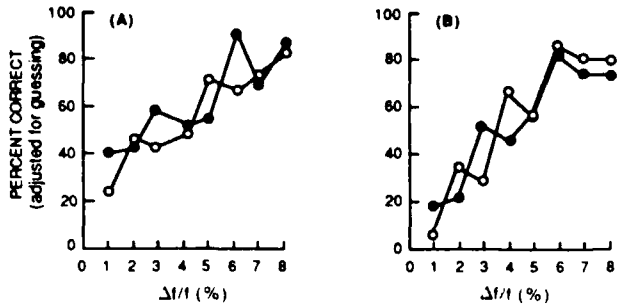

Fig. 2. Psychometric functions for frequency discrimination. The two gratings that constituted a trial were presented sequentially either on one screen located at 2 m (filled circles) or on different screens located at 1 and 2 m from the observer (open circles). The object stimuli were identical in the two experiments; the distances to the screens and the retinal frequencies differed. Observers were JDC (A) and CAB (B).

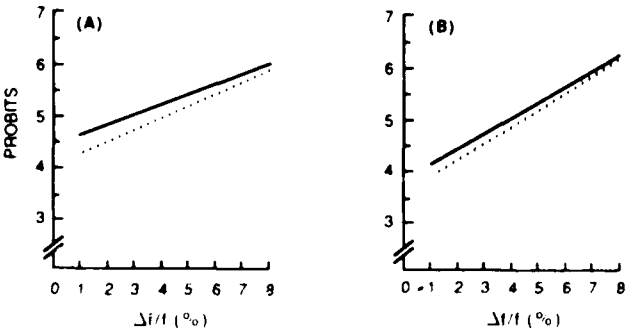

Fig. 3. Best-fitting lines to the linearized psychometric functions for standard frequency discrimination (solid lines) and for object-spatial-frequency discrimination (dotted lines). Observers were JDC (A) and CAB (B).

ing of higher object frequency appeared. This task was unambiguous because there was only one way of seeing the gratings; observers could not simply choose to ignore the depth cues (see Sections 5 and 6). Right–wrong feedback was given after each trial, and enough practice trials were conducted to ensure that the observer's performance had reached a plateau.

The data were adjusted for guessing as follows: (original percent correct − 50) × 2 = adjusted percent correct.

Results

Results of the standard spatial-frequency-discrimination experiments are shown by the filled symbols in Fig. 2. Frequency-discrimination thresholds (determined by standard probit analysis techniques)[14] were 2.6 and 3.9% for observers JDC and CAB, respectively. These thresholds are consistent with values obtained previously.[15]

Data for object-frequency discrimination are shown by the open symbols in Fig. 2. There is no obvious difference between the psychometric functions for standard frequency discrimination (filled symbols) and for object-frequency discrimination, but there is a small tendency for accuracy to be higher for standard frequency discrimination. To illustrate this more clearly, the individual psychometric functions were linearized by converting the percentages to probits[14] and then were summarized by the best-fitting lines. These lines are shown in Fig. 3. The object-discrimination function (dotted line) lies slightly below the standard frequency-discrimination function (solid line). This small difference could readily be accounted for by the fact that the errors in two estimates of a single depth (standard discrimination) are undoubtedly more highly correlated than are the errors in the estimates of two depths (object discrimination).

Discussion

The small differences in the data reported above do not support the hypothesis that there are two distinct underlying mechanisms. Without strong evidence for two mechanisms, only a single mechanism should be assumed, simply on the basis of parsimony. However, one can also consider whether a stronger inference can be made from these data. It was argued above that the psychometric function for object-frequency discrimination should differ from that for retinal-frequency discrimination. The question, of course, is how different it should be. Specifically, do the data reported above actually contradict the hypothesis that retinal frequencies are being compared in the standard spatial frequency-discrimination task? To answer this question, a quantitative theoretical assessment of the effect of depth error on the psychometric function for frequency discrimination is required.

3. EXPECTED EFFECTS OF ERROR IN THE DEPTH JUDGMENT

The two most plausible explanations for the data reported in Section 2 are that both tasks are mediated by a common mechanism that is sensitive to depth and, alternatively, that they are mediated by different mechanisms but the additional error introduced by the depth judgment (required in object-frequency discrimination) is so small that it makes only a slight change in the psychometric function for frequency discrimination. To assess the plausibility of this small-depth-error explanation, the following quantitative analysis was performed.

For this analysis, it was assumed that the error in the retinal-frequency representation is given by the results of the standard frequency-discrimination experiments. This assumption has also been made for channel models of frequency discrimination. Several estimates of the depth error were then made to determine the magnitude of the error that would be consistent with the object-frequency-discrimination data (Figs. 2 and 3) under the assumption that performance in object-frequency discrimination is limited only by the accuracy of the retinal frequency and depth information. A Gaussian probability-density function was used for the depth-error estimate, with σ being changed to obtain the different estimates. The mean was assumed to be zero, consistent with size constancy. The depth information that the observer needs to discriminate between object frequencies is the ratio of the two viewing distances. There are no data in the literature, of which I am aware, that pertain to this point, and our laboratory conditions were not suitable for making this measurement (because of the large number of depth cues). Therefore we consider several values of σ.

The estimated effects of depth error were calculated as follows: the probability of a correct response for a given $\Delta f/f$ is the product of the probability of a correct response in the absence of depth error (i.e., the value from the standard frequency-discrimination experiment) multiplied by the

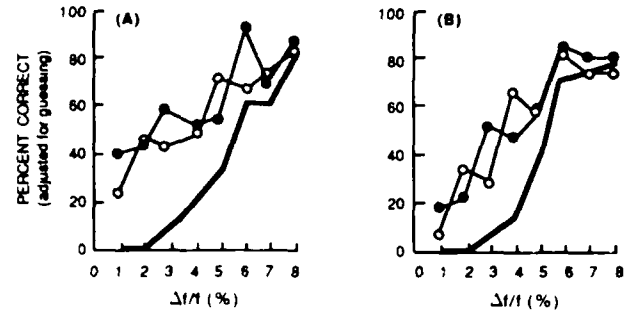

Fig. 4. Effect of adding error from a depth estimate to the psychometric function obtained in the standard frequency-discrimination experiments. An estimate of the psychometric function resulting from adding a depth judgment to the spatial-frequency-discrimination process is shown (bold lines). The probability-density function of depth error is Gaussian with $\sigma = 3\%$ (see the text). Results of standard frequency-discrimination experiments (filled symbols) and object-frequency discrimination experiments (open symbols) are also shown. Observers were JDC (A) and CAB (B).

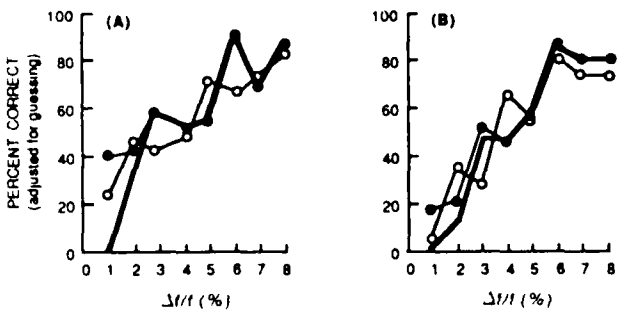

Fig. 5. Same as Fig. 4 except that σ for the depth error is 1%.

(one-tailed) probability that the depth error would exceed $\Delta f/f$ percent. (A depth error of $n\%$ or more, in the appropriate direction, would reverse the observer's judgment if the frequency difference was $n\%$ or less.)

Figure 4 (bold lines) shows the results of including a $\sigma = 3\%$ depth error in the psychometric function for frequency discrimination. (Although this error is larger than the lowest obtained with some stereo paradigms,[16] it should be considered because our viewing situation was not designed to elicit stereo hyperacuity.) The effects of depth error were calculated separately for each observer. Also shown for comparison are the original psychometric functions for standard frequency discrimination and object-frequency discrimination (filled and open symbols, respectively). For both observers, the standard frequency-discrimination function with ($\sigma = 3$) error added differs substantially from the object-frequency-discrimination function. The largest difference occurs at small values of $\Delta f/f$ because when $\Delta f/f$ is small, even small depth errors can affect the results, whereas when $\Delta f/f$ is large, only large depth errors have an effect.

In the next estimate, σ is assumed to be 1. The effects of this depth error are shown in Fig. 5 for both observers. With $\sigma = 1$, the depth-error-added and object-frequency-discrimination functions are clearly different at the low end for one observer [Fig. 5(A)] but not for the other [Fig. 5(B)], because the second observer's low accuracy at the smallest values of $\Delta f/f$ forces the curves to come together. For $\sigma < 1$, the differences are not significant for either observer.

If σ for the depth error under the experimental conditions of Section 2 is more than about 1%, then the data contradict the hypothesis that retinal frequencies are being compared in standard frequency discrimination. If σ for the depth error is less than about 1%, then these results would be consistent with either a single-mechanism explanation (object frequencies compared) or with a two-mechanism explanation (object or retinal frequencies compared). However, even if the depth error were that small, the null hypothesis—that there is only one mechanism for frequency discrimination—should still be assumed in the absence of positive evidence for a second mechanism. I therefore assume that in the standard spatial-frequency-discrimination experiment described in Section 2, the observers actually compared estimates of object frequencies. That conclusion is tested further in the following sections.

4. EFFECT OF INTERSTIMULUS INTERVAL

In the experiments reported in Section 2 a long ISI was used to provide the observer with time to shift between the two stimulus depths in the object-frequency-discrimination task. However, the long ISI makes the results difficult to relate to previous studies of frequency discrimination, in which shorter ISI's have generally been used. Furthermore, one might expect the sensitivity of more primitive spatial-frequency representations to be revealed if the ISI were reduced. Long ISI's might favor comparison of the object frequencies, and shorter ISI's might favor the comparison of retinal frequencies. In the following experiments, frequency-discrimination thresholds were measured as a function of ISI by using a single-screen (single-distance) paradigm.

Methods

The experimental procedure used in these experiments was similar to that used in the standard frequency-discrimination experiment (Section 2) except that the duration between the two grating presentations was varied between experimental sessions. The relative phases of the gratings were randomized from trial to trial. The ISI's were 0, 85, 255, 510 and 1020 msec. Each grating was presented for 204 msec. Viewing distance was 1 m, and the mean spatial frequency was 1.36 cycles/deg at the retina. Viewing was monocular. Two naive observers were used, neither of whom had served in the previous experiments.

Results

Frequency-discrimination thresholds for all ISI's and both observers are shown in Fig. 6. Although both observers show some variation across this large range of ISI's, the variation is not systematic across observers. The individual psychometric functions underlying these thresholds are

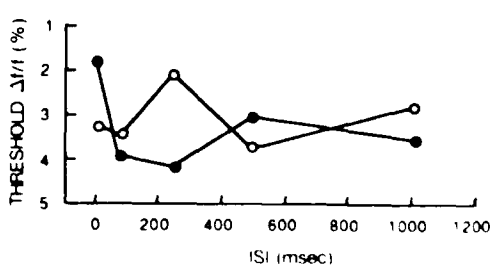

Fig. 6. Frequency discrimination thresholds as a function of time between presentations of the gratings being compared (ISI). Observers were MBO (filled circles) and EBF (open circles).

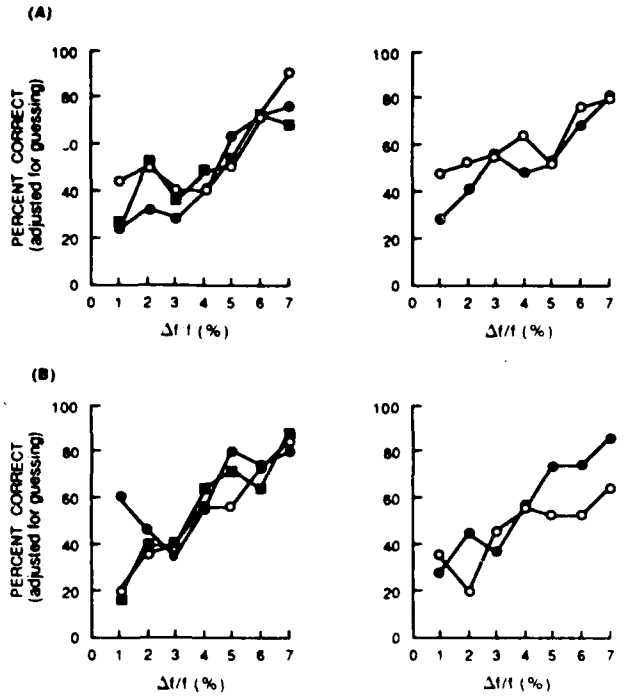

Fig. 7. Psychometric functions for frequency discrimination underlying the thresholds shown in Fig. 6, for observers MBO (A) and EBF (B). The two extreme ISI's are shown on the right: 0 msec (open circles) and 1020 msec (filled circles). The three intermediate ISI's are shown on the left: 510 msec (open circles), 255 msec (filled circles), and 85 msec (filled squares).

shown in Fig. 7. Frequency-discrimination thresholds do not vary systematically with ISI over the range from 0 to 1020 msec. In particular, there is no evidence that the longest ISI taps a different mechanism than briefer ISI's. Thus the standard spatial-frequency-discrimination task (Section 2) was, in fact, representative. These results replicate and extend the results of Regan's study[17] in which frequency-discrimination thresholds were measured with ISI's ranging from 0.4 to 20 sec.

Discussion

The study noted earlier[17] on the effect of ISI on spatial-frequency discrimination focused on the storage of spatial-frequency information. This view of the results of the ISI manipulations is particularly interesting in the present context. The results reported in Section 2 suggest that it is the object frequency, not the retinal frequency, that is stored. At very long ISI's (i.e., several seconds), intuition supports the idea that only the object-frequency information would remain. The interesting result is that this effect appears to hold also when the two gratings are presented in immediate succession. The results of the ISI manipulations and the comparison of standard frequency-discrimination results with object-frequency-discrimination results thus point to the primacy of an object-frequency representation in spatial frequency-discrimination tasks.

5. RETINAL-SPATIAL-FREQUENCY DISCRIMINATION

The data obtained thus far suggest that under standard experimental conditions, observers compare the object frequencies and not the retinal frequencies of the gratings, even though the representation of the object frequencies must include more error than does the representation of the retinal frequencies. A logical question is whether the observer can learn to access the retinal-frequency representation directly. The aim of the following experiment was to try to teach observers to compare retinal frequencies directly.

Methods

The gratings were presented at different viewing distances (1 and 3 m) and were paired according to their retinal frequencies, making their object frequencies differ by about a factor of 3. The average retinal frequency was 4.05 cycles/deg (which was 2.32 cycles/cm on the 1-m screen). The observer's task was to indicate which display had the grating of higher retinal frequency. Auditory feedback was used to define the task, as it was in all previous experiments. Rather than presenting grating pairs that shared a common mean frequency in this experiment, I presented grating pairs that had different mean frequencies. $\Delta f/f$ was fixed at 10%. (This paradigm was used to prevent the observer from making judgments by comparing the frequency of one of the gratings with the average frequency previously presented on that screen.) This experiment was otherwise identical to the object-frequency-discrimination experiments reported in Section 2.

The observer whose data are shown was completely inexperienced with this and related tasks. She had not served in any of the previous experiments and was not informed of the results of those experiments until all data were collected. Her only instructions were to be correct as often as possible. Other observers were told to try to ignore the distances to the screens. Their performance was no better.

Results

Frequency-discrimination thresholds for this retinal-frequency discrimination and for an associated object-frequency discrimination (same viewing distances; average object frequency, 2.32 cycles/cm) are shown in Fig. 8. Performance on this task was initially very poor, but it improved with practice until it nearly equaled that obtained by this observer for object frequency discrimination.

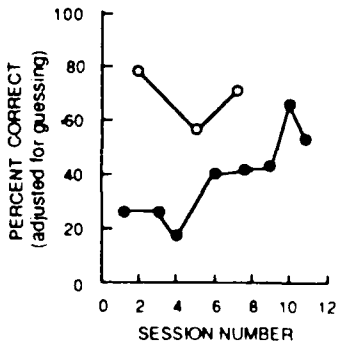

Fig. 8. Effects of learning on frequency discrimination with viewing distances of 1 and 3 m for observer VP. Results for retinal frequency discrimination (filled circles) and object frequency discrimination (open circles) are shown. Each datum represents the result of one session of 80 trials. In these experiments, $\Delta f/f$ was fixed at 10%, and the center frequency f was varied. This paradigm yields higher overall thresholds but ensures that the observer does not make same-screen comparisons.

Discussion

One might conclude from these data that an observer can eventually learn to ignore depth and to compare retinal frequencies directly. However, two problems stand in the way of this interpretation. First, if the observer is comparing retinal frequencies directly, then he or she should be more accurate at this task than at object-frequency discrimination. However, none of the four observers who participated in this portion of the study was more accurate at the retinal-frequency discrimination. Second, there is another means by which the observer could be performing this task: the object frequencies of the two gratings differ by approximately a factor of 3. This ratio is more than 3 if the far screen has the lower retinal spatial-frequency grating and is less than 3 if the near screen has it. Thus the observer needs only to compare the ratios of the object frequencies with the average objective-frequency ratio to obtain the required answer. All four observers who were trained on the retinal-frequency-discrimination task independently reported adopting this strategy.

6. FREQUENCY-RATIO DISCRIMINATION

The informal observations made in the retinal-frequency-discrimination experiments were tested and confirmed experimentally as follows. After the observer mastered the retinal frequency-discrimination task, the viewing distances were changed while the stimulus objects remained the same. Because the object frequencies were unchanged, their average ratio was also unchanged. However, because the viewing distances were changed, the retinal frequencies were now related by an arbitrary ratio. The auditory right-wrong feedback to the observer was also unchanged. Therefore the observer's task was the same as in the previous experiment when considered in terms of the object frequencies but became arbitrary when considered in terms of the retinal frequencies. If the observer were actually comparing retinal frequencies in the retinal-frequency-discrimination experiment, then he or she should initially be at a loss about how to perform this frequency ratio discrimination. However, if the observer were comparing the ratios of the object frequencies in the retinal-frequency-discrimination task, then the change in viewing distance should have no effect on his or her performance.

Methods

The experimental conditions were the same as those used previously (Section 2) except that the viewing distances were 1 and 2 m for the retinal-frequency discrimination that served as the control and the 2-m screen was moved to 1.5 m for the frequency-ratio discrimination. At the 1- and 2-m viewing distances, the average retinal frequency was 4.05 cycles/deg.

Results

Figure 9 (filled circles) shows data obtained in the frequency-ratio discrimination experiment without practice. Also shown for comparison (open symbols) are data from the retinal-frequency discrimination experiment, obtained after a stable level of performance had been reached. The observer performed the frequency-ratio discrimination as well as he performed the retinal-frequency discrimination. Furthermore, the learning transferred completely from retinal-frequency discrimination to frequency-ratio discrimination. Performance on the frequency-ratio discrimination began at the high level of accuracy shown here even though the relationship between the retinal frequencies was arbitrary. Thus it seems clear that observers did not compare the retinal frequencies in the original task but instead compared estimates of the object frequencies of the gratings.

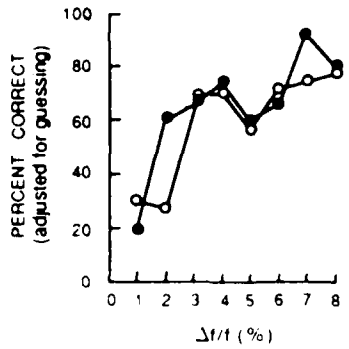

Fig. 9. Psychometric functions for frequency-ratio discrimination (filled circles) and retinal-frequency discrimination (open circles) for observer JDC.

7. DISCUSSION

The data reported here do not support the hypothesis that observers compare retinal frequencies directly in standard spatial-frequency-discrimination xperiments. Instead, observers appear to compare estimates of object frequencies even when the retinal frequencies are similar and the object frequencies are dissimilar. This conclusion contradicts the basic assumption of current spatial-frequency-channel models of frequency discrimination. The reliance of spatial-frequency discrimination on an estimate of stimulus depth as well as on the retinal frequencies implies that frequency discrimination cannot be performed at the theoretical frequency-channels stage of processing. It also suggests that discrimination and detection do not "involve the application of different decision processes to the same neural representation of the visual scene"[10] but instead are based on fundamentally different representations that may be serially related.

The idea that detection threshold and perceived frequency are based on different neural representations was previously proposed by Klein *et al.*[18] Using an adaptation paradigm, they found that perceived spatial frequency shifts in the same way when the test stimulus is surrounded by a simultaneous grating annulus set at the adapting frequency as it does when the test stimulus is preceded by adaptation to a grating stimulus that covers the test area. Detection thresholds, on the other hand, are unaffected by the presence of the surrounding annulus but are raised if preceded by adaptation to a superimposed grating of similar spatial frequency. Klein *et al.* concluded from these results that contrast threshold elevation and the perceived spatial frequency shift arise from adaptation at different sites in the visual pathway. Graham[19] has also noted discrepancies be-

tween the results of detection and identification experiments.

The idea that frequency discrimination occurs subsequent to the frequency-channels stage (a two-stage model) is not contradictory to experimental results that have been cited as evidence for the spatial-frequency-channels model of frequency discrimination. The strongest argument for a single stage for detection and discrimination is the finding that the ratio of z scores for identifiability and detectability remains constant as the contrast of the grating is changed in the near-threshold region.[20] Although this linkage has been thought to imply that detection and discrimination occur at a common site, in fact the contrast result implies only that the effect of contrast on frequency discrimination can be completely accounted for by the effect of contrast at the detection stage of processing. This conclusion is consistent with a two-stage model in which spatial-frequency discrimination is based on representations of both the retinal frequencies of the gratings (at the purported detection stage) and their depths. The accuracy of the retinal-frequency information is affected by stimulus contrast; the accuracy of the depth information, for these grating stimuli, is not. Therefore, even in a two-stage model, the only effect of contrast on frequency discrimination is its effect on the retinal-frequency representation, that is, on the detection stage in current channel models.

Other evidence cited in favor of a single site of detection and discrimination[1] is the existence of multiple, tuned pathways and pathway labeling. Neither of these concepts conflicts with the idea that discrimination occurs at a site subsequent to detection. The information may be transmitted along the multiple, tuned, labeled, pathways and then used for spatial-frequency discrimination at a later site, in conjunction with other visual information.

The results and conclusions reported here are also not inconsistent with the observation of Hirsch and Hylton[21] that frequency-discrimination accuracy is limited by the foveal mosaic. Just as the accuracy of the retinal-frequency representation limits the accuracy with which object frequencies can be estimated, so the receptor mosaic may impose its limitations, which carry through to higher perceptual levels.

Finally, it is interesting to note that the psychometric function for spatial-frequency discrimination shows remarkable insensitivity to the detailed spatial and temporal conditions of the stimulus presentations that so affect detection thresholds. Frequency discrimination thresholds are insensitive to such basic stimulus parameters as the relative distances to the gratings being compared, the mean frequency of the experiment, the ISI,[1] and the relative orientations of the stimuli. This insensitivity is consistent with the idea presented here that spatial-frequency discrimination is based on a more sophisticated representation of the stimuli than is commonly assumed. Although this conclusion contradicts current channel models, it has intuitive appeal. The ultimate goal of the visual system is to gather information about the external world, and object, not retinal, frequency is the coin of that realm.

ACKNOWLEDGMENT

This research was supported by the Air Force Office of Scientific Research, Air Force Systems Command, U.S. Air Force, under contract number F49620-85-K-0024.

REFERENCES

1. J. P. Thomas, "Underlying psychometric functions for detecting gratings and identifying spatial frequency," J. Opt. Soc. Am. **73**, 751–758 (1983).
2. A. B. Watson, "Detection and recognition of simple spatial terms," NASA Tech. Memo. 84353 (Ames Research Center, Moffett Field, Calif., 1983).
3. H. R. Wilson and D. J. Gelb, "Modified line-element theory for spatial-frequency and width discrimination," J. Opt. Soc. Am. A **1**, 124–131 (1984).
4. J. Hirsch and R. Hylton, "Limits of spatial-frequency discrimination as evidence of neural interpolation," J. Opt. Soc. Am. **72**, 1367–1374 (1982).
5. D. Regan and K. I. Beverley, "Spatial-frequency discrimination and detection: comparison of postadaptation thresholds," J. Opt. Soc. Am. **73**, 1684–1690 (1983).
6. A. B. Watson and J. G. Robson, "Discrimination at threshold: labelled detectors in human vision," Vision Res. **21**, 1115–1122 (1981).
7. F. W. Campbell and J. G. Robson, "Application of Fourier analysis to the visibility of gratings," J. Physiol. **197**, 551–566 (1968).
8. C. Blakemore and F. W. Campbell, "On the existence of neurones in the human visual system selectively sensitive to the orientation and size of retinal images," J. Physiol. **203**, 237–260 (1969).
9. M. B. Sachs, J. Nachmias, and J. G. Robson, "Spatial frequency channels in human vision," J. Opt. Soc. Am. **61**, 1176–1186 (1971).
10. J. P. Thomas, "Detection and identification: how are they related?" J. Opt. Soc. Am. A **2**, 1457–1467 (1985).
11. J. P. C. Southall, ed., *Helmholtz's Treatise on Physiological Optics, 1910* (Dover, New York, 1962), Vol. III.
12. A. H. Holway and E. G. Boring, "Determinants of apparent visual size with distance variant," Am. J. Psychol. **54**, 21–37 (1941).
13. C. Blakemore, E. T. Garner, and J. A. Sweet, "The site of size constancy," Perception **1**, 111–119 (1972).
14. D. J. Finney, *Probit Analysis* (Cambridge U. Press, Cambridge, Mass., 1971).
15. C. A. Burbeck and D. Regan, "Independence of orientation and size in spatial discriminations," J. Opt. Soc. Am. **73**, 1691–1694 (1983).
16. S. P. McKee, "The spatial requirements for fine stereoacuity," Vision Res. **23**, 191–198 (1983).
17. D. Regan, "Storage of spatial frequency information and spatial-frequency discrimination," J. Opt. Soc. Am. A **2**, 619–621 (1985).
18. S. Klein, C. F. Stromeyer III, and L. Ganz, "The simultaneous spatial frequency shift: a dissociation between the detection and perception of gratings," Vision Res. **14**, 1421–1432 (1974).
19. N. Graham, "Detection and identification of near-threshold visual patterns," J. Opt. Soc. Am. A **2**, 1468–1482 (1985).
20. J. P. Thomas, "Underlying psychometric function for detecting gratings and identifying spatial frequency," J. Opt. Soc. Am. **73**, 751–758 (1983).
21. J. Hirsch and R. Hylton, "Limits of spatial frequency discrimination as evidence of neural interpolation," J. Opt. Soc. Am. **72**, 1367–1374 (1982).
22. F. W. Campbell, J. Nachmias, and J. Jukes, "Spatial frequency discrimination in human vision," J. Opt. Soc. Am. **60**, 555–559 (1970).

Appendix B

Vision Res. Vol. 27, No. 3, pp. 417–427, 1987
Printed in Great Britain

0042-6989/87 $3.00 + 0.00

POSITION AND SPATIAL FREQUENCY IN LARGE-SCALE LOCALIZATION JUDGMENTS

CHRISTINA A. BURBECK

Visual Sciences Program, Sensory Sciences Research Laboratory, SRI International, Menlo Park, CA 94025, U.S.A.

(*Received* 19 *February* 1986, *in revised form* 24 *July* 1986)

Abstract—The frequency-channel model and the position, or "local-signs," model that have been proposed to account for hyperacuity (i.e. small-scale relative spatial localization) are examined in the context of large-scale relative spatial localization. As a basis for subsequent experiments, localization accuracy is measured over a large range of object separations, and previous findings that the "Weber fraction for localization" is constant are replicated. The effects on localization accuracy of both high- and low-spatial frequency components in the objects being localized are examined in some detail. Localization accuracy is found not to rely exclusively on either the high- or the low-frequency components. Neither the frequency-channel nor the position hypothesis as defined here is consistent with all of the observed results. However, with a slight modification, the position hypothesis can account qualitatively for all of the observed results, whereas no reasonable modification of the frequency-channel hypothesis appears able to do as well.

Position Spatial frequency channels Spatial vision Contrast Localization

1. INTRODUCTION

At its finest, the human visual system can detect a few photons, a few tenths of a percent of contrast, a nanometer shift in wavelength, or a second of arc displacement (Hecht *et al.*, 1942; Van Nes and Bouman, 1967; Wright, 1946; Klein and Levi, 1985). Such abilities are impressive, and, as visual scientists, we are eager to understand them, but they may not exemplify the basic visual functions that underlie our more mundane perceptions.

Research on relative spatial localization (that is, detection of the position of objects relative to one another) has usually focused on the upper limit of visual performance. The ability to detect offsets that are less than the width of a retinal cone (i.e. hyperacuity) has been so intriguing that we cannot resist trying to understand it. However, the small-scale stimuli that are required to evoke hyperacuity responses are not only uncommon in our ordinary experience, they may not even be ideal probes of the localization process. In the research reported here, large-scale stimuli are used to explore further the spatial properties of the localization process and to provide new tests of existing theories of localization.

Models

Historically, hyperacuity has been analyzed in terms of the nature of the encoding of local position information. The first prominent theory of localization, suggested by Lotze and then advocated by Hering (described in Matin, 1972) was the theory of local signs. In this theory, components of the stimulus excite receptors, which signal their positions relative to the fovea. These retinal positions are then compared to yield judgments about the relative positions of various stimulus components. Although this model and its subsequent modifications have been invoked primarily to account for hyperacuity thresholds (Marshall and Talbot, 1942; Hirsch and Hylton, 1982) they could also be generalized to include localization of more widely separated objects.

Recently, several investigators have considered an alternative to the local sign, or position, approach; they have been exploring the possibility of accounting for hyperacuity directly in terms of the frequency selectivity of the units that are tuned to limited ranges of spatial frequency and orientation (Wilson and Gelb, 1984; Carlson and Klopfenstein, 1985; Klein and Levi, 1985). [For brevity the theoretical

stage of visual processing that consists of such units will be referred to as the primary representation, and the models that are based on this representation will be referred to collectively as channel models.] Although details of various channel models differ, they share the common basic assumption that the distance between objects is encoded by those units that have receptive fields that are large enough to be stimulated by both objects simultaneously. It is this basic concept that is tested in the experiments reported below.

The requirement of channel models that the responsible units be stimulated simultaneously by both objects being localized has traditionally restricted applicability of these models to small object separations, and Wilson has found that this model does not apply for separations larger than about one degree (Wilson and Gelb, 1984). However, this restriction is not essential. Localization of more widely separated objects could also be accounted for if the primary representation contains units that are tuned for low spatial frequencies and have large receptive fields. This premise may not be unreasonable: Stromeyer *et al.* (1982) provided evidence for channels with peak spatial frequencies considerably less than 0.5 c/d. Therefore, a frequency channel model of spatial localization could plausibly be expanded to include objects that are separated by 2 or 3 deg, or even more, by including channels that are tuned to lower spatial frequencies. In principle, this type of model could account for the relative spatial localization of any two objects that are visible simultaneously.

The position model that will be considered here is a modification of that invoked by previous local signs models. This modification is prompted by the considerable quantitative modeling of small-scale localization that has recently been done (e.g. Carlson and Klopfenstein, 1985; Klein and Levi, 1985; Wilson, 1986). The model to be considered here assumes that the primary representation constitutes the initial stage of processing for the localization mechanism. However, this model assumes that each unit carries information not only about its spatial frequency and orientation selectivity, but about its receptive field position as well. It further assumes that the distance between objects is not encoded explicitly in the primary representation, but rather is inferred, at a subsequent stage of visual processing, from the retinal position information. The model also assumes that the accuracy with which the distances can be inferred is determined solely by the accuracy of the position information obtained from the primary representation. Because the high-spatial-frequency units have the smallest receptive fields, they carry the most precise position information. The assumption of no additional noise from the localization mechanism itself is made because of its simplicity; it is implausible physiologically. Alternative assumptions are considered in the Discussion.

Predictions of models

Quantitative models are deliberately avoided in this paper because the aim is to determine the general validity of the basic frequency-channel and position concepts rather than the specific validity of any particular embodiments. However, some additional constraining assumptions are required before testable predictions can be made. I make the following assumptions about the primary representation: (1) the retinal receptive field density and the spatial frequency bandwidths of the channel units scale with the peak spatial frequencies of these units (Blakemore and Campbell, 1969; Sakitt and Barlow, 1982) so that there is a constant relationship between the sampling rate and the peak spatial frequency; (2) the units in the primary representation have bandwidths of approximately one to two octaves, so that, for example, a unit that is most sensitive to high spatial frequencies cannot simultaneously detect two stimuli that are separated by several degrees (Ejima and Takahashi, 1984). Alternative possible assumptions are considered in the Discussion (Section 7).

Weber fraction for localization. The frequency-channel hypothesis implies that the localization threshold, Δs, will scale with the separation, s, between the objects, yielding a constant "Weber fraction for localization," $\Delta s/s$. Conversely, the position hypothesis implies that, for separations above some minimal value, Δs will be constant (i.e. $\Delta s/s$ will decrease linearly with increasing s) because the accuracy of the positional information for one object is unaffected by the presence of another, nonadjacent, object.

Adding high spatial frequency components. The channel hypothesis implies that, for a pair of widely separated, spectrally complex objects, enhancing the high spatial frequency components in the objects will not affect localization accuracy. According to this hypothesis, widely separated objects are localized by mechanisms

that are selectively sensitive to low spatial frequencies, and hence insensitive to high spatial frequencies. On the other hand, the position hypothesis implies that localization accuracy will be improved by the enhancement of high spatial frequencies in the objects to be localized, because units that are tuned to high spatial frequencies yield more precise positional information (due to their spatially more localized receptive fields), and it is assumed that the precision of the information in the primary representation completely determines the degree of accuracy obtainable.

Subtracting low spatial frequency components. The channel hypothesis includes no provision for localizing widely separated objects that have no detectable energy at low spatial frequencies (i.e. narrow band high frequency objects). Therefore, if this hypothesis is correct then there must be another mechanism for localizing such stimuli. On the contrary, the position hypothesis does not require another mechanism to deal with these stimuli. It implies that widely separated, narrowband, high spatial frequency objects will be localized (by the mechânism that is responsible for localization of less esoteric stimuli) as accurately as spectrally complex stimuli (and more accurately than low frequency objects).

Although either the position or frequency-channel hypothesis could conceivably be fit into a theoretical framework that accounts for almost any result, that could not be done without seriously contradicting the essences of the basic hypotheses. The predictions made above are those that seem to follow most naturally from the basic position and frequency-channel concepts.

2. THE WEBER FRACTION FOR LOCALIZATION

Previous findings

Volkmann performed the classic study of localization thresholds for a wide range of object separations in 1863 (von Helmholtz, 1910). In Volkmann's experiments, observers centered a middle line between two flanking lines. The flanking lines were separated by distances ranging from 0.7 to 16.7 deg. He found $\Delta s/s$ to be approximately constant over that range, contradicting the prediction of the position hypothesis as sketched above. I repeated his experiments under somewhat different conditions, and obtained similar results.

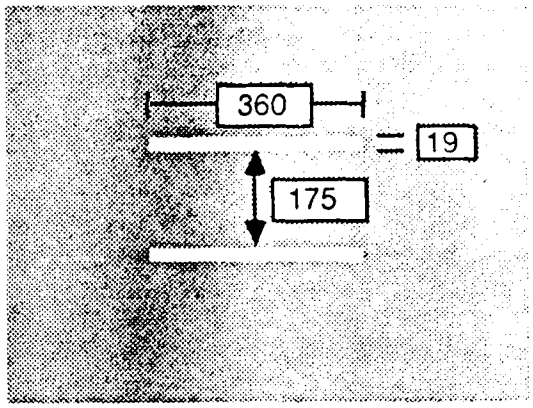

Fig. 1. Representation of the two-bar stimulus. The size of the bars was scaled with the separation between them, according to the ratio shown here.

Methods

Two paradigms were used: the three-bar bisection task of Volkmann, and a two-bar task in which the interbar distance is compared to a learned reference distance. In both the two-bar and three-bar experiments, the objects to be localized were horizontal rectangular bars, as sketched in Fig. 1 for the two-bar case. They were displayed on a video monitor (Conrac, Model 2400, 19 in. diagonal, 60-Hz noninterlaced frame rate, 512 × 512 pixels) that also provided a constant background luminance of 90 cd/m^2. The luminance of the bars was 171 cd/m^2, which resulted in 45% contrast. (Contrast in these experiments is defined to be $(L_{max} - L_{min})/2L_{bkgrd}$, where L_{bkgrd} is the luminance of the background, which was constant. (For these rectangular bar stimuli $L_{min} = L_{bkgrd}$, but in subsequent experiments, a more general definition is required.) The visual angles subtended by the two dimensions of each bar were always proportional to the distance between the bars, as if the viewing distance alone were changed. The relationship between bar size and mean separation is that shown in Fig. 1.

Actually, both the viewing distance and the stimulus itself were changed to achieve the wide range of object separations used. At the smallest separations, a camera lens was used to reimage the stimulus at a smaller scale. When the lens was used, the stimulus was imaged in an aperture that was surrounded by a large uniform field that was illuminated to match the screen approximately in brightness and hue. The effects on localization accuracy of viewing distance and optical minification were checked by using different combinations of viewing distance,

stimulus size, and optical minification to achieve a single object separation and bar size. No significant effects of viewing distance, *per se*, or of optical minification were observed. To prevent the observer from using the distance to the edge of the screen as a cue, the bars were kept well away from the edge, and the position of the pair of bars relative to the upper and lower edges was varied randomly from trial to trial. Viewing was monocular.

The method of constant stimuli was used to measure localization accuracy at each of 10 object separations, approximately equally spaced on a log scale, covering the range 3.4–764 min of arc in the two-bar condition, and 3.6–405 min of arc in the three-bar condition. In a given experimental session, measurements were made at a single object separation, with a single type of stimulus and task, i.e. either two- or three-bar.

Each stimulus was presented with an abrupt onset and was left on at full (i.e. 45%) contrast until the observer responded. Right/wrong feedback was given after each trial.

Two-bar condition. For each object separation, s, the test separations were $s + n(\partial s)$, for $n = \pm 1$ to ± 5. The increment, ∂s, was determined in preliminary experiments for each observer and for each value of s, so that the observer was correct about 90% of the time when $|n|$ equaled 5. Each of the ten stimuli was presented 5 times in a given session, and at least 5 sessions were conducted at each object separation, yielding at least 250 trials for each psychometric function. Data were collapsed across the sign of n, so that a single percent correct value represented a given offset value (without regard to whether the test separation was that much larger or that much smaller than the reference separation).

On each trial, a single pair of bars was presented. The observer's task was to determine whether the distance between the bars was more or less than the average object separation seen during the previous trials. The experienced observers quickly learned the standard and typically performed at a stable level after 50–100 trials. At least two practice sessions of 50 trials each were conducted whenever the mean object separation was changed, and at least one practice session (of 50 trials) was conducted at the beginning of each data collection period. The results of these practice sessions were not included in the calculations of localization accuracy.

Three-bar condition. In this paradigm, there was no fixed reference distance. The observer compared the distance between the top bar and middle bar to the distance between the middle bar and bottom bar. If the mean separation was s, then the bars in a given trial were separated by $s + n(\partial s/2)$ and $s - n(\partial s/2)$, with the larger separation occurring equally often on the top and bottom. The observer's task on each trial was to determine which separation was larger. Data were averaged over the "top distance larger" and "bottom distance larger" conditions. The three-bar experiments were otherwise identical to the two-bar experiments.

Data analysis

Standard probit analysis techniques (Finney, 1971) were used to analyze the data. The per cent correct value for each offset was corrected for guessing [(percent correct − 50) × 2], converted to probits, and then plotted as a function of the offset value. The resulting function was approximated by a straight line, using linear regression, and the offset corresponding to the 50% correct point was determined from the linear approximation. This value, Δs, is a measure of the localization threshold. To relate this value to the scale of the stimulus, Δs was divided by the mean separation, s, yielding the "Weber fraction for localization," $\Delta s/s$.

Results

Localization accuracy for both stimulus conditions is plotted as a function of mean separation in Fig. 2. Data were obtained from two observers for the three-bar condition, and from one observer for the two-bar condition. The average standard error was approximately twice the width of a data point. It is clear that, when localization accuracy is expressed as a per-

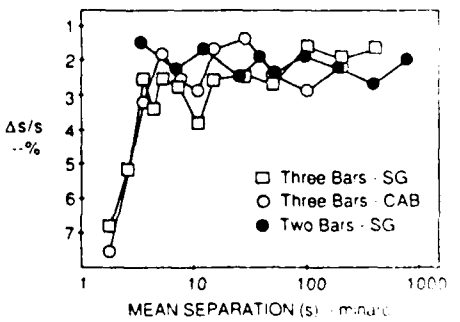

Fig 2. Localization accuracy, plotted as a function of mean separation between the objects being localized, is essentially constant once a minimum separation is exceeded.

centage of the mean separation between the objects, as it is here, it does not vary substantially with object separation, once the separation exceeds a minimum value of a few minutes of arc.

The results of these experiments verify Volkmann's finding that the threshold, Δs, is proportional to the mean separation, s, over a large range of object separations. Thus, the Weber fraction for localization, $\Delta s/s$, is essentially constant. Note that this result is not specific to either stimulus configuration (or task). The two-bar and three-bar paradigms yield the same estimates of localization accuracy, over the large range of object separations tested. Therefore, either paradigm can be used without loss of generality.

3. SPATIAL FREQUENCY EFFECTS—ENHANCING THE HIGH-SPATIAL-FREQUENCY COMPONENTS

The following experiments investigate the role of high spatial frequencies in the localization of spectrally complex stimuli that are separated by several degrees of visual angle. The channel concept implies that high frequencies play no part in this task; the position concept relies on *them for highest precision*.

It is impossible to understand the role of high-spatial-frequency components in localization without investigating the effects of contrast simultaneously, because high spatial frequencies could appear to provide poor support for localization judgments simply because of their lower effective contrasts. To separate frequency effects from contrast effects, I measured localization accuracy over a range of contrasts and examined the functions relating localization accuracy to contrast. I used "bars" with different luminance profiles, as shown in Fig. 3(a) and (b).

Methods

In the absence of prior knowledge, it seemed reasonable to adopt the common practice of using the contrast detection threshold for each stimulus as a normalization constant. This was done, and localization accuracy was measured at several fixed multiples of the contrast detection threshold. The use of several stimulus contrasts provided a check on the appropriateness of the normalization procedure, and also revealed the effects of contrast, *per se*, which will be considered later.

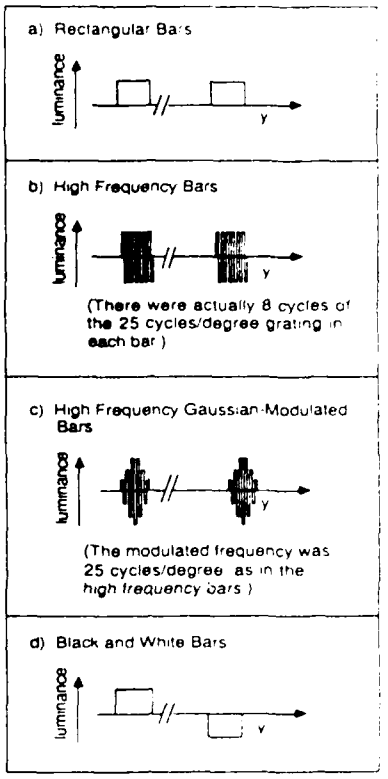

Fig. 3. Sketches of the vertical luminance profiles of the stimuli used in the experiments reported in Sections 3–6.

All stimuli were presented for 225 msec with abrupt onsets and terminations. The mean object separation was fixed at 175 min of arc, consistent with the goal of investigating large-scale localization. At the 142 cm viewing distance that was used, one line of the raster display subtended 1.20 min of arc, so the highest displayable frequency was 25 cy/deg. The stimuli were stabilized on the observer's retina by means of an SRI Dual-Purkinje-Image eye-tracker (Crane and Steele, 1978) and stimulus deflection system (Crane and Clark, 1978) to ensure that the observer maintained central fixation. This was important because of the well-known variation in contrast sensitivity with retinal eccentricity.

Contrast detection thresholds were measured by a yes–no staircase procedure. Localization accuracy was measured by the method of constant stimuli, as in the previous experiments. The two-bar paradigm was used.

The rectangular bar stimulus used in the previous experiments serves as the reference stimulus for the experiments that follow. This stimulus is spectrally complex, with most of its energy at low spatial frequencies. The Fourier

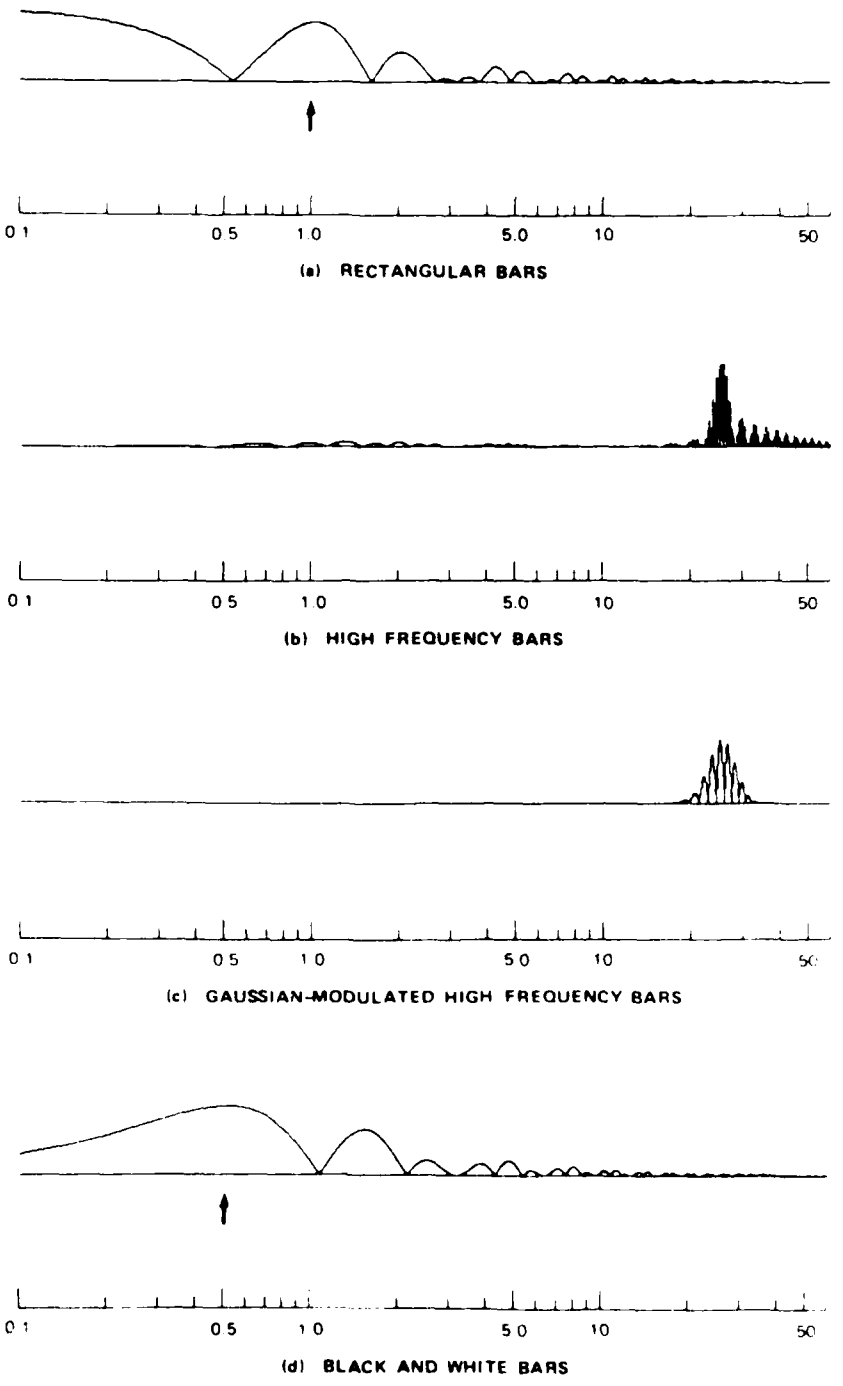

Fig. 4. Fourier transforms of the stimuli used in the experiments reported in Sections 3–6.

spectrum of the rectangular bar stimulus (before it was convolved with the line spread function of the display) is shown in Fig. 4(a). Separation between the bars was set at the mean value of 1.75 min of arc for this calculation.

To determine the role of the high-spatial-frequency components in this type of large-scale localization task, I changed to a stimulus in which most of the energy is in the high rather than the low frequency region. This stimulus, sketched in Fig. 3(b), consisted of a strip of horizontal grating of 2.5 c/deg. The vertical and horizontal extent of the grating strips matched that of the rectangular bars (as shown in Fig. 1).

The one-dimensional Fourier spectrum of this stimulus (before it was convolved with the line spread function of the display) is shown in Fig. 4(b).

It is important to note that this spectrum does not accurately reflect the impact of this stimulus on the visual system. The variation in contrast sensitivity with spatial frequency must also be factored in. Threshold for a 1 c/degree grating is approximately 1/100th that for a 25 c/deg grating, even at the fovea (Koenderink and van Doorn, 1978), whereas in the Fourier spectrum of this high-frequency-bar stimulus, the (small) peak at 1 c/deg has 1/25th the amplitude of that at 25 c/deg. Thus, from a frequency-channels perspective, it is not surprising that, at threshold, this stimulus does not appear to be a high-frequency stimulus, that is, the gratings are not resolved and the bars appear uniform in luminance. This appearance suggests that a more-sensitive, low-frequency mechanism is active at the contrast threshold. However, as the stimulus contrast is increased, the differences between the high-frequency and the rectangular-bar stimuli become significant. Even a qualitative comparison of the Fourier transforms of these two stimuli suggests that high-spatial-frequency components should become suprathreshold at much lower stimulus contrasts for the high-frequency bars than they do for the rectangular bars. Thus, if localization accuracy is enhanced by high spatial frequencies, as the position hypothesis implies, then, at high stimulus contrasts, localization accuracy for the high-frequency bars should exceed that for the rectangular bars.

Results

Graphs of localization accuracy as a function of stimulus contrast (expressed as multiples of the detection threshold) for both conditions are shown in Fig. 5. The curves have essentially the same shape, which suggests that the use of the contrast threshold as a normalizing constant was appropriate. Furthermore, the thresholds for the two conditions are essentially the same at all contrasts. The largest difference in the localization thresholds for these two conditions is at 5 times the detection thresholds. The psychometric functions underlying those data points are shown in Fig. 6.

The data of Figs 5 and 6 give no hint of the large difference in the relative amplitudes of the high- and low-frequency regions for the two stimuli that is evident in their Fourier transforms [Fig. 4(a) and (b)]. This result contradicts the prediction of the position hypothesis that enhancing the high-spatial-frequency components will improve localization accuracy (by improving the precision of the position information available from the primary representation).

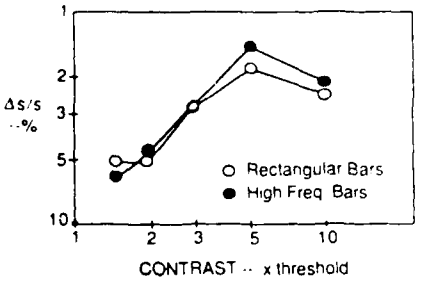

Fig. 5. Localization accuracy, $\Delta s/s$, as a function of the contrast of the bars. Contrast is expressed as multiples of the contrast detection threshold for each stimulus. Observer: SG.

4. SPATIAL FREQUENCY EFFECTS—SUBTRACTING THE LOW-SPATIAL FREQUENCY COMPONENTS

The results of the two previous experiments were consistent with the hypothesis that localization of widely separated objects is done on the basis of low-spatial-frequency information. To test this hypothesis directly, I measured localization accuracy as a function of contrast using a narrower-bandwidth, high-spatial-frequency stimulus that has no detectable energy at low spatial frequencies. The vertical luminance profile of this stimulus is sketched in Fig. 3(c) and its Fourier transform is shown in Fig. 4(c). This stimulus consists of a pair of "bars," each of which is a horizontal sinewave

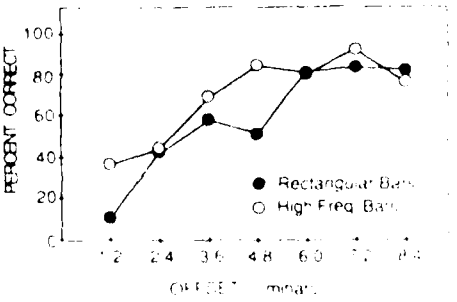

Fig. 6. Psychometric functions for localization of the rectangular bars and high-frequency (25 c/degree) bars at 5 times the contrast thresholds for the individual stimuli. Observer: SG.

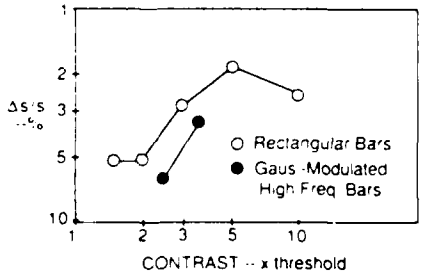

Fig. 7. Localization accuracy, $\Delta s/s$, as a function of the contrast of the bars (expressed as multiples of the detection threshold) for solid rectangular bars and for strips of 25 c/degree horizontal grating with Gaussian contrast envelopes [see Figs. 3(c) and 4(c)]. Localization accuracy for the Gaussian-modulated high frequency bars was measured at 2.3 and 3.6 times the contrast threshold.

grating of 25 c/degree whose contrast is modulated by a Gaussian function with $\sigma = 9.6$ min of arc.

The contrast detection threshold for this stimulus was more than 25% (measured at the retinal eccentricity at which it was presented in the localization experiments), so localization accuracy could not be measured at more than 3–4 times threshold. Furthermore, this narrow-band stimulus quickly caused significant pattern adaptation effects, even though the stimulus presentations were brief (225 msec). Thus, localization accuracy also could not readily be measured when the contrast was near the detection threshold. Data for the two conditions that could be measured are shown in Fig. 7. (Data from the original rectangular bar condition are also shown for comparison.)

As with the other stimuli, localization accuracy improves with increasing contrast, and, as far as can be ascertained from these limited data, it increases at the same rate. However, there is a small overall reduction in accuracy for this condition relative to the others. Detailed exploration of the cause of this difference is beyond the scope of the present paper. However, in experiments reported elsewhere (Burbeck, 1986), I explored the effects of exposure duration on localization accuracy and found that, when the stimulus is left on until the observer responds (as in the first experiments reported above), localization accuracy is essentially as high for these Gaussian-modulated, high-frequency bars as it is for the rectangular bars. Thus, it appears that activation of low-spatial-frequency mechanisms is not required for optimal localization of widely separated objects. The data also do not suggest the existence of a second localization mechanism.

5. SPATIAL FREQUENCY EFFECTS—CHANGING THE LOW-SPATIAL-FREQUENCY COMPONENTS

Since I have established (Section 2) that the Weber fraction for localization is constant with separation over a wide range, another inference can be drawn from the frequency-channel hypothesis of localization. In this hypothesis, widely separated objects are localized by channels tuned to low spatial frequencies, and the accuracy with which a given frequency can be represented scales with the frequency. Therefore, if the dominant low spatial frequency of the stimulus, f, is halved—for example, by doubling the mean separation—then the accuracy with which the frequency is represented, Δf, should also be halved. In this theory, the internal constant $\Delta f/f$ is responsible for the observed constant $\Delta s/s$. However, the dominant low spatial frequency, f, may be changed by other means as well. In particular, if the contrast polarity of one bar is reversed [Fig. 3(d)], then f is halved [arrows in Fig. 4(a) and (d)], but s is unchanged. If the frequency-channel hypothesis is correct, this change to the stimulus should double $\Delta s/s$. If the position model is correct, there will be no change in localization accuracy.

To test these predictions, I measured localization accuracy as a function of contrast for one black bar and one white bar. The results of this experiment are shown in Fig. 8, together with the previous rectangular-bar data from Fig. 5.

The effect on localization accuracy of this stimulus manipulation does not come close to the factor-of-two change in localization threshold predicted by the frequency-channel hypothesis. This result is consistent with the position hypothesis, however.

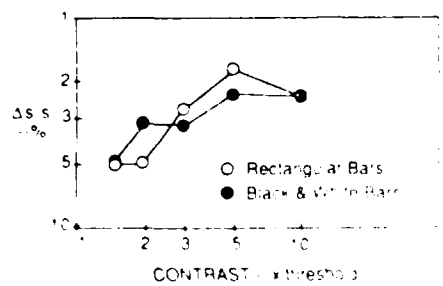

Fig. 8. Localization accuracy, $\Delta s/s$, as a function of the contrast of the bars (expressed in multiples of the detection thresholds).

6. CONTRAST EFFECTS

Although neither of the hypotheses considered here leads to specific predictions about how contrast should affect localization accuracy, it is interesting to consider what contrast effects can tell us about the localization process. Contrast effects have been reported previously in the context of hyperacuity studies, and some explanations have been suggested for them in that context. The two that I will consider here are that as contrast is increased, (1) the high-frequency mechanisms, which provide the best positional information but which have lower contrast sensitivity, become activated—the change-of-channel hypothesis (Wilson and Gelb, 1984; Carlson and Klopfenstein, 1985), and (2) the signal-to-noise ratio improves in a way predictable from contrast increment thresholds—the signal-to-noise hypothesis (Klein and Levi, 1985).

The change-of-channel hypothesis is not supported by my data on the effects of enhancing the high-spatial-frequency content of the bars: if localization accuracy for the rectangular bars improves with increasing contrast because the high-frequency components of the stimulus become suprathreshold as contrast is increased, then this improvement ought to be even more evident for the high-frequency bars. In particular, the slope of the contrast vs localization-accuracy curve should be steeper for the high-frequency bars than for the rectangular bars. It is not. Therefore, this result argues against the change-of-channel hypothesis.

On the other hand, the signal-to-noise hypothesis can account for the contrast effects reported above, and it is compatible with both the frequency-channel and the position hypotheses. In fact, the magnitude of the contrast effect obtained here is in reasonable agreement with predictions made by Klein and Levi (1985) for hyperacuity stimuli, using contrast increment detection data. However, there is a suggestion in the data (Fig. 5) of a decline in localization accuracy between 5 and 10 times the contrast threshold, which would not be consistent with a signal-to-noise hypothesis. For a more detailed picture of the effects of contrast on localization, the psychometric functions from which the data of Fig. 5 were generated are shown in Fig. 9. The improvement in localization accuracy between 2 and 5 times threshold [Fig. 9(a)] is clear and systematic. However, the slight decline in accuracy as contrast is increased further [Fig. 9(b)] is insufficient to reject the signal-to-noise hypothesis. Thus, the signal-to-noise hypothesis could reasonably account for these data.

7. DISCUSSION

Neither the frequency-channel hypothesis nor the position hypothesis, as outlined above, can account for all of the results reported here. The frequency-channel hypothesis is consistent with the constant Weber fraction for localization, and it accounts for the insensitivity of the localization mechanism to the presence of high spatial frequencies (in spectrally complex stimuli). However, the channel hypothesis is contradicted by the high localization accuracy obtainable with widely separated, narrow-band high-spatial-frequency bars, and by the insensitivity of the localization threshold to the relative polarities of the widely-separated bars. The position hypothesis, on the other hand, is contradicted by both sets of "high-frequency-bar" data, because it predicts that localization should be even more accurate for high-frequency stimuli than for stimuli that have less energy at high spatial frequencies. The position hypothesis is also contradicted by the constant Weber fraction for localization. Therefore, the problem clearly is not whether the position hypothesis or the frequency-channel hypothesis accounts for the data, but whether either hypothesis can be modified to account for the observed results.

The frequency-channel hypothesis is consistent with more of the observed results than is the position hypothesis, but modifying or adding to it seems less promising. There is no apparent way to deal with the lack of effect of bar polarity. Localization of the narrow-band high-frequency bars is also fundamentally inconsistent with his hypothesis. To account for the narrow-band, high-frequency data, one would have to postulate either that high-spatial-frequency units have very large spatial extents or that there are two equally sensitive mechanisms, one for localizing stimuli with detectable energy at low spatial frequencies and one for localizing all other stimuli. Neither of these alternatives is very attractive.

Modification of the position hypothesis seems more promising simply because it is less constrained. The subsequent stage of processing in which the distance between objects is inferred from the retinal position information can easily be modified to account for the findings reported above. For example, a plausible mechanism that

yields constant Δs / s can be obtained simply by postulating that the same type of operations that created the primary representation act analogously on that representation to yield a secondary representation. This postulated secondary representation would encode the pattern of excitation in the (retinotopic) primary representation and hence contain information about the distance between those areas of excitation. If the sampling principles that have been theorized for the primary representation (Sakitt and Barlow, 1982) also apply to the secondary representation, then large separations will be encoded with proportionately less accuracy than small separations, yielding a constant Weber fraction for localization. [A similar scheme has been suggested by Hirsch and Hylton (1982) in a somewhat different theoretical context.] This model can also account for the localization mechanism's insensitivity to the frequency content of the stimulus when localization accuracy is limited by the resolution of the secondary representation (i.e. when the objects to be localized are well-defined discrete objects, as they were in all of the experiments reported here). Highly diffuse, or near-threshold-contrast stimuli would be expected to yield quite different results.

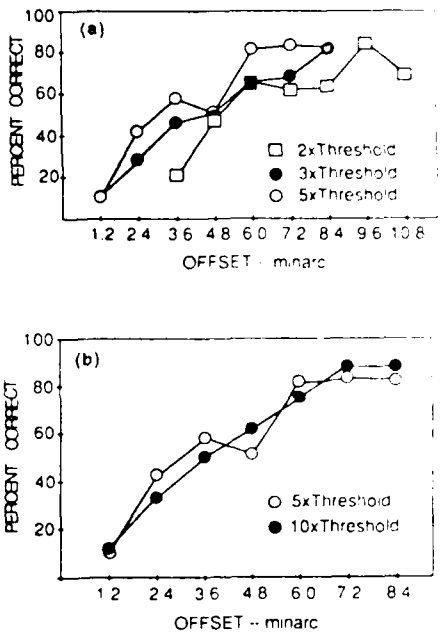

Fig. 9. Psychometric functions for the rectangular bar stimuli from which the thresholds shown in Fig. 5 were calculated. (a) Between 2 and 5 times threshold, the improvement in localization accuracy with increasing contrast is clearly systematic and statistically significant. (b) Psychometric functions for the rectangular bar stimuli at 5 and 10 times the contrast threshold.

Objects that are separated by only a few minutes of arc would also be expected often to yield different results, according to this modified position-model. With such small-scale stimuli, the local spatial-frequency response changes with the separation between the targets, even though localization, *per se*, is not done at the primary representation (i.e. frequency channels stage). Thus, with such stimuli, localization accuracy may be determined by the properties of units in the primary representation rather than by the properties of the (secondary) localization mechanism itself. Stimulus parameters such as contrast, line length, and gap width, which have a large effect in the primary representation, could reasonably be accounted for by channel models. However, Morgan and Ward (1985) have elegantly shown that, even with small-scale stimuli, careful experimental design can break the connection between local channel responses and localization accuracy. When this is done, channel models are inadequate to account for the observer's performance.

The approach taken here has been to separate the properties of the localization mechanism from those of the primary representation by separating the targets by several degrees. With such widely separated targets the local spatial frequency response is unaffected by changes in target separation. Therefore, the spatial properties that are observed are those of the localization mechanism itself. It is, of course, possible that there are two mechanisms for localization, one for small-scale and one for large-scale stimuli. However, there is some evidence against this (Smith, 1982; Burbeck, 1986) and without specific evidence for two mechanisms, a single mechanism is the more parsimonious assumption. According to the model proposed here, there is a single localization mechanism, and differences between localization of large- and small-scale stimuli are accounted for by differences in the response of the primary representation.

Alternatives to the primary representation

All of the models that were considered here rely on the assumption that, at an early stage of spatial processing, units exist that are selective to a limited range of spatial frequencies and orientations. This hypothesis could be false. An alternative, which has been considered in the context of hyperacuity studies, is the ze-

crossing model cogently described by Marr (1982). In this model, the human visual system begins its spatial analysis by determining the locations of the zero-crossings of the second derivative of the luminance distribution. Morgan *et al.* (1984) have proposed that these zero crossings are used in small-scale localization judgments. Such a scheme could be used as the initial stage in the position model just described. However, the analog relationship between the primary and secondary representations would be lost. The position model as described above with two recursive stages is more parsimonious and appears to be able to account for all of the results reported above. Quantitative development of such a model would be a major undertaking, but it may provide important insights into the mechanisms behind some basic visual abilities.

Acknowledgements—This research benefited from many interesting discussions with James R. Bergen, and the manuscript benefited from insightful comments by Thomas P. Piantanida. The research was sponsored by the Air Force Office of Scientific Research, under Contract Numbers AFOSR F49620-82-K-0024 and AFOSR F49620-85-K-0022. The United States Government is authorized to reproduce and distribute reprints for Governmental purposes notwithstanding any copyright notation thereon.

REFERENCES

Blakemore C. and Campbell F. W. (1969) On the existence of neurones in the human visual system selectively sensitive to the orientation and size of retinal images. *J. Physiol., Lond.* **203**, 237–261.

Burbeck C. (1986) Exposure-duration effects in localization judgments. *J. opt. Soc. Am. A.* In press.

Carlson C. R. and Klopfenstein R. W. (1985) Spatial-frequency model for hyperacuity. *J. opt. Soc. Am. A* **2**, 1747–1751.

Crane H. D. and Clark M. R. (1978) Three-dimensional visual stimulus deflector. *Appl. Opt.* **17**, 706–714.

Crane H. D. and Steele C. M. (1978) Accurate three-dimensional eyetracker. *Appl. Opt.* **17**, 691–705.

Ejima Y. and Takahashi T. (1984) Facilitatory and inhibitory after-effects of spatially localized grating adaptation. *Vision Res.* **24**, 979–985.

Finney D. J. (1971) *Probit Analysis*. Cambridge Univ. Press.

Hecht S., Shlaer S. and Pirenne M. H. (1942) Energy, quanta, and vision. *J. gen. Phys.* **25**, 819–840.

von Helmholtz H. (1910) *Handbuch der Physiologischen Optik*, Verlag von Leopold Voss, Hamburg und Leipzig [*Helmholtz's Treatise on Physiological Optics, Volume III* (Edited by Southall J. P. C.) Dover, New York (1962)] (1962)].

Hirsch J. and Hylton R. (1982) Limits of spatial-frequency discrimination as evidence of neural interpolation. *J. opt. Soc. Am.* **72**, 1367–1374.

Klein S. A. and Levi D. M. (1985) Hyperacuity thresholds of 1 sec: theoretical predictions and empirical validation. *J. opt. Soc. Am. A* **2**, 1170–1190.

Koenderink J. J. and van Doorn A. J. (1978) Visual detection of spatial contrast: influence of location in the visual field, target extent and illuminance level. *Biol. Cybernet.* **30**, 157–167.

Marr D. (1982) *Vision*. W. H. Freeman, San Francisco.

Marshall W. H. and Talbot S. A. (1942) Recent evidence for neural mechanisms in vision leading to a general theory of sensory acuity. *Biol. Symp.* **7**, 117–164.

Matin L. (1972) Eye movements and perceived visual direction. In *Handbook of Sensory Physiology, Vol. VII 4, Visual Psychophysics* (Edited by Jameson D. and Hurvich L. M.). Springer, Berlin.

Morgan M. J. and Ward R. M. (1985) Spatial and spatial-frequency primitives in spatial-interval discrimination. *J. opt. Soc. Am. A* **2**, 1205–1210.

Morgan M. J., Mather G., Moulden B. and Watt R. J. (1984) Intensity response nonlinearities and the theory of edge localization. *Vision Res.* **24**, 713–719.

Sakitt B. and Barlow H. B. (1982) A model for the economical encoding of the visual image in cerebral cortex. *Biol. Cybernet.* **43**, 97–108.

Smith R. A. Jr (1982) Size discrimination with low spatial frequencies. *Perception* **11**, 707–720.

Stromeyer C. F. III, Klein S., Dawson B. M. and Spillman L. (1982) Low spatial-frequency channels in human vision: adaptation and masking. *Vision Res.* **22**, 225–233.

Van Nes F. L. and Bouman M. A. (1967) Spatial modulation transfer in the human eye. *J. opt. Soc. Am.* **57**, 401–406.

Wilson H. R. (1986) Responses of spatial mechanisms can explain hyperacuity. *Vision Res.* **26**, 453–469.

Wilson H. R. and Gelb D. J. (1984) Modified line element theory for spatial-frequency and width discrimination. *J. opt. Soc. Am. A* **1**, 124–131.

Wright W. D. (1946) *Researches on Normal and Defective Colour Vision*. Henry Kimpton, London.

Appendix C

Reprinted from Journal of the Optical Society of America A, Vol. 3, page 1983, November 1986

Exposure-duration effects in localization judgments

Christina A. Burbeck

Visual Sciences Program, SRI International, Menlo Park, California 94025

Received February 18, 1986; accepted June 27, 1986

The effects on localization accuracy of increasing exposure duration beyond 100 msec are explored for a wide range of object separations. Previous reports that localization accuracy for objects separated by a few minutes of arc increases for exposures up to at least 400 msec are confirmed. I report here that localization of larger objects at larger separations does not improve when the exposure duration is increased beyond 100 msec. This difference between the small- and large-scale results can be explained by the difference in the spatial-frequency content of the objects being localized: When high-frequency objects are substituted for spectrally broadband objects in the large-scale case, the exposure-duration effects for widely separated objects become similar to those obtained in the small-scale case. These results suggest that the exposure-duration effect previously reported in hyperacuity studies is not specific to the localization task *per se* but rather is a suprathreshold version of the familiar form of spatiotemporal interaction seen in contrast-threshold results. They also suggest that a single type of mechanism underlies small- and large-scale localization.

1. INTRODUCTION

Previous studies of the effects of exposure duration on localization accuracy[1-4] have focused on the localization of objects that are separated by only a few minutes of arc, where hyperacuity thresholds are obtained. In these studies, localization accuracy was found to improve with increasing exposure duration up to 400 msec or more, leading the various investigators to conclude that the localization mechanism has a much longer integration time than does the mechanism underlying simple detection, where a critical duration of 100 msec is more typical.[2,5] The research reported here examines the effects of exposure duration on localization over a wide range of object separations and investigates the source of the exposure-duration effects obtained.

2. EXPOSURE-DURATION EFFECTS AT A RANGE OF OBJECT SEPARATIONS

A. Methods

The objects to be localized were horizontal rectangular bars, as sketched in Fig. 1. They were displayed on a video monitor [Conrac Model 2400, 19-in. (48.26-cm) diagonal, 60-Hz noninterlaced frame rate, 512 × 512 pixels] that also provided a constant background luminance of 90 cd/m^2. The luminance of the bars was 162 cd/m^2, or approximately 80% contrast, which was more than 10 times the contrast threshold for each stimulus used. [Unless indicated otherwise, contrast is defined to be $(L_{max} - L_{bkgrd})/L_{bkgrd}$, where L_{bkgrd} is the luminance of the background, which was constant.] The visual angles subtended by the two dimensions of each bar were always proportional to the distance between the bars, as if only the viewing distance were being changed. The relationship between bar size and mean separation is shown in Fig. 1.

Actually, both the viewing distance and the stimulus itself were changed to achieve the wide range of object separations. At the smallest separations, a camera lens was also used to reimage the stimulus at a smaller scale. When the lens was used, the stimulus was imaged in an aperture that was surrounded by a large uniform field that was illuminated to match the screen approximately in brightness and hue. The effects on localization accuracy of viewing distance and optical minification were checked by using different combinations of viewing distance, stimulus size, and optical minification to achieve a single object separation and bar size. No significant effects of viewing distance, *per se*, or of the lens were observed. Viewing was monocular.

To prevent the observer from using the distance to the edge of the screen as a cue, the bars were kept well away from the edge, and the position of the pair of bars relative to the edge was varied randomly from trial to trial. The adequacy of these procedures was tested in experiments in which only one bar was presented and the observer was required to guess whether the bar was a member of a pair that was farther apart or closer together than the average. When this single-bar paradigm was used, observers performed at chance level with all the stimulus configurations used in the experiments reported here.

The method of constant stimuli was used to measure localization accuracy at each of five object separations, ranging from 6.7 to 405 minutes of arc (arcmin). In a given experimental session, measurements were made at a single mean object separation. For each object separation, s, the test separations were $s + n(\delta s)$, for $n = \pm 1$ to ± 5. The increment, δs, was determined in preliminary experiments for each observer and for each value of s, so that the observer was correct about 90% of the time when $|n| = 5$. Each of the 10 stimuli was presented five times in a given session, and at least five sessions were conducted at each object separation, yielding at least 250 trials for each psychometric function. Data were collapsed across the sign of n, so that a single percent-correct value represented a given offset value (without regard to whether the test separation was that much larger or that much smaller than the reference separation). Threshold was obtained by correcting the data for guessing

0740-3232/86/111983-06$02.00

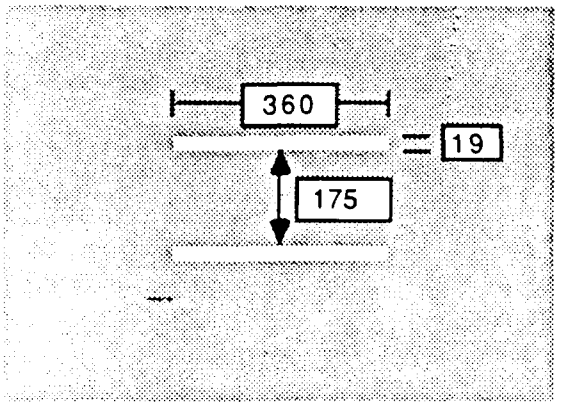

Fig. 1. Representation of the two-bar stimulus. The size of the bars was scaled with the separation between them, according to the ratio shown here.

[(percent correct − 50) × 2], converting to probits to linearize the data,[6] using linear regression to determine the best-fitting line to the transformed data, and then calculating the 50% point on the resulting line.

On each trial, a single pair of bars was presented. The observer's task was to determine whether the distance between the bars was more or less than the average object separation that he had seen during the previous trials. Right/wrong feedback was given after each trial in the form of audible tones. The experienced observers quickly learned the standard and typically performed at a stable level after 50 to 100 trials. At least one practice session of 50 trials was conducted at the beginning of each data-collection period, and two or more practice sessions (of 50 trials each) were conducted whenever the mean object separation was changed. The results of these practice sessions were not included in the calculations of localization accuracy.

Localization accuracy was measured for three stimulus durations: 102 msec, 408 msec, and observer-controlled. (For brevity, the 102- and 408-msec conditions will be referred to as the 100- and 400-msec conditions, respectively.) In the observer-controlled condition, the stimulus remained on until the observer responded with his decision. Because the observer was encouraged to be correct as often as possible, this condition presumably represents the observer's optimal performance—that is, the value of the plateau in an exposure-duration versus localization-accuracy curve. Data for the three conditions were collected in interleaved sessions for each mean separation to avoid artifacts arising from day-to-day variation in localization accuracy.

During preliminary experiments, I found a high degree of variability in the 100-msec data when large object separations were used: The observer would often not even see one or both of the briefly presented objects. (The observer's attention seemed to return to the fovea between trials, and this may have been the cause.) The problem was alleviated by presenting one bar for 306 msec before the onset of the other bar. The two bars then remained on together for the designated duration (102 or 408 msec) and were terminated simultaneously. In the observer-controlled condition, the stimuli appeared simultaneously. The 306-msec preview of one bar had no significant effect on the results obtained at small object separations, but it significantly reduced the variability of the data obtained at large object separations. The preview was used at all object separations to ensure comparability of the data.

B. Results

Data for two observers are shown in Fig. 2. Both observers in this experiment were naive to the purposes of the experiment. The findings were also confirmed with the author as an observer. With the long (i.e., observer-controlled) exposure duration, localization accuracy is essentially constant with mean separation, as has previously been reported.[7] However, with brief exposure durations, localization accuracy is substantially poorer at small separations than at large. In other words, exposure duration has little effect on localization accuracy for mean separations larger than approxi-

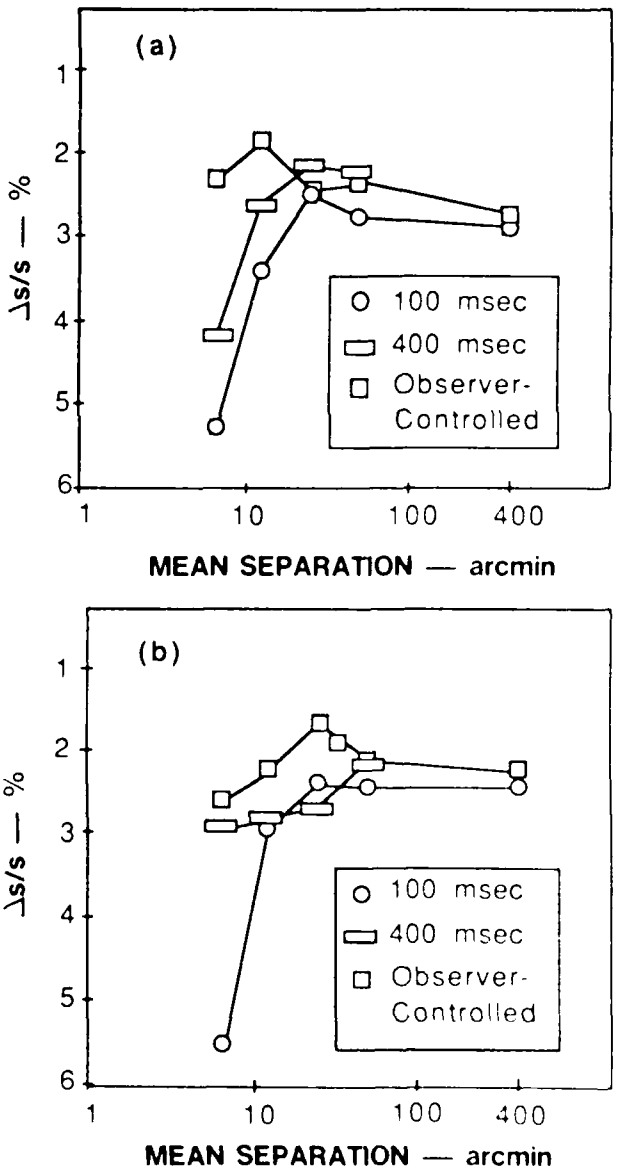

Fig. 2. Localization accuracy measured at a range of object separations using 100-msec, 400-msec, and observer-controlled exposure durations with abrupt onsets and terminations. (a) Observer SG; (b) observer AM.

mately 25 arcmin, whereas it has a profound effect at smaller separations. The data obtained at the smallest object separation, 6.7 arcmin, are consistent with several previous reports of the effects of exposure duration in other hyperacuity tasks.[1-3] The finding that exposure duration has a negligible effect at larger separations has not, to my knowledge, been reported previously. I will consider two plausible explanations for the difference in the exposure duration effects at large and small separations: differences in the effective contrasts of the stimuli used and differences in the spatial-frequency content of the stimuli.

3. CONTRAST EFFECTS

Hadani *et al.*[4] have shown that, with briefly presented hyperacuity stimuli, the effect of exposure duration on relative localization can be accurately modeled in terms of the effect of exposure duration on stimulus strength. Specifically, if contrast is decreased as exposure duration is increased, keeping stimulus energy constant, then localization accuracy is essentially constant. If the effects of contrast and exposure duration also interact when large separations are used, then the difference in exposure-duration effects at small and large separations found here (Fig. 2) might be confounded by differences in the effective contrasts of the small- and large-scale stimuli. In particular, stimuli with high effective contrasts (as in the large-separation experiments) might be less susceptible to exposure-duration effects than are stimuli with lower effective contrasts (as in the small-separation experiments).

If the lower localization accuracy for small, briefly presented stimuli arose from the lower effective contrasts of these stimuli, then equating the effective contrasts of the stimuli used at all separations should equate the localization accuracies. To test this explanation, I measured localization accuracy over a range of stimulus contrasts and separations, using a briefly presented stimulus. The effective contrasts of the stimuli were equated by normalizing the stimulus contrast by the detection threshold. The validity of this normalization procedure is supported by the data that resulted.

A. Methods

Localization accuracy was measured as a function of stimulus contrast at five mean separations ranging from 6.7 to 175 arcmin. The experimental paradigm was the same as that used above, with the size of the bars scaled to the mean separation. However, in this set of experiments, contrast was set at 1.5, 2, 3, 5, or 10 times the detection threshold for the stimulus being used. The stimuli were presented with abrupt onsets and terminations and were on for 225 msec.

Contrast-detection thresholds were measured using a yes/no staircase procedure, contrast being reduced if the observer responded yes (seen) and increased if the observer responded no (not seen). The contrast increment was 10%, and half of the trials were blank to discourage false alarms. The stimuli were presented in the same retinal locations that they occupied in the localization tasks. Threshold was obtained by taking the average of at least 10 contrast reversals. The contrast thresholds for the various separations are given in Table 1.

B. Results

Figure 3 shows results for all five mean separations. There are several points of interest in these data. First, at all object separations, localization accuracy increases with increasing contrast up to about five times the detection threshold and then reaches a plateau. Therefore the contrast used in the previous experiments, which was always more than 10 times the detection threshold, was high enough to eliminate contrast effects. Similar contrast effects were reported previously by Watt and Morgan[5] for vernier acuity tasks.

The second point of interest is that the rate of increase in sensitivity with contrast and the saturation point for this contrast effect are similar for all separations tested. The common curve shape validates the use of the detection threshold as a normalizing factor. It also suggests that there is a single type of mechanism underlying localization at all object separations in this range.

The third point of interest is that localization accuracy for this brief exposure duration increases with increasing object separation at all stimulus contrasts. It is clear from Fig. 3 that sensitivity for the smallest separation used (6.7 arcmin) is depressed relative to that for larger separations. To show more clearly that the sensitivity changes systematically across separations, the data of Fig. 3 (excluding the 6.7-

Table 1. Contrast Thresholds for Scaled Stimuli (225-msec Duration). Observer SG

Separation Condition (arcmin)	Contrast Threshold (% modulation)
6.7	6.22
10	2.31
19	3.08
54	1.77
175	1.02

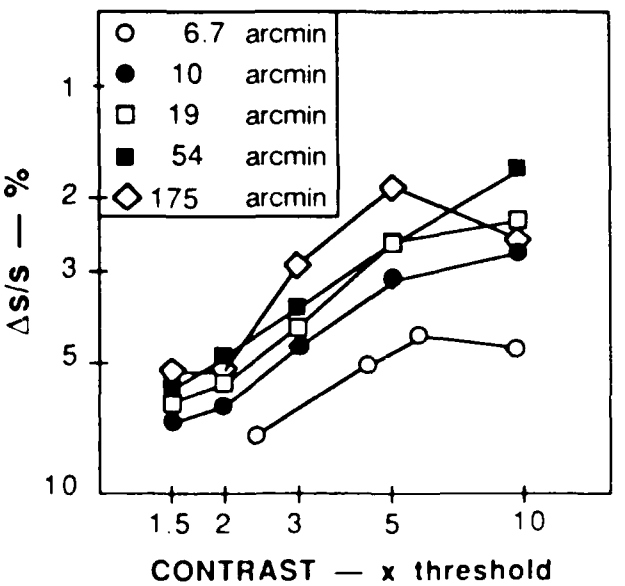

Fig. 3. Localization accuracy, $\Delta s/s$, as a function of contrast for a wide range of object separations. Observer SG.

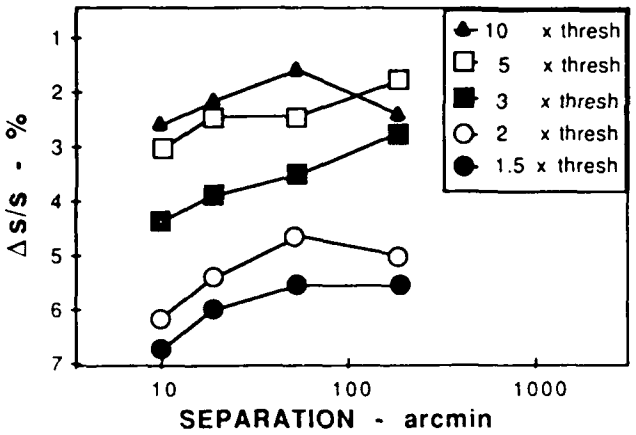

Fig. 4. Localization as a function of mean separation for five contrast levels. Data from Fig. 3. Observer SG.

arcmin condition) have been replotted in Fig. 4, where localization accuracy is shown as a function of mean separation for the various contrast levels. A linear ordinate has been used to enhance visual clarity. It can be seen from this figure that localization accuracy increases consistently up to about 50 arcmin at all stimulus contrasts.

The data of Figs. 3 and 4 show that, for a brief exposure duration, the increase in localization accuracy with increasing separation is independent of the effective contrast of the stimulus. Therefore the difference in exposure-duration effects at large and small separations is not due simply to differences in the effective contrasts of the stimuli used in the two conditions.

4. SPATIAL-FREQUENCY EFFECTS

An alternative explanation for the exposure-duration effects reported above is that they are a suprathreshold version of the spatiotemporal interaction found at the detection threshold. At threshold, information about higher spatial frequencies is integrated over a longer duration than is information about lower spatial frequencies.[9] Such spatiotemporal interaction could theoretically account for the observed results, because the Fourier transform of the small-scale stimulus has substantial energy at high spatial frequencies, whereas that of the large scale stimulus does not. These transforms are shown in Fig. 5. Qualitatively, the spatiotemporal interaction explanation is acceptable. The magnitudes of the exposure duration effects at small and large separations seen in Fig. 2 are similar to the magnitudes of the contrast threshold effects for high and low spatial frequencies, respectively.[9] A quantitative comparison cannot be made without a complete theory of how the localization mechanism uses various frequency components of the stimulus. However, experimental tests can be made of this explanation.

If suprathreshold spatiotemporal interaction at a spatial-frequency specific level of visual processing is responsible for the exposure duration effect obtained here, then changing the spatial frequency content of the stimulus should change the exposure duration effects. Specifically, a stimulus that consists of a pair of high frequency objects that are separated by more than about 25 arcmin should yield exposure duration effects that are similar to those obtained with rectangular bars that are separated by a few minutes of arc.

A. Methods

To test this explanation, localization accuracy was measured as a function of exposure duration at a large object separation (175 arcmin) using high-frequency bar stimuli. Each high-frequency bar consisted of a 25-cycle/deg grating whose contrast was modulated by a one-dimensional (vertical) Gaussian envelope with σ equal to 9.6 arcmin. The width and length of the high-frequency bars were scaled to the object separation, as in the previous experiments. The Fourier transform of this high-frequency, wide-separation stimulus is shown in Fig. 5(c).

Contrast for the high-frequency stimulus was raised to 90% to minimize contrast effects. [For this stimulus, contrast is defined to be $(L_{max} - L_{min})/(L_{max} + L_{min})$.] To determine where on the curve of contrast versus localization accuracy this value lay, detection thresholds were measured for these high-frequency stimuli in the retinal locations that they occupied in the localization experiments. The stimuli were stabilized on the observer's retina[10,11] to ensure that the appropriate retinal location was stimulated. (This precau-

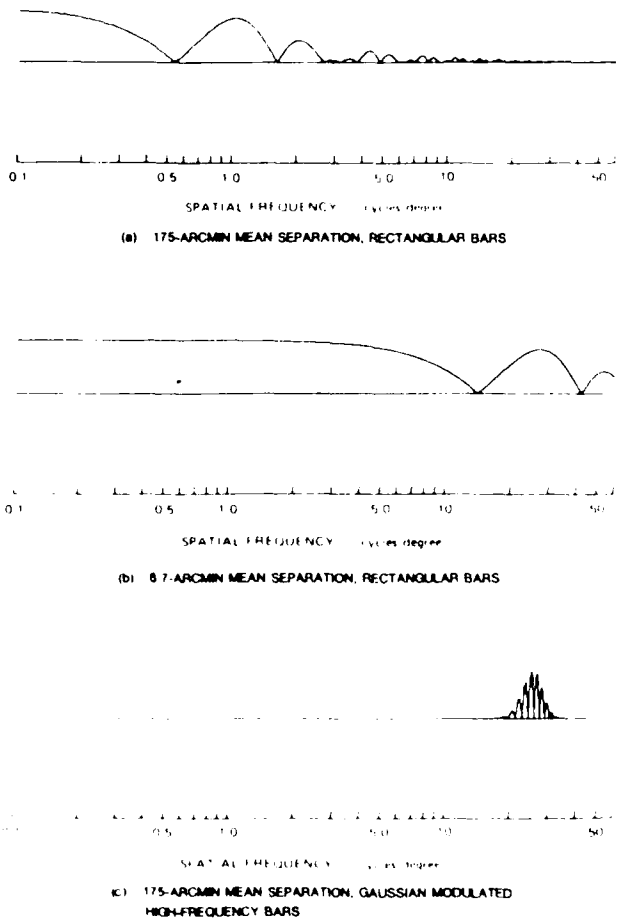

Fig. 5. One dimensional Fourier transforms of the stimuli used in the experiments on spatial frequency effects (Section 4). The transforms of these simple stimuli were determined analytically and then plotted using a standard plotting program on a Symbolics computer. One-dimensional transforms are appropriate under the assumptions that (1) the observer estimates the shortest distance between the two bars and (2) the bars extend horizontally beyond the limits of the relevant receptive fields. These assumptions were confirmed by unpublished data obtained in my laboratory showing that line length has no appreciable affect on localization accuracy.

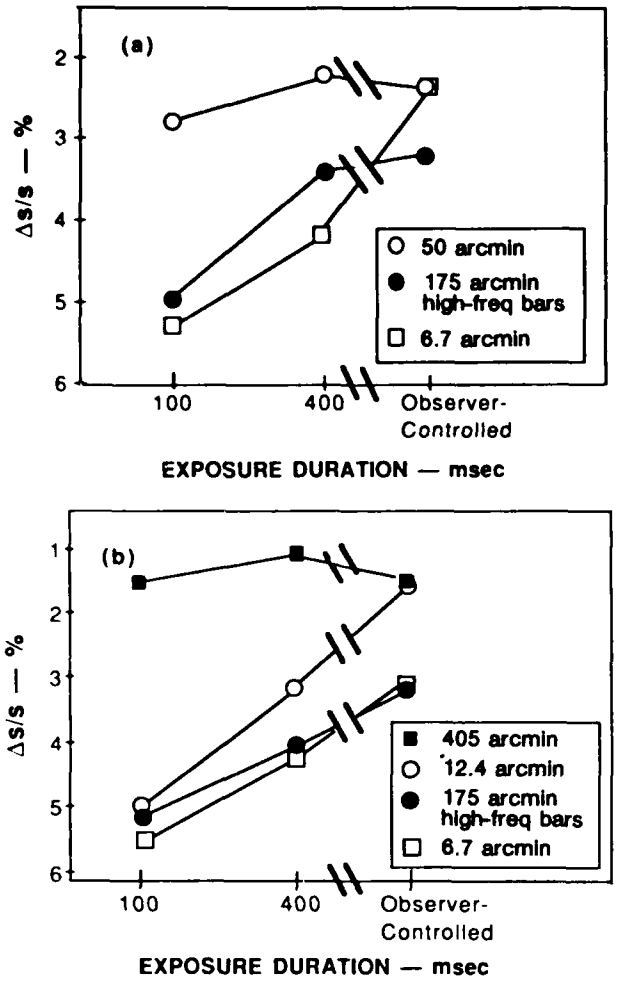

Fig. 6. Localization accuracy as a function of exposure duration for two observers. (a) Observer SG, (b) observer CAB.

tion was more critical with these higher-frequency stimuli than it was for the broadband stimuli used previously.) Detection thresholds were 26 and 22%, respectively, for observers SG and CAB. Thus the 90% contrast was 3.5 to 4 times the detection threshold for the 100-msec condition. Although this is not on the plateau of the contrast versus localization-accuracy curve (Fig. 2), the residual contrast effect is only a 15–20% change in threshold. A difference in thresholds that exceeds about 20% can therefore be attributed to exposure duration.

B. Results

Data for this 175-arcmin-separation, high-frequency bar condition are shown in Fig. 6 together with the comparable data for the 6.7- and 50-arcmin conditions from Fig. 2 for observer SG and data for the 6.7-, 12.4-, and 405-arcmin conditions for observer CAB.

Localization accuracy for the high-frequency, widely separated bars varies with exposure duration in a way that mimics the exposure-duration effects seen at small object separations and that differs substantially from the effects seen previously at large object separations. Furthermore, this effect is significantly larger than the residual contrast effect for these stimuli and hence cannot be attributed solely to a change in effective contrast with change in exposure duration. The similarity of the small-separation data and the high-frequency, large-separation data implies that the effect of exposure duration is not related primarily to the separation between the objects but rather is related to the spatial-frequency content of the objects themselves. These data suggest that it is not the localization mechanism *per se* that is continuing to acquire information at the longer durations; instead it is a mechanism (or set of mechanisms) that precedes localization and that integrates information about different spatial frequencies at different rates.

5. DISCUSSION

The earliest report of the effects of exposure duration on localization accuracy[1] was concerned with determining the role of eye movements in vernier acuity. If spatial integration played an important role in vernier acuity (the "dynamic" theory), then stabilizing the retinal image should have a larger effect at long than at small exposure durations. It did not, and the dynamic theory of vernier acuity suffered a blow, but the effect of exposure duration on localization accuracy remained as an important phenomenon to be explained.

This exposure-duration effect has usually been attributed to the fact that localization is a more complex process than simple detection; however, that attribution does not explain the phenomenon. The results reported here suggest that the effects of exposure duration on localization occur at a site of processing in which the spatial-frequency content of the individual stimuli is fundamental to their representation. An obvious candidate is the processing site that is responsible for frequency-specific pattern adaptation and masking effects as modeled by Thomas,[12] Wilson and Bergen,[13] Watson,[14] Sakitt and Barlow,[15] and others. The cause of the exposure-duration effect may simply be an improved signal-to-noise ratio in the output of this frequency-channel stage, as has been suggested by Klein and Levi[16] to account for the effect of contrast on localization. In this scheme, determination of the relative positions of objects occurs subsequent to the frequency-channel stage of visual processing. Alternatively, the exposure-duration effect might be accounted for in terms of statistical sampling, as has been done for contrast effects by Watt and Morgan.[8]

The data reported above indicate that the signal-to-noise ratio does improve with increasing exposure duration (for durations longer than about 100 msec) but only for the high spatial frequencies in the stimulus. This finding is consistent with the results of an early study by Hood[17] and supports the conclusion drawn by Morgan *et al.*[18] from their comparison of exposure-duration effects for stationary and for moving hyperacuity targets. Morgan *et al.* found no effects of exposure duration on the moving targets and replicated previous findings of a large effect with stationary targets (as also replicated here). They concluded that exposure duration affects the high-frequency components of the stimuli, which are blurred by the stimulus motion, and not the low-frequency components, which are less affected by stimulus motion.

In summary, localization accuracy appears to be a constant function of mean separation at both long and short exposure durations, provided that the spatial-frequency

content of the objects being localized is sufficiently similar. Furthermore, this relationship is independent of stimulus contrast when that contrast is expressed as a multiple of the detection threshold. Localization accuracy improves with increasing contrast in the same way for all mean separations tested, ranging from the hyperacuity region (6.7 arcmin) to large separations (405 arcmin). The results suggest that the effects of exposure duration on hyperacuity thresholds, which have been widely studied, are linked to the spatial-frequency content of the stimulus and not to the localization task *per se*. The localization process appears to be sensitive to the quality of the signal that it receives, but this process is unable to improve the quality of the information it receives by further temporal integration.

ACKNOWLEDGMENTS

This research was sponsored by the Air Force Office of Scientific Research, Air Force Systems Command, U.S. Air Force, under contracts AFOSR F49620-82-K-0024 and F49620-85-K-0022.

REFERENCES

1. U. T. Keesey, "Effects of involuntary eye movements on visual acuity," J. Opt. Soc. Am. **50,** 769–774 (1960).
2. W. S. Baron and G. Westheimer, "Visual acuity as a function of exposure duration," J. Opt. Soc. Am. **63,** 212–219 (1973).
3. J. M. Foley and C. W. Tyler, "Effect of stimulus duration on stereo and vernier displacement thresholds," Percept. Psychophys. **20,** 125–128 (1976).
4. I. Hadani, A. Z. Meiri, and M. Guri, "The effects of exposure duration and luminance on the 3-dot hyperacuity task," Vision Res. **24,** 871–874 (1984).
5. H. B. Barlow, "Temporal and spatial summation in human vision at different background intensities," J. Physiol. **141,** 337–350 (1958).
6. D. J. Finney, *Probit Analysis* (Cambridge U. Press, Cambridge, 1971).
7. H. von Helmholtz, *Handbuch der Physiologischen Optik* (Voss, Hamburg, 1910) [*Helmholtz's Treatise on Physiological Optics*, J. P. C. Southall, ed. (Dover, New York, 1962), Vol. III].
8. R. J. Watt and M. J. Morgan, "The recognition and representation of edge blur: evidence for spatial primitives in human vision," Vision Res. **23,** 1465–1477 (1983).
9. J. Nachmias, "Effect of exposure duration on visual contrast sensitivity with square-wave gratings," J. Opt. Soc. Am. **57,** 421–427 (1967).
10. H. D. Crane and M. R. Clark, "Three-dimensional visual stimulus deflector," Appl. Opt. **17,** 706–714 (1978).
11. H. D. Crane and C. M. Steele, "Accurate three-dimensional eyetracker," Appl. Opt. **17,** 691–705 (1978).
12. J. P. Thomas, "Underlying psychometric function for detecting gratings and identifying spatial frequency," J. Opt. Soc. Am. **73,** 751–758 (1983).
13. H. R. Wilson and J. R. Bergen, "A four mechanism model for spatial vision," Vision Res. **19,** 19–32 (1979).
14. A. B. Watson, "Detection and recognition of simple spatial forms," NASA Tech. Memo **84353** (National Aeronautics and Space Administration, Washington, D.C., 1983).
15. B. Sakitt and H. B. Barlow, "A model for the economical encoding of the visual image in cerebral cortex," Biol. Cybern. **43,** 97–108 (1982).
16. S. A. Klein and D. M. Levi, "Hyperacuity thresholds of 1 sec: theoretical predictions and empirical validation," J. Opt. Soc. Am. A **2,** 1170–1190 (1985).
17. D. C. Hood, "The effects of edge sharpness and exposure duration on detection threshold," Vision Res. **13,** 759–766 (1973).
18. M. J. Morgan, R. J. Watt, and S. M. McKee, "Exposure duration affects the sensitivity of vernier acuity to target motion," Vision Res. **23,** 541–546 (1983).

Appendix D

Large-Scale Localization Across Spatial Frequency Channels

submitted to Vision Research

RESEARCH NOTE

Large-Scale Localization Across Spatial Frequency Channels

CHRISTINA A. BURBECK,

Visual Sciences Program, SRI International, Menlo Park, CA 94025, U.S.A.

Abstract – Large-scale localization accuracy is measured with objects that stimulate different ranges of spatial frequencies. The author has previously made measurements using objects that stimulate only high-spatial-frequency channels or only low-spatial-frequency channels and found no effect of spatial frequency. In the present study, localization accuracy is measured with an object pair consisting of a low-spatial-frequency object and a high-spatial-frequency object. Localization accuracy for this cross-channel stimulus is as high as for the same-channel stimuli used previously, showing that the localization mechanism operates effectively across spatial frequency channels.

Large-Scale Localization Across Spatial Frequency Channels
C. A. Burbeck

In a previous study (Burbeck, 1987), I reported that over a large range of spatial frequencies, the spatial frequency content of widely separated objects does not affect localization of those objects, provided the signal strength of the objects is kept constant. This conclusion was also drawn by Toet et al. (1987) in a concurrent study. In both studies, the two objects being localized were always identical; e.g. both were Gaussian-modulated high-spatial-frequency (HSF) bars, or both were low-spatial-frequency (LSF) Gaussian bars. Those experiments left open this question: Can large-scale localization be done accurately if the objects being localized do not stimulate the same type of frequency channel? For example, if one object stimulates only HSF channels and the other only LSF channels?

To answer this question, I measured large-scale localization accuracy with an HSF/LSF stimulus pair and compared the results to localization accuracy measured with a pair of HSF stimuli and with a pair of LSF stimuli. All stimuli were horizontal bars, 5.5 deg long, with an average vertical separation of 173 arcmin. (Because of equipment limitations, all stimuli had rectangular contrast profiles in the direction orthogonal to the direction of the distance judgment.) The method of constant stimuli was used with a single separation presented on each trial. Observers judged the vertical separation between the bars, reporting whether it was greater or less than the average separation they had seen on previous trials. Auditory right/wrong feedback was given after every trial.

The HSF object was a strip of 21 c/deg horizontal grating whose contrast in the vertical direction was modulated by a Gaussian envelope (with σ = 11.4 arcmin). The LSF stimulus was a horizontal bar whose vertical luminance profile was Gaussian (σ = 11.4 arcmin). Exposure duration was 500 msec (with abrupt onset and offset) to enhance sensitivity to the HSF objects. Contrast was maintained at 90% to ensure that localization accuracy was optimal for both the HSF and LSF stimuli. All other details of the experiments were identical to those reported previously

(Burbeck, 1987).

Figure 1 shows the psychometric functions for localization under three conditions: HSF/HSF, LSF/LSF, and HSF/LSF object pairs. Data are shown for two observers, both of whom were naive. Localization accuracy is the same for the LSF pair as for the HSF pair, confirming the conclusion of the previous studies. The new finding is that localization accuracy also remains the same if an HSF/LSF pair is used.

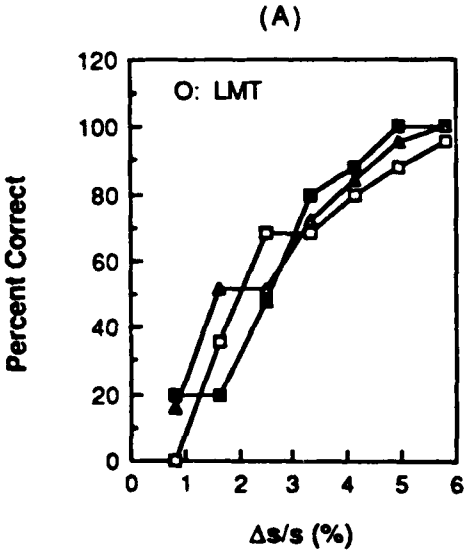

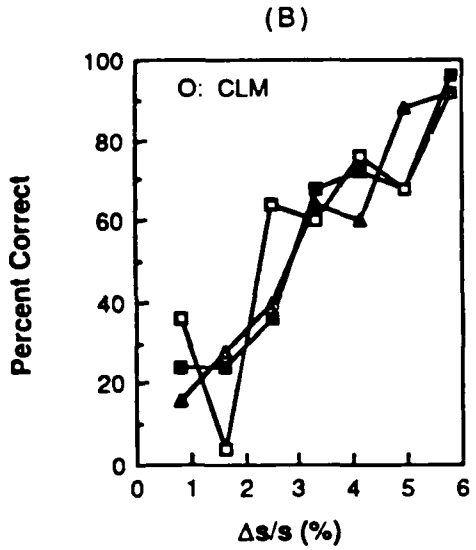

Fig. 1. Psychometric functions for localization of objects separated by an average of 173 arcmin. Objects are both low spatial frequency (triangles), both high spatial frequency (open squares,) or one is high spatial frequency and one low spatial frequency (filled squares). The data have been corrected for guessing by the formula (Original Percent Correct - 50) x 2. Data for two observers are shown.

It has been suggested that results such as these and HSF perceptual grouping phenomena (Janez, 1984; Carlson et al., 1984) can be accounted for by assuming that there is a nonlinear process that allows LSF channels to respond to HSF stimuli (Peli, 1987). The nonlinearity invoked is the one known to occur in the initial transduction of luminance. However, that nonlinearity is quite weak over the small range of luminances present in the stimuli used here (Shapley and Enroth-Cugell, 1984). Furthermore, I have shown previously that when the objects are HSF stimuli, localization accuracy increases with increasing exposure duration, whereas it does not when they are LSF stimuli (Burbeck, 1987). Thus, it is unlikely that LSF channels are responsible for localization of both types of stimuli. A much more plausible assumption is that different frequency channels are involved.

The results of previous experiments showed that the large-scale localization process can operate equally well on the responses of either LSF or HSF channels. The present result shows that it can operate as accurately across channel types as it can within a single channel type. Thus, theories of spatial vision that postulate multiple independent channels at each retinal location (Graham et al., 1978; Wilson, 1978; Wilson and Bergen, 1979, and others since), must allow the localization process to operate across, not just within, channels. More generally, the finding reported here reinforces the idea that large-scale localization is a fairly high-level process, being insensitive to those aspects of the retinal image that appear to be most important in detection tasks.

Acknowledgement

This research was sponsored by the U.S. Air Force Office of Scientific Research, Air Force Systems Command, United States Air Force, under Contract AFOSR F49620-85-0022. The United States Government is authorized to reproduce and distribute reprints for governmental purposes notwithstanding any copyright notation thereon.

REFERENCES

Burbeck C. A. (1987) Position and spatial frequency in large-scale localization judgments. *Vision Res.* **27**, 417-427.

Carlson C. R., Moeller J. R. and Anderson C. H. (1984) Visual illusions without low spatial frequencies. *Vision Res.* **24**, 1407-1413.

Graham N., Robson J. G. and Nachmias J. (1978) Grating summation in fovea and periphery. *Vision Res.* **18**, 815-825.

Jañez L. (1984) Visual grouping without low spatial frequencies. *Vision Res.* **24**, 271-274.

Peli E. (1987) Seeing the forest for the trees: The role of nonlinearity. *Suppl. to Invest. Ophth. and Vis. Science* **28**, 365.

Shapley R. and Enroth-Cugell C. (1984) Visual adaptation and retinal gain controls. In *Progress in Retinal Research*, Pergamon, New York.

Toet A., van Eekhout M. P., Simons H. L. J. J. and Koenderink J. J. (1987) Scale invariant features of differential spatial displacement discrimination. *Vision Res.* **27**, 441-452.

Wilson H. R. (1978) Quantitative characterization of two types of line-spread function near the fovea. *Vision Res.* **18**, 971-981.

Wilson H. R. and Bergen J. R. (1979) A four mechanism model for threshold spatial vision. *Vision Res.* **19**, 19-32.

Appendix E

No Orientation Selectivity in Large-Scale Localization

submitted to J. Opt. Soc. Am. A

No Orientation Selectivity in Large-Scale Localization

Christina A. Burbeck
Visual Sciences Program
SRI International, Menlo Park CA 94025

Although orientation sensitivity is clearly evident in contrast thresholds of one-dimensional gratings, I find no orientation sensitivity at the level of suprathreshold localization judgments. This conclusion is supported by three pieces of evidence: First, localization accuracy does not vary reproducibly with orientation. Second, the result still holds when the stimuli are misaligned relative to the measurement axis. To test this, one of the objects to be localized is randomly misaligned relative to the measurement axis; the observer's task is to infer the distance between the targets along the measurement axis. Observers can infer the distance along, for example, a 15° angle, as well as they can infer the vertical distance. Third, localization thresholds for misaligned stimuli are higher at all orientations than those for aligned stimuli by an amount that can be completely accounted for under the assumption that the localization mechanism is isotropic.

No Orientation Selectivity in Large-Scale Localization
C. A. Burbeck

I. Introduction

Localization -- our ability to determine the relative positions of objects -- has received increasing attention in recent years. Westheimer was one of the early active proponents of the importance of this ability,[1] and Morgan and Watt,[2] Klein and Levi,[3] and Hirsch and Hylton,[4] among others, have also made major contributions. Why is this visual ability of such interest? Historically, it has been a major subject of inquiry primarily because localization thresholds can be subcellular in size, i.e., smaller than the width of the foveal cones that are detecting the stimuli. The challange posed by this fact prompted Westheimer to coin the term hyperacuity and prompted many investigators to seek an explanation.

Extremely small thresholds, however, are obtained only when the objects to be localized are separated by a few minutes of arc.[5] Much more common in our daily experience are object separations of degrees or tens of minutes of arc, so one must ask whether the localization process that is being investigated in hyperacuity studies is also responsible for the larger-scale tasks.

If the small- and large-scale localization processes are fundamentally different,[6] then large-scale localization should be studied in its own right. If they are not fundamentally different,[7] then studies of the large-scale task may yield information about the common underlying process that is not easily accessible from studies using small-scale stimuli. The problem with small-scale stimuli is that, the properties of the localization process may be obscured by local spatial interactions at stages of visual processing distal to the site of localization, e.g. at the retina itself.[3] This confounding does not occur with large-scale stimuli, where the object separation and the local spatial characteristics of the stimulus can be manipulated independently.[8,9]

In the research reported here, I take advantage of the additional flexibility afforded by large-scale stimuli to study the orientation selectivity of the localization process with objects that are locally isotropic, i.e. the individual objects are isotropic, although together they form an oriented stimulus. If the initial stage of cortical spatial processing consists of neurons that are selectively sensitive to a limited range of orientations, as is generally believed,[10] then the use of a locally isotropic stimulus becomes especially important. If the stimulus were locally oriented, then the orientation selectivity of this initial cortical stage could affect the results, even if the localization process itself were not sensitive to orientation. Thus, using a locally isotropic stimulus allows any orientation selectivity found in the localization results to be attributed unambiguously to the localization mechanism. For this reason, in the experiments reported here, I used locally isotropic stimuli to determine whether the process underlying the localization of widely separated objects is

sensitive to the orientation of the localization axis.

II. Effect of Orientation on Localization Accuracy

Orientation selectivity has previously been found in orientation discrimination[11] and in contrast detection.[12] One indication of orientation selectivity is lower thresholds for visual tasks with vertical and horizontal than with oblique orientation of the stimuli. Following this lead, we might suppose that, if the localization process is sensitive to the orientation of the measurement axis, then localization accuracy might also vary with orientation. The following experiment tests this possibility.

Methods

Localization accuracy was measured using a pair of small squares separated by an average distance of 100 arcmin edge to edge. (Hardware limitations prevented us from using disks.) Each square was 5x5 arcmin (without taking the optical point spread function of the eye into account) and, because of its small size, had no strong apparent orientation. The large object separation made it unlikely that the two objects were detected by a common unit at distal stages of visual processing, e.g. at an oriented spatial-frequency-channels stage. Thus, we assume that the stimulus was effectively isotropic at any such stages.

The stimuli were displayed on a high-resolution monitor (Conrac 2400 C19, 512x512 pixels, 60 Hz noninterlaced). The background luminance was 78 cd/m^2 and the dots were set at 90% contrast (that is, when the entire screen was set at the luminance value of the dots, the screen measured 140 cd/m^2). The observers viewed the display through a dove prism that was rotated to achieve the various orientations used. The display surround was circular and the room was dark. Viewing was monocular.

The method of constant stimuli was used with 14 object separations ranging from 91 to 109 arcmin, unless otherwise indicated. The observer's task was to indicate on each trial whether the pair of dots was closer together or farther apart than the average separation he had seen on previous trials. Auditory right/wrong feedback was given after every trial. Practice trials were conducted prior to data collection to teach the observer the reference distance. Each stimulus was presented five times in a given session. At least five sessions were conducted in each condition for each observer, yielding 350 or more trials per calculated threshold. Thresholds were calculated by correcting the data for guessing [(percent correct-50)x2], converting to probits,[13] and then using linear regression to find the line that best fitted the transformed data. The 50% value on this line

was taken as the threshold separation, Δs. Threshold is plotted as Δs/s, in percent, where s is the average object separation.

Results

Figure 1 shows data for both observers. The error bars indicate plus and minus on standard error.[13] Sensitivity is significantly higher for one observer than for the other. The observer with the higher thresholds was experienced, whereas the other observer was quite inexperienced. Thus, the difference in thresholds was not due to practice. I have no explanation for the difference, but have found this magnitude of intersubject variability with other subjects in similar tasks.

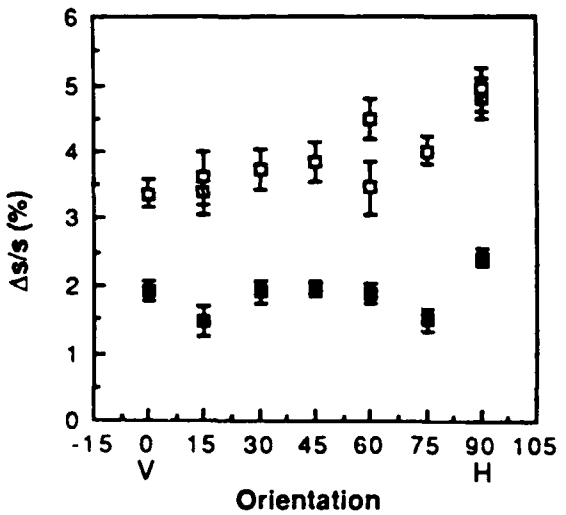

Fig. 1 Localization accuracy as a function of the orientation of the measurement axis. Open symbols, observer SG. Filled symbols, observer AM. Repeat measurements were made for observer SG. V indicates vertical measurement axis, H, horizontal.

Both observers showed some slight variation in threshold with orientation during the initial measurements. Repeat measurements were made on observer SG, and the pattern of variation was not replicated, as can be seen in Fig. 1. The psychometric functions for repeat measurements at 0°

15°, 30°, and 45° are shown in Fig. 2. (Observer AM was unavailable for further testing.) Collectively, the data suggest that there is no significant difference in localization accuracy across orientation, at least if the observer is given sufficient practice on the task. Therefore, it is reasonable to make the more parsimonious assumption of an isotropic model of localization.

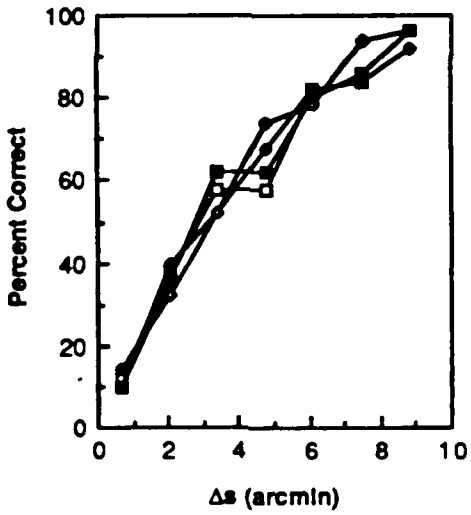

Fig. 2 Psychometric functions for localization obtained at 0° (open squares), 15° (filled diamonds), 30° (filled squares), and 45° (open diamonds). The data have been corrected for guessing. Observer SG.

III. Localization with Nonaligned Stimuli

For a further test of the hypothesis that the localization mechanism is isotropic, we devised the following experimental paradigm.

The idea was to create a task in which the localization judgment required orientation information explicitly. The stimulus configuration is shown diagramatically in Fig. 3. In the condition represented in this figure, the observer's task was to infer the vertical distance between the two dots; the horizontal position of the bottom dot was varied from trial to trial. This measurement was repeated at a range of orientations of the measurement axis. The lower dot was always displaced orthogonally to the measurement axis. (That is, the entire stimulus was rotated to each new orientation.)

There are two fundamentally different ways in which this task could be done. First, if the localization process is an oriented mechanism, e.g. a mechanism of the type postulated to account for contrast detection, then it consists of oriented subprocesses, each of which has receptive fields that are elongated in the direction orthogonal to their measurement axes. These oriented subprocesses should be essentially insensitive to variation in the position of a dot over a considerable distance in the direction orthogonal to the measurement axis. If localization of widely separated objects is done by processes with such large, oriented, receptive fields, then observers should be able to infer the projected distances nearly as well as they judge actual interobject distances.

Furthermore, if the localization mechanisms are oriented, they may be tuned to only a few orientations. If so, observers may be able to infer projected distances better along some orientations than along others. *A priori* it would seem likely that observers could infer distances projected onto the vertical or horizontal more accurately than, for example, distances projected onto an angle that is 15° to the vertical.

On the other hand, if the localization mechanism is isotropic, then the only data that it can convey is the actual distance between the objects (s, in Fig. 3). Thus, if the observer did not take into account the obvious orthogonal variation in the lower dot's position, then his responses would be determined solely by his judgment of the distance, s. This would result in a large decrease in accuracy relative to the aligned condition. His performance would be improved if he estimated the orthogonal displacement (or the orientation of the two dots) and adjusted his responses accordingly. (Quantitative details relating to this alternative are considered in Section IV.) For

now, I simply observe that if the localization mechanism is isotropic, then accuracy should be reduced by the introduction of random orthogonal displacement of one dot.

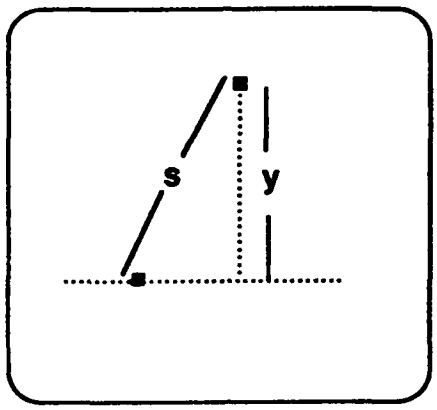

Fig. 3 Randomly misaligned stimulus. The observer's task was to determine the projected distance y between the two objects. One dot was displaced in the direction orthogonal to the direction of measurement by an amount that varied randomly from trial to trial over the range -87 and +87 arcmin from the measurement axis. The average distance between the objects projected along the measurement axis (which in this drawing is vertical) was 100 arcmin. The targets are not drawn to scale.

Methods

Localization accuracy was measured using a pair of dot stimuli as shown in Fig. 3. The equipment and experimental designs were the same as those used in the previous experiments. However, in these experiments the lower dot (the rightmost dot for a horizontal measurement axis) was displaced randomly from trial to trial in the direction orthogonal to the measurement axis by a distance in the range ±87 arcmin. The observer knew the nominal orientation of the measurement axis but he acquired a more precise estimate of it during practice trials. The observer's task was to report, on each trial, whether the projected separation along the measurement axis was greater or less than the average projected separation. This judgment had to be made in the presence of large trial-to-trial variations in the orientation of the dot separation (s, in Fig. 3). Despite the large random misalignments, observers quickly learned the task; one practice session of 70 trials was found to be sufficient to reach a stable level of performance.

Results

Data for both observers are shown in Fig. 4. Contrary to intuition, we saw no systematic variation in accuracy with orientation of the measurement axis. Although one observer shows a tendency to have higher thresholds for more horizontal orientations, this trend is not evident in the other observer. In general, thresholds are not lower at the horizontal and vertical orientations than they are at the obliques. For example, both observers can estimate a distance projected on an angle of 15° as well as they can estimate a distance projected on the vertical (0°). Thus, there is no evidence for a set of oriented mechanisms tuned to only a few orientations. Furthermore, randomly misaligning the objects results in a substantial change of the localization threshold, which was elevated by an average of 1.5x for one observer and 2.5x for the other. This, too, might suggest the absence of orientation-selective mechanisms, as argued above, but a more quantitative analysis is required to draw clear conclusions. Such an analysis is reported in Section IV.

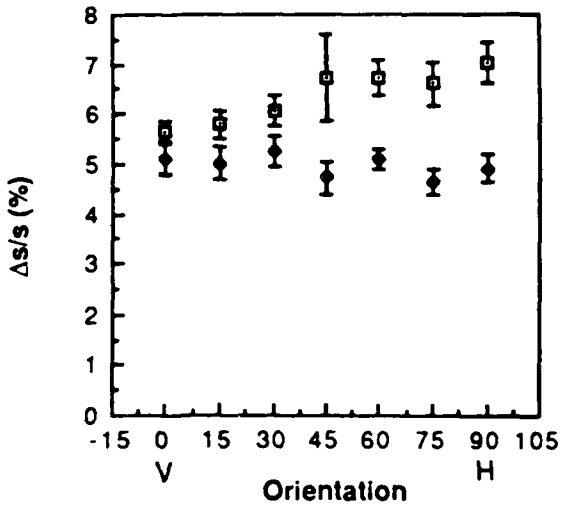

Fig. 4 Localization thresholds for two observers. Open symbols, observer SG. Filled symbols, observer AM. V indicates a vertical measurement axis and H a horizontal one.

IV. Isotropic Prediction for Misaligned Condition

A. Simple Prediction

Can an isotropic localization process account for the threshold elevation produced by randomly misaligning one of the objects? This question can be answered quantitatively with very few assumptions.

If the localization mechanism is isotropic, it can provide information only about the actual interobject distance (s, in Fig. 3). Information about the lateral position of the lower dot could be contributed via other visual mechanisms, but let us assume for the moment that it is not. The observer's performance in the misaligned condition should then be predictable from his performance on the aligned condition, because the same visual information is being used in both cases. This "simple isotropic prediction" of the misaligned-condition results can easily be calculated and then compared to the observer's actual data on this condition, as described below. This simple analysis is not sufficient, but we include it because it provides a basis for the subsequent analysis.

The first step in calculating the simple isotropic prediction is to determine what the auditory feedback would mean to the observer if he were judging s instead of y. Because the observer's nominal task was to judge the distance y, the feedback indicated he was correct if he responded "closer" when y was less than 100 arcmin and "farther" if y was >100 arcmin. However, when considered in terms of the value of s, the feedback was probabilistic. The calculation required to determine the probability that a response of "closer" was correct for each value of s is shown schematically in Fig. 5, using a vertical orientation as an example.

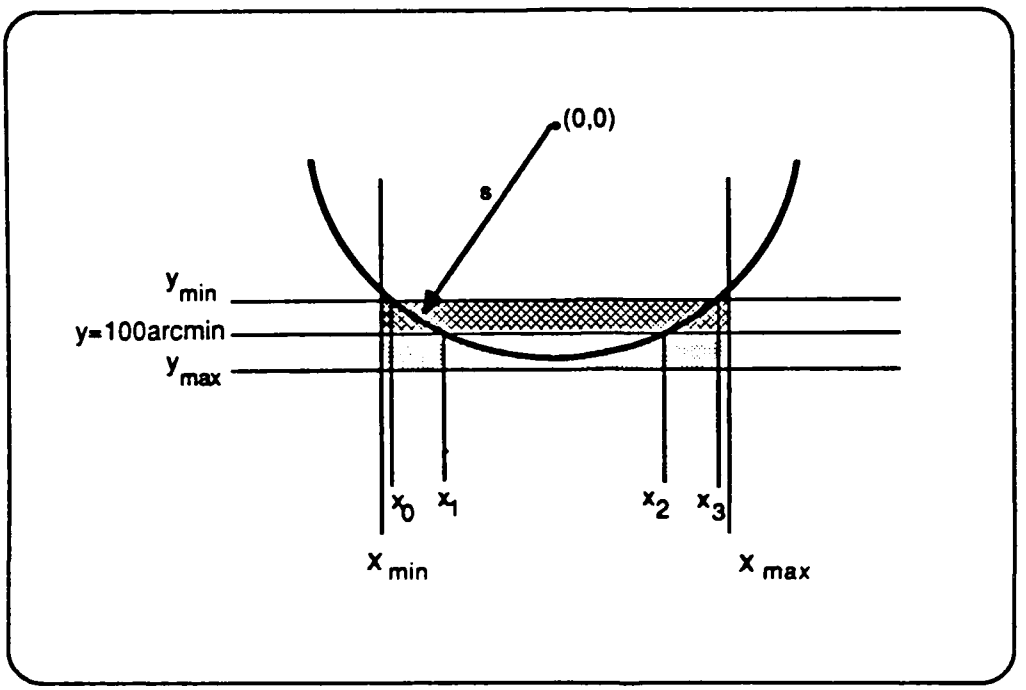

Fig. 5 Sketch of feedback calculation.

The solid bold arc in Fig. 5 represents a constant value of s. The horizontal and vertical lines labeled y_{min}, y_{max}, x_{min}, and x_{max} are limits of the range of positions that the lower dot could occupy. The ordered pair (0,0) represents the upper dot. The response "closer" was correct when the curve lay in the cross-hatched region (i.e. between x_0 and x_1 and between x_2 and x_3,) and incorrect when it lay in the dotted region (i.e. between x_1 and x_2). We calculated the percentage of the time that "closer" was the correct response by dividing the sum of the lengths of the arcs lying within the cross-hatched region by the total arc length within the stimulus range. The results of this calculation show that "closer" was more likely to be the correct response for s ≤103 arcmin, and "farther" was more likely to be correct for s >103. (Details of the calculation are given in Appendix

A.) Thus, s = 103 arcmin was the optimum crossover point if the observer made his judgments solely on the basis of s, ignoring the lateral position of the lower dot. This is the assumption used in the simple isotropic model.

The accuracy with which each observer can judge the distance s is given by the observer's psychometric function for the aligned condition. This function is independent of orientation (Fig. 1), and it scales with the average value of s over a large range.[8] Therefore, a single representative psychometric function for the aligned condition covers all orientations and a wide range of mean separations. The psychometric function that was used in these calculations to represent the aligned condition was obtained by averaging each observer's data across orientations. The calculation was simplified by using the percentage of "closer" responses instead of the standard percentage correct. (The psychometric functions shown earlier considered percent correct, independent of what the correct response was.) Linear interpolation was used to connect the data points that defined the function. The function was then translated and scaled so that its 50% value was 103 (the cross-over point for the simple isotropic model).

The hypothesis being tested is that the observer uses the value of s, not y, in making his judgment and that he completely ignores the orthogonal position of the lower dot. To determine what his responses would be in this case, we rotated the psychometric function for the aligned condition around the upper dot [by substituting $(x^2+y^2)^{1/2}$ for s]. A sketch demonstrating this revolution and its intersection with the range covered by the stimuli is shown in Fig. 6. The circles are constant values of s and hence represent constant values of percentage of "closer" responses. These curves indicate the shape of the rotated psychometric function. The cross-hatched area indicates the range of positions actually occupied by the lower dot. The simple isotropic prediction for the misaligned condition is obtained by integrating across the rotated psychometric function at fixed values of y, and dividing by the horizontal extent of the surface (x_{max}- x_{min}) to obtain the average height of the surface at each value of y. This gives the probability that the observer responded "closer" for each value of y. The details of these calculations are given in Appendix B. The results of these calculations are shown by the solid lines in Fig. 7. Also shown are each observer's data for the misaligned condition. The data curves shown are the average of the psychometric functions obtained at orientations of 0°, 15°, 30°, and 45° in the misaligned condition for each observer.

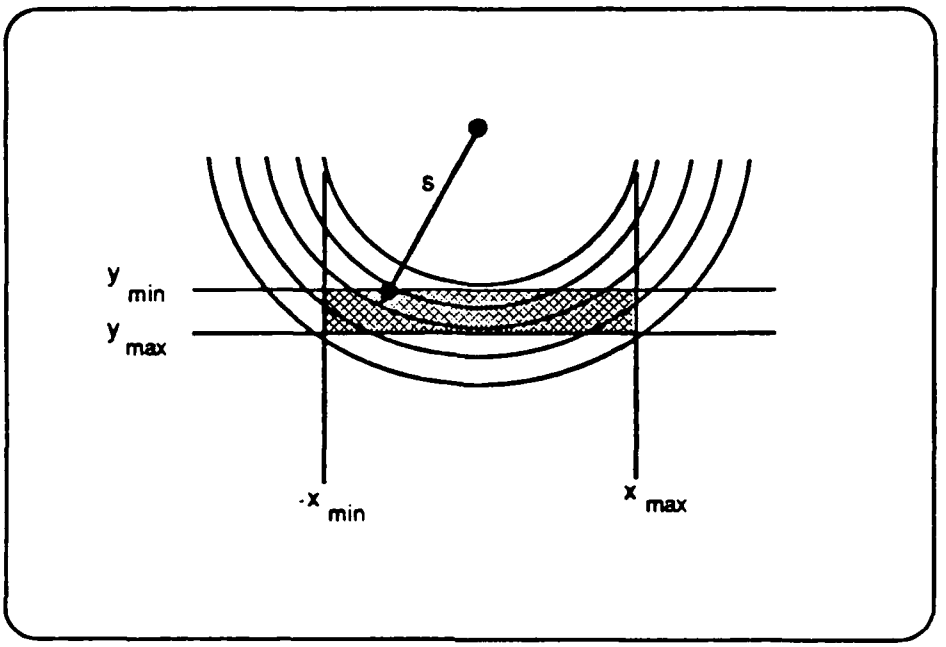

Fig. 6 Contour map suggesting the shape and location of the rotated psychometric function.

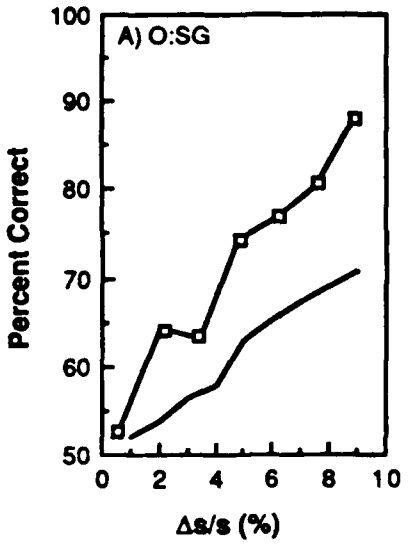

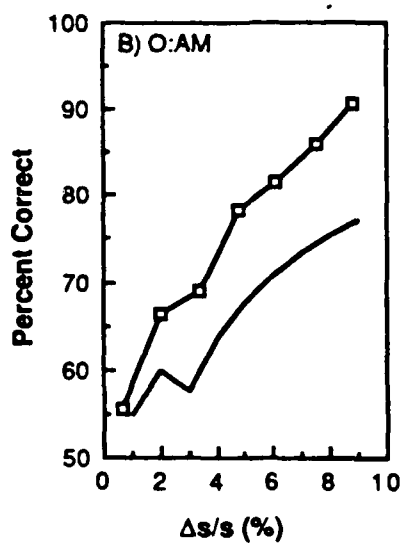

Fig. 7 Simple isotropic predictions for the misaligned condition, solid lines. Also shown for comparison, open squares, are each observer's data for the misaligned condition.

The simple isotropic prediction clearly differs from the observers' data. It predicts lower accuracy than was actually achieved. Thus, if the localization mechanism is isotropic, the observer must be making some use of his knowledge of the lateral position of the lower dot (that is, of the orientation of the stimulus axis). What is a reasonable assumption to make about the nature of that knowledge? If the observer had perfect knowledge of the orthogonal position, then his performance would equal that for the aligned condition. If he had no knowledge (as was assumed in the simple isotropic prediction), then his performance would be well below that achieved (as illustrated in Fig. 7). If he had imperfect knowledge, his performance would be somewhere between these extremes. The problem then is to estimate the accuracy of that knowledge.

B. Three-Interval Isotropic Prediction

To avoid the problem of adjusting the assumptions until they fit the data, I made a single *a priori* assumption. I assumed that the observer could accurately assign the absolute-value of the orthogonal displacement of the lower dot into one of three equal intervals. The value three was initially chosen intuitively. It was subsequently tested experimentally, as reported below. No published data were available on the accuracy with which observers can make such judgments. In particular, the judgments required here are not the same as those required in orientation discrimination or vernier acuity tasks.

With this tripartite information about the lateral position, the observer could use the feedback to determine three crossover values, one for each of the three ranges of orthogonal displacement, and hence improve his performance. The calculations for this three-interval prediction are similar to those required for the isotropic prediction. The predictions for the two observers are shown in Fig. 8, together with each observer's data for the misaligned condition.

For Observer SG, the accuracy predicted by the three-interval isotropic model is a good approximation to the data; for Observer AM, the predicted accuracy is higher than that actually achieved. Although changing the number of intervals could improve the fit for Observer AM, it would make it worse for Observer SG. Thus, the *a priori* choice of three intervals seems to have been a good one, and that choice makes the model approximately correct. However, the agreement of the isotropic prediction and the misaligned data depends heavily on the accuracy of the observer's information about the orthogonal position. Therefore, it is important to test the assumption that the observer can accurately assign the orthogonal position of the lower dot into one of three intervals (each side of center).

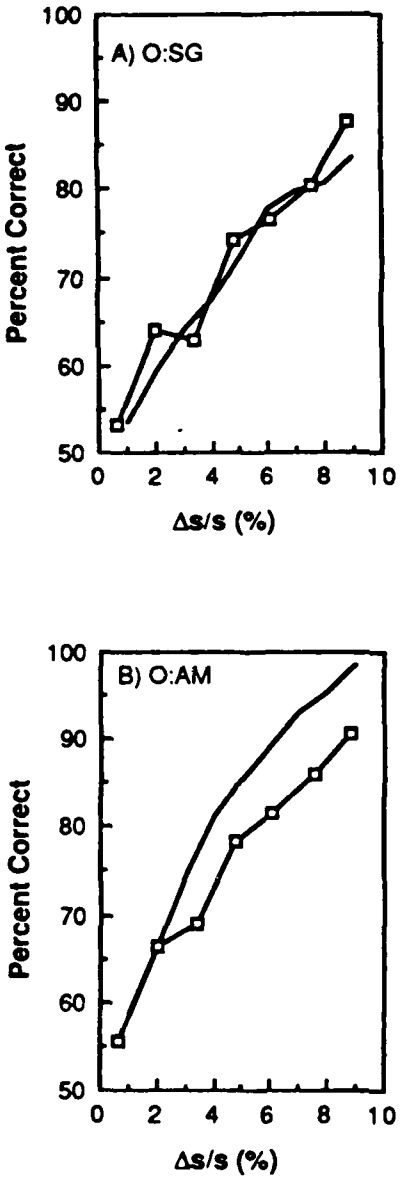

Fig. 8 Three-interval isotropic prediction for the misaligned condition, solid lines. Also shown for comparison, by the open squares, are each observer's data for the misaligned condition.

C. Test of the Three-Interval Assumption

To test the assumption underlying the three-interval isotropic prediction, the following experiment was conducted. The stimuli were the same as those used in the misaligned-dot experiment except that the separation between the two dots, y, was fixed at 100 arcmin. The orthogonal position of the lower dot was random over the same range as in the previous experiment. However, in this experiment, the lateral position of the lower dot was recorded, and the lower dot was constrained to appear in each of six equal intervals (three right and three left of center) during each block of trials. (There was no end-of-block signal to the observer, and 21 blocks were presented sequentially, so the restrictions inherent in the block design provided, at most, weak cues to the observer.) The observer's task was to assign each stimulus to one of three intervals: lower dot in the center third of the horizontal range, lower dot far to the right or left, or lower dot between those two extremes. No trial-to-trial feedback was given. The observer had one practice session (21 blocks of 6 trials each) in which he learned the range of displacements that would be presented. In subsequent sessions, 21 blocks of 6 trials were again presented; the first block was discarded, as is the custom in our laboratory. Five or more such data sessions were conducted for each observer at each of four orientations: 0°, 15°, 30°, and 45°. Figure 9 shows the percentage of correct assignments for each orientation for two observers. Both observers assigned the lower dot into one of three intervals on the basis of its orthogonal displacement with a high degree of accuracy that was independent of the orientation of the measurement axis. Therefore, the three-interval isotropic model is a plausible explanation of the data obtained with the misaligned-dots.

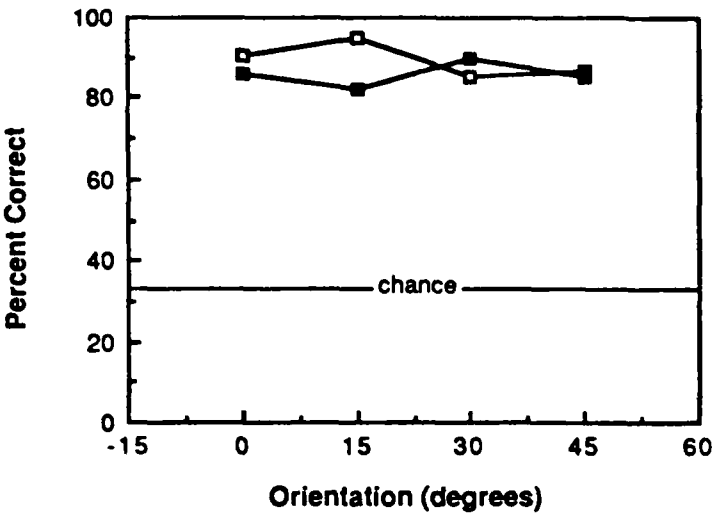

Fig. 9 Percent correct assignment of orthogonal position of lower dot to one of three intervals: center, far left or right, and intermediate left or right. Observer RLW, open squares; Observer LMT, filled squares.

V. Summary

Unlike contrast detection and orientation discrimination, large-scale localization appears to exhibit no orientation selectivity. The isotropic nature of this process was indicated in three ways:

- The lack of reproducible variation in localization thresholds with the orientation of the stimulus axis,
- The lack of variation in the localization thresholds with the orientation of the projected measurement axis for misaligned stimuli,
- The ability of a (plausible) isotropic model to account for the data obtained in a task that specifically elicited an oriented localization judgment.

We conclude that the localization process is probably not selective for orientation. This conclusion supports the idea that localization cannot, in general, be accounted for at a frequency-channels stage of processing, which is sensitive to orientation. Instead, it seems likely that localization occurs at a subsequent stage that is less sensitive to the exact details of the original retinal image.

VI. Acknowledgments

This research was sponsored by the Air Force Office of Scientific Research, Air Force Systems Command, USAF, under contract number AFOSR F49620-85-K-0022. The United States Government is authorized to reproduce and distribute reprints for Governmental purposes notwithstanding any copyright notation thereon.

REFERENCES

1. G. Westheimer, "Visual hyperacuity," Progress in Sensory Physiology, 1, Springer, Berlin (1981).

2. R. J. Watt and M. J. Morgan, "Spatial filters and the localization of luminance changes in human vision," Vision Res. 24, 1387-1397 (1984).

3. S. A. Klein and D. M. Levi, "Hyperacuity thresholds of 1 sec: theoretical predictions and empirical validation," J. Opt. Soc. Am. A 2, 1170-1190 (1985).

4. J. Hirsch and R. Hylton, "Limits of spatial frequency discrimination as evidence of neural interpolation," J. Opt. Soc. Am. 72, 1367-1374 (1982).

5. G. Westheimer and S. P. McKee, "Spatial configurations for visual hyperacuity," Vision Res. 17, 941-947 (1977).

6. S. A. Klein and D. M. Levi, "Position sense in the peripheral retina," J. Opt. Soc. Am. A 4, 1543-1553 (1987).

7. C. A. Burbeck, "Exposure-duration effects in localization judgments," J. Opt. Soc. Am. A 3, 1983-1988 (1986).

8. C. A. Burbeck, "Position and spatial frequency in large-scale localization judgments," Vision Res. 3, 417-428 (1987).

9. A. Toet, M. P. van Eekhout, H. L. J. J. Simons and J. J. Koenderink, "Scale invariant features of spatial displacement discrimination," Vision Res. 3, 441-452 (1987).

10. R. L. DeValois and K. K. DeValois, "Spatial Vision," Ann. Rev. Psychol. 31, 309-341 (1980).

11. T. Caelli, H. Brettel, I. Rentschler and R. Hilz, "Discrimination thresholds in the two-dimensional spatial frequency domain," Vision Res. 23, 129-133 (1983).

12. F. W. Campbell, J. J. Kulikowski and J. Levinson, "The effect of orientation on the visual resolution of gratings," J. Physiol. 187, 427-436 (1966).

13. D. J. Finney, Probit Analysis (Cambridge University Press, Cambridge, 1977).

Appendix A
Calculation of Probabilistic Feedback

The percentage of time that "closer" was the correct response for a given value of s is most easily calculated in terms of the angles subtended by the arcs. Figure A-1 shows the terminology used in the following calculations. For pictorial clarity the separation and the angles are not to scale.

Five conditions can obtain, as indicated by the five arcs. For arc 1, "closer" is always the correct response; for arc 5, "farther" is correct. For the rest, feedback is probabilistic. The most general case is given by arc 3.

θ_0 is one half of the full range of the arc. (Half-angles are used for computational simplicity.) θ_2 is (one half of) the section of arc that is outside of the stimulus range. Thus θ_0-θ_2 represents the range of possible stimuli at separation s. θ_1 is determined by the vertical and by the intersection of the arc with the y=100 line. Thus θ_0-θ_1 represents the range of possible stimuli for which the correct response is "closer". The probability that "closer" is correct for a given value of s is then given by

$$\frac{\theta_0 - \theta_1}{\theta_0 - \theta_2},$$

where θ_0, θ_1, and θ_2 are functions of s, as described below.

If $s \leq (y_{min}^2+x_{min}^2)^{1/2}$ (arcs 1, 2 and 3 in Fig. A-1), then θ_0 is determined by the intersection of the arc with y_{min}. Thus

$$\theta_0 = \arccos \frac{y_{min}}{s} \quad \text{for } s \leq (y_{min}^2+x_{min}^2)^{1/2}.$$

Under our conditions, $(y_{min}^2+x_{min}^2)^{1/2} = 125.6$.

If $s > (y_{min}^2+x_{min}^2)^{1/2}$ (arcs 4 and 5), then x_{min} and x_{max} determine the end points of the arc. Thus

$$\theta_o = \arcsin \frac{x_{min}}{s} \quad \text{for } s > (y_{min}^2+x_{min}^2)^{1/2}.$$

For all s,

$$\theta_1 = \arccos \frac{100}{s} .$$

However, θ_2 depends on the value of s:

$$\theta_2 = 0 \text{ for } s < y_{max}, \text{ (arcs 1 and 2)}$$

and

$$\theta_2 = \arccos \frac{y_{max}}{s} \quad \text{for } s > y_{max} \text{ (arcs 3, 4 and 5).}$$

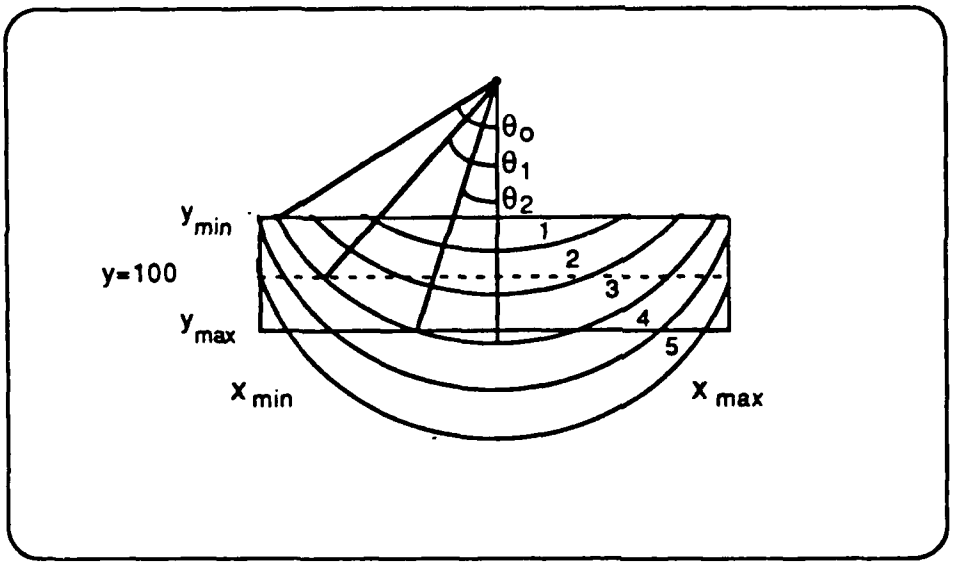

Fig. A-1 In arcmin, $y_{max} = 109$, $y_{min} = 81$, $x_{min} = -87$, $x_{max} = 87$.

Appendix B

Calculation of Simple Prediction of Percent "Closer"

Because linear interpolation was used to complete the psychometric function for the aligned condition, the rotated function was easy to integrate. For each segment of the rotated function, the integral was:

$$R_i(y) = \int_{a_i(y)}^{a_{i+1}(y)} (x^2 + y^2)^{1/2}\, dx \qquad (1)$$

where $a_i(y)$ and $a_{i+1}(y)$ are the values of x over which a given rotated line segment is to be integrated. These endpoints vary with the value of y and are calculated as follows. Let e_i, i=0,..,15 be the endpoints of the line segments that collectively constitute the psychometric function for the aligned condition. Then for each value of y, $a_i(y) = (y^2 - e_i^2)^{1/2}$.

The integral, (1), can be solved analytically. For each interval, i, the integral is:

$$R_i(y) = (m_i/2)\,\{x(x^2+y^2)^{1/2} + y^2 \log|x + (x2+y2)^{1/2}|\}\Big|_{x=a_i(y)}^{x=a_{i+1}(y)}$$

where m_i is the slope of the line segment for that interval, and y is fixed. The average percent "closer" for this segment of the integral, weighted by the length of the interval $(a_i(y), a_{i+1}(y))$, is

$$S_i(y) = R_i(y) + \text{intercept}_i * [a_{i+1}(y) - a_i(y)].$$

The average percent "closer" for a given value of y is then

$$S(y) = \sum_i 2S_i(y) / (x_{max}-x_{min}).$$

(For simplicity, the calculations were all done on the basis of one half of the symmetric rotated function, hence the factor of 2.)

S(y) was calculated for y values ranging from 89 to 109. To obtain the predicted psychometric function from these values, I converted S(y) to average percent *correct* by subtracting S(y) from 100 for y<100 and then averaging these predicted percent corrects across constant values of Δy, where $\Delta y = |100-y|$. These are the values plotted in Fig. 7.

Appendix F

Serial Stages in Spatial Processing
Evidence from Pattern Adaptation Effects

DRAFT

To be submitted to Vision Research

Serial Stages in Spatial Processing:
Evidence from Pattern Adaptation Effects

Christina A. Burbeck

Visual Sciences Program

SRI International

Menlo Park, California 94025

Serial Stages in Spatial Processing: Evidence from Pattern Adaptation Effects
C. A. Burbeck

Abstract – Several effects of pattern adaptation are examined and compared in this study of the relationship between a spatial frequency channels representation and higher levels of spatial processing. Specifically, we conducted experiments to determine whether the various pattern adaptation effects are tied to the retinal spatial frequencies of gratings or to their object spatial frequencies. The results of these experiments (1) verify a previous finding that contrast-threshold elevation is tied to the retinal, not object, spatial frequency of the adapting and test gratings (Blakemore, *et al.*, 1972), (2) fail to replicate the finding (Regan and Beverley, 1983) that frequency-discrimination thresholds are elevated by pattern adaptation, and (3) show that the perceived spatial frequency shift (PSFS) is also tied to retinal spatial frequencies, despite evidence that contrast-threshold elevation and the PSFS occur at different sites (Klein, *et al.*, 1974). The PSFS implies that frequency discrimination thresholds should be altered by pattern adaptation, but not in the way reported in the literature. The magnitude of this implied threshold change is calculated and compared to the experimental findings. Collectively the results support the idea that a spatial frequency channels for analogous stage of processing as revealed in classical pattern adaption effects, is fundamental to higher levels of spatial representation.

Keywords: Pattern adaptation, spatial frequency discrimination, contrast detection, perceived spatial frequency shift.

Serial Stages in Spatial Processing: Evidence from Pattern Adaptation Effects
C. A. Burbeck

INTRODUCTION

Recent research in spatial vision has been dominated by the idea that the early stages of spatial vision can be accurately modeled as a set of filters that are selectively sensitive to a limited range of spatial frequencies (DeValois and DeValois, 1980; Kelly and Burbeck, 1984). Although the original spatial frequency channels concept has been modified to reflect the spatially localized nature of early spatial processing (refs), the basic concept of multiple spatial-frequency-selective mechanisms remains a dominant theme. With this basic theoretical foundation, two major research questions at this time are:

- Which perceptual phenomena can be accounted for by a spatial frequency channels approach, and which require that we postulate subsequent or alternative types of spatial processing?

- What is the relationship between the spatial frequency channels representation (assuming one exists) and these other spatial processes? In particular, is there evidence for a serial relationship, as suggested by the idea that channels model the processing that occurs in layer V4 of visual cortex, or is parallel processing suggested?

In the research reported here, we examine the relationships between the detectability and the discriminability of spatial frequency gratings. We use pattern adaptation effects as probes, seeking to determine 1) the sites of the various pattern adaptation effects and 2) the relationship between those pattern adaptation effects and the perceived spatial frequency and discriminability of gratings.

For many years now spatial frequency discrimination has been modeled using a spatial frequency channels approach: Thomas and his colleagues model the ability in terms of a metric on

the space of spatial frequency channel responses, and Regan and Beverley postulate that the ratios of frequency channel responses is the relevant quantity. Thomas' model is based on a comparison of the detectability and discriminability of gratings, whereas Regan's theory is based on the results of his study of the effects of pattern adaptation on spatial frequency discrimination thresholds. Both theories assume that detection and frequency discrimination are based on a common neural representation.

However, evidence against that assumption is mounting. The first argument against this assumption that I have seen was in a paper by Klein *et al.* in 1974. They found that the perceived spatial frequency shift (PSFS) has the same properties whether it results from prior exposure to an adapting grating or from simultaneous exposure to a surrounding "adapting" grating, whereas the contrast-threshold elevation effect occurs only after prior exposure to an adapting grating. A surrounding "adapting" grating has no effect on the detection threshold. These results raise the possibility not only that detection and discrimination are dissociated as Klein *et al.* concluded, but also that there are two sites of pattern adaptation, one that affects contrast thresholds and one that affects perceived spatial frequency.

The idea that detection and discrimination are based on different representations is also supported by a recent study by Gorea (1987). He studied the effects of backward masking on identification and detection of sinewave gratings and found that the ratio of detection to identification is a U-shaped function of SOA (stimulus-onset-asynchrony). He argued from this that detection and discrimination are serial processes.

I have also suggested that there is a serial relationship between these two processes (Burbeck, 1987). Specifically, I found that frequency discrimination is not done on the basis of retinal spatial frequencies at all, but instead is done on the basis of a higher level representation in

which information about the distances to the gratings is included to achieve estimates of the actual properties of the objects (Burbeck, 1987). In short, observers compare the perceived spatial frequencies and not the retinal spatial frequencies of the gratings. Contrast detection thresholds, on the other hand, appear to be determined solely by the retinal spatial frequencies of the gratings, independently of their perceived spatial frequencies. For brevity, I will refer to the stage in which perceived spatial frequencies are represented as the "object spatial frequency representation", but this name does not imply any assumptions about the manner in which information about object properties is stored. The name was chosen to parallel the term spatial frequency channels representation, that is used to describe the more distal stages of processing in which local retinal spatial frequencies are represented.

In the present study, I use pattern adaption paradigms to pursue the question of the seriality of a retinal spatial frequency channels representation, which can account for some detection thresholds, and an object spatial frequency representation, which is required to account for discrimination thresholds. If the effects of pattern adaptation on perceived frequency occur at a retinal spatial frequency channels (or analogous) stage then the seriality of the two stages is supported. On the other hand, if the effects of pattern adaptation on perceived frequency are tied to the object spatial frequencies, i.e. to the site of discrimination, then the seriality of these two stages is neither supported nor rejected. In the experiments described below, we determine the sites of several pattern adaptation effects to see if they occur at the retinal spatial frequency channels stage or at the more proximal stage in which object spatial frequencies are estimated.

The research by Klein *et al.* (1974) suggests that the PSFS might occur at a stage that is proximal to the frequency channels stage, and that idea is lent credence by the fact that perceived spatial frequencies are estimates of object, not retinal, spatial frequencies. Also providing indirect support for the idea that some pattern adaptation effects might occur in an object-spatial-frequency

representation are Regan and Beverley's data on the effects of pattern adaptation on frequency discrimination. They found that frequency discrimination thresholds are most elevated when the test frequency is 2.5 times the adapting frequency. This is significant because the diameter of their adapting stimulus was 2.5 times that of their test stimuli. Thus, the maximum effect occurred when the number of cycles in the test and adapting stimuli was the same. In their experiment, observers viewed the stimuli monocularly in a dark room, so they might well have perceived the adapting stimulus as having the same physical (object) diameter as the test stimulus, only seen at a shorter viewing distance. If this percept were dominant, then the maximum effect occurred when the perceived spatial frequencies of the adapting and test gratings were equal. Thus, there are some suggestions in the literature that pattern adaptation effects do not all occur in a common retinal-spatial-frequency-based representation of the stimulus.

To test this intriguing possibility, and to investigate further the relationship between the postulated retinal spatial fequency representation and object spatial frequency representation, we conducted several experiments in which we manipulated the perceived spatial frequencies and the retinal spatial frequencies of the gratings independently. If two gratings are presented at a single viewing distance, as is normally used, then the relationship between their perceived spatial frequencies is the same as that between their retinal spatial frequencies. However, if the gratings are presented at different viewing distances and depth information is available to the observer, that connection is broken. We can then determine whether the pattern adaptation effect is occurring at a stage of processing in which the retinal spatial frequencies are represented, or at a stage of processing in which the object spatial frequencies are represented, e.g., at the site of spatial frequency discrimination. This is the basis of the experiments described below.

CONTRAST-THRESHOLD ELEVATION

This experiment lays some groundwork by confirming that the contrast-threshold-elevation pattern-adaptation effect is maximum when the retinal spatial frequency of the test grating matches that of the adapting grating, not when their perceived spatial frequencies match. It replicates an experiment performed by Blakemore *et al.* in 1972. Observers adapted to a high-contrast grating that was presented either at the same viewing distance as the test stimuli, or at a closer viewing distance. The retinal spatial frequency of the adapting grating was fixed. However, it appeared to have a much higher spatial frequency when it was closer to the observer than when it was farther away. This is because the object frequency (cycles/cm in the stimulus plane) is higher when it is closer, and the perceived frequency estimates the object frequency, consistent with size constancy. If the contrast-threshold elevation effect is tied to the perceived spatial frequencies, it should peak at different retinal spatial frequencies for the two conditions.

Methods

The stimuli were displayed on CRT monitors (Conrac C2400, 512x512, 60 Hz, noninterlaced), with mean luminance of 78 cd/m^2. The room was dimly lit (approximately 3 cd/m^2), and viewing was binocular to facilitate acquisition of depth information. A headrest was used to keep the viewing distance constant. The stimuli were all horizontal sine wave gratings. The adapting grating had a contrast of 80% and was flickered in counterphase at 2 Hz to prevent the formation of negative afterimages (Burbeck, 1986). The initial adaptation period was 1 min and the intertrial adaptation periods were 15 sec. The adapting grating was presented on one monitor, the

test gratings on another. The two monitors were placed so that the observer perceived them as juxtaposed. The observer simply shifted his gaze between them at the beginning and end of each test interval.

There were two experimental conditions in these contrast detection experiments. In the *equidistant* condition, the test and adapting gratings were both presented 3 meters from the observer. In the *nonequidistant* condition, the test and adapting gratings were presented at different distances: the adapting grating was at 1 meter, and the test was at 3 meters. At 1 m, the gratings subtended 21x15 deg; at 3 m, they subtended 7.8x5.5 deg. The retinal spatial frequency of the adapting grating was 4 c/deg in both the equidistant condition and the nonequidistant condition. However, the perceived spatial frequencies of the adapting gratings in the two conditions differed by approximately a factor of three, because their viewing distances differed by a factor of three.

The spatial frequency of the test grating was varied to determine the spatial frequency at which the peak adaptation effect occurred. The test grating was presented for 500 msec with an abrupt onset and termination. Detection thresholds were measured by a yes/no staircase procedure (increment factor 1.1), with two interleaved staircases (Cornsweet, 1962). At least ten contrast reversals were used to estimate each threshold. In the sessions without adaptation, the same procedures were used, but the adapting stimulus was a uniform field of the same mean luminance as the other stimuli. Contrast-threshold elevation ratios were calculated by dividing the contrast threshold obtained after adaptation to the grating by the contrast threshold obtained after adaptation to the uniform field.

Results

Figure 1 shows the contrast-threshold-elevation ratios for the equidistant condition (open

symbols), and for the nonequidistant condition (filled symbols), plotted as a function of the retinal spatial frequency of the test grating. The solid arrows show the retinal spatial frequency of the adapting grating. The shaded arrows show the spatial frequency at which the test and adapting gratings have the same perceived spatial frequency in the nonequidistant condition.

The contrast threshold is elevated at 4 c/deg regardless of the relationship between the perceived frequencies of the test and adapting gratings. If this pattern adaptation effect were tied to the perceived spatial frequencies of the stimuli, then presenting the adapting grating at 1 meter instead of 3 meters should have shifted the peak effect to approximately 1.3 c/deg, where the perceived spatial frequencies of the test and adapting gratings match. However, in agreement with the previous finding of Blakemore *et al.* (1972), we find that threshold is elevated most when the retinal spatial frequencies of the adapting and test gratings are equal, independent of any differences in their perceived spatial frequencies. Thus, the contrast-threshold elevation effect occurs at a stage of processing in which retinal spatial frequencies are represented.

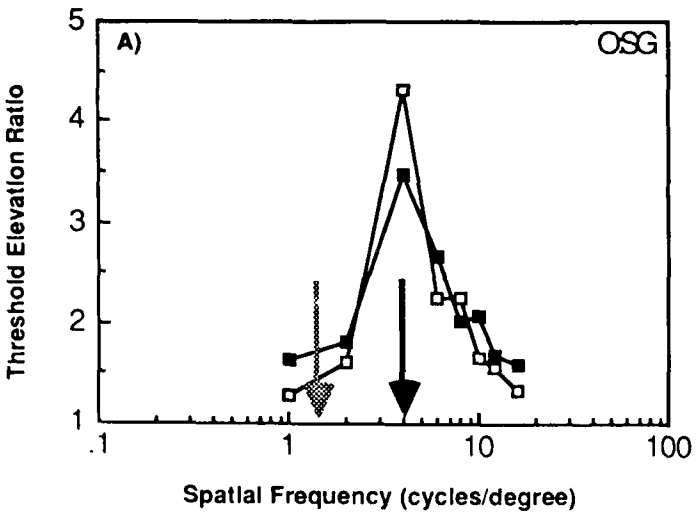

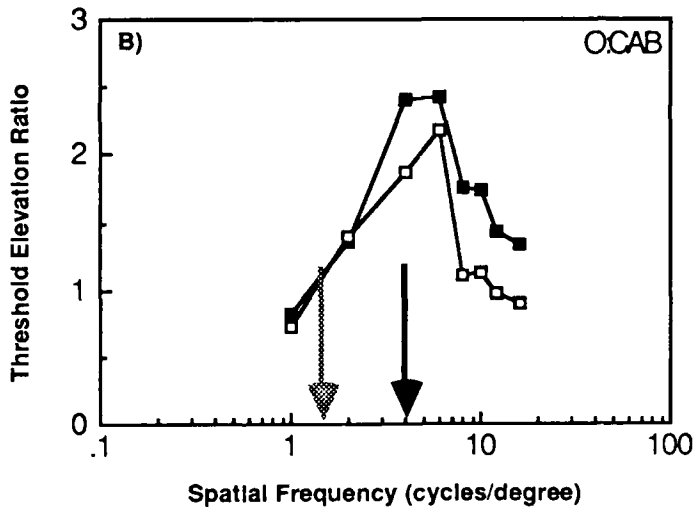

Figure 1. Threshold elevation ratios for detecting a grating at 3 meters following adaptation to a high-contrast grating of 4 c/deg. Adapting grating at 1 meter (filled squares) or at 3 meters (open squares). The solid arrows indicate the retinal spatial frequency of the adapting grating. The shaded arrows show the spatial frequency of the test grating at which the perceived frequencies of the test and adapting gratings in the nonequidistant condition match. Two observers.

FREQUENCY-DISCRIMINATION-THRESHOLD ELEVATION

As noted in the Introduction, the findings of Regan and Beverley (1983), Klein *et al.* (1974), and Burbeck (1987) combine to suggest that one form of grating adaptation might occur at a stage of processing in which perceived spatial frequency is represented. Pursuing this possibility, we attempted to replicate Regan and Beverley's finding that pattern adaptation elevates frequency-discrimination thresholds, with the peak effect occurring at 2.5 times the adapting frequency. The original goal of this experiment was to determine whether the frequency-discrimination adaptation result was tied to the retinal or to the perceived spatial frequencies of the test and adapting gratings. However, repeated attempts to replicate their findings failed.

Methods

Several conditions were tried; the results were the same in each. Data from two conditions are shown. The data shown in Fig. 2 were collected under the following conditions.

Figure 2 conditions:

Observers viewed the stimuli monocularly at a distance of 1 meter in an otherwise dark room. The test and adapting stimuli appeared sequentially at the same location so that no saccade was required between the adapting and test intervals. (A beam splitter and two computer-controlled shutters were used to superimpose the positions of the test and adapting stimuli.) Test stimulus diameter was 13.3 deg, and adapting stimulus diameter was 5.3 deg (larger than Regan and Beverley's stimuli, but with the same 2.5:1 ratio of adapting to test diameter). All stimuli were horizontal sine-wave gratings, as in the previous experiment. The mean luminance of the test was 17 cd/m^2, and of the adapting stimulus, 78 cd/m^2. (The test and adapting luminances were chosen to replicate Regan and Beverley's conditions.) Adapting contrast was 80%. The test contrast was random in the range 40-60% to prevent perceived contrast, which varies with spatial frequency, from being used as a cue to frequency. The phases of the test gratings were varied randomly in the range 0 to 180 deg relative to the edge of the display.

The adapting stimuli were counterphase-flickered at 2 Hz. The initial adapting duration was 3 min. The intertrial adaptation interval was 25 sec. At the end of each adapting interval, the observer initiated the test interval by pressing a button. The test gratings, which were not flickered, were each presented for 250 msec with abrupt onsets and terminations. The time between presentations of the two test gratings in a trial was 1.2 sec. The observer's task was to indicate which grating had the higher spatial frequency. Auditory right/wrong feedback was given after

each trial. After the observer's response, the adapting grating would reappear. In the control runs, the conditions were identical except that the adapting stimulus was uniform.

The method of constant stimuli was used, and at least 210 trials contributed to each psychometric function. The frequencies of the test gratings presented on a given trial differed by 1% to 7%. The average test frequency was 5.9 c/deg. The relationship between the test and adapting frequencies was varied by changing the adapting frequency. The adapting frequencies were: 5.9 c/deg (test=adapt), 2.9 c/deg (test=2x adapt), 2.35 c/deg (test=2.5x adapt), and 1.9 c/deg (test=3x adapt). The data for the unadapted, the test=adapt, and the test=2.5x adapt conditions were collected in interleaved sessions, with an unadapted session before each adapted session. Data for the other conditions were collected later under slightly different conditions, as described below.

Figure 3 conditions:

The data in Fig. 3 were collected under conditions that are similar to those used for the data in Fig. 2, with some slight modifications to replicate Regan and Beverley's conditions more exactly. The viewing distance was 145 cm; the test screen was 3.5 deg in diameter and the adapting screen was 9 deg in diameter. The contrast of the adapting grating was 100%. The gratings were counterphase flickered at 1.5 Hz. Initial adaptation was 5 min with subsequent intertrial adapting intervals of 10 sec. Test gratings were presented with the same temporal envelope as that used by Regan and Beverley (1983, see their Fig. 1). All of these changes were made to make our conditions more like theirs. Two adapting frequencies were tested under these conditions: test = 2x adapt, and test = 3x adapt.

Results

Typical pre- and postadaptation psychometric functions for frequency discrimination obtained under our initial conditions are shown in Fig. 2. There is no evidence of elevation in either of the conditions. If anything, the frequency discrimination threshold is lower following adaptation – i.e. the psychometric function is higher. Figure 3 shows data obtained with the modifications described above that made our conditions as similar to those of Regan and Beverley as we could achieve. These data also show that adaptation does not elevate frequency discrimination thresholds at frequencies 2 to 3 times the test frequency for this naive observer. Two other observers were also tested in the test = 2.5x adapt condition, and no threshold-elevation effects were found.

A) Test Frequency = Adapting Frequency

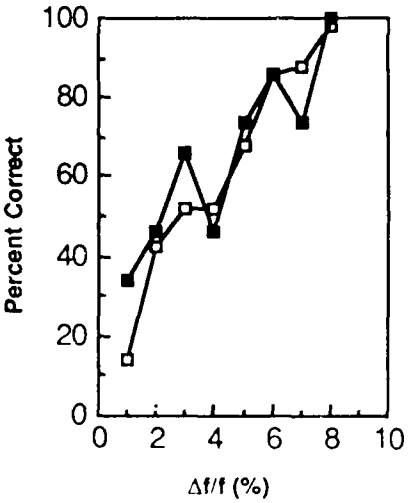

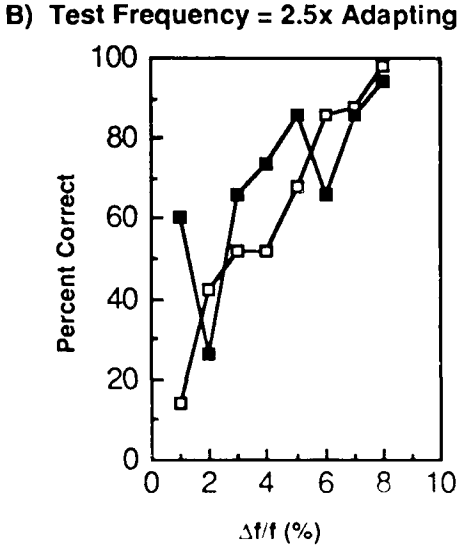

Figure 2. Psychometric functions for frequency discrimination at 5.9 c/deg, measured after adaptation to a uniform field (open squares) and after adaptation to a flickering grating (filled squares). (A) Adapting frequency, 5.9 c/deg. (B) Adapting frequency, 2.35 c/deg.

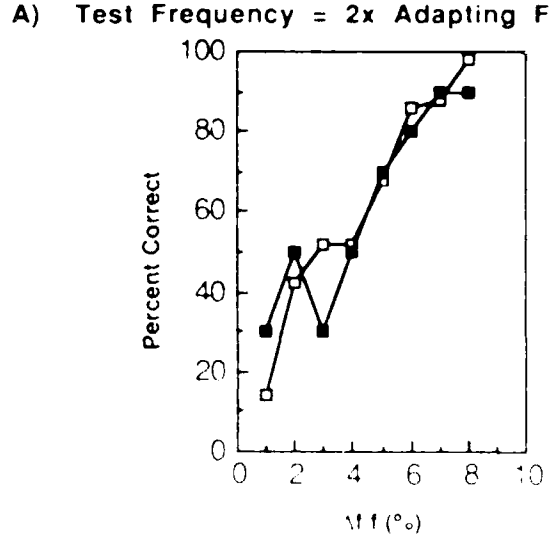

AD-A187 668 SPATIOTEMPORAL CHARACTERISTICS OF VISUAL LOCALIZATION PHASE 2(U) SRI INTERNATIONAL MENLO PARK CA SENSORY SCIENCES RESEARCH LAB C A BURBECK 30 SEP 87 2/2

UNCLASSIFIED AFOSR-TR-87-1637 F49620-85-K-0022 F/G 6/4 NL

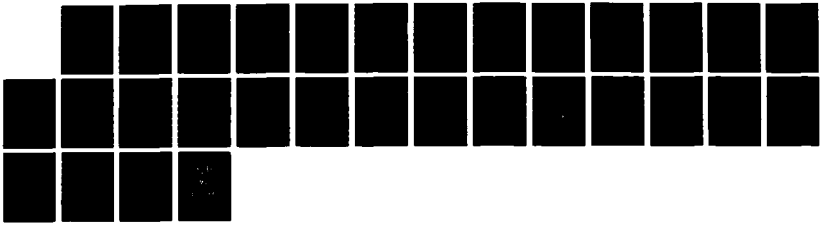

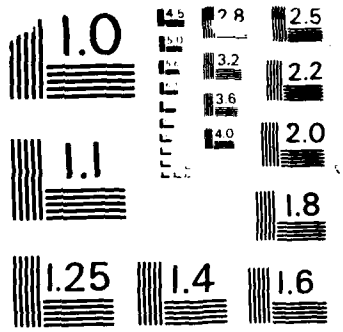

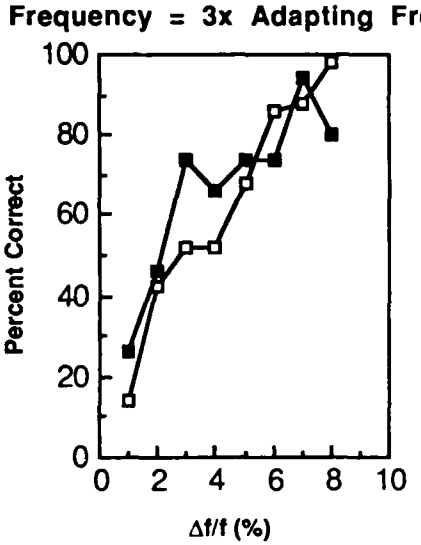

Figure 3. Same as Figure 2 except that details of adaptation and test presentation differed slightly. See text. (A) Adapting frequency, 2.9 c/deg. (B) Adapting frequency 1.9 cy/deg.

PERCEIVED SPATIAL FREQUENCY SHIFT FOLLOWING PATTERN ADAPTATION

Failing to reproduce the frequency-discrimination threshold-elevation effect, we turned to the perceived spatial frequency shift, which has been replicated repeatedly (Blakemore and Sutton, 1969; Blakemore *et al.*, 1970; Klein *et al.*, 1974). The suggestion that the PSFS is a fundamentally different type of pattern adaptation effect than contrast-threshold elevation (Klein *et al.*, 1974) raises the possibility that the PSFS might be tied, not to the retinal spatial frequencies of the stimuli, but to their perceived frequencies instead. To investigate this possibility, we measured the PSFS with the test and adapting gratings at different viewing distances, using an experimental design that was similar to that used in the previous experiments.

Methods

In this experiment, the adapting grating was restricted to the upper half of a 21x15 deg bipartite field. Viewing distance was 1 m. During the adapting intervals, the lower hemifield was always uniform at the mean luminance of the other stimuli. A small bar was presented in the middle of the display, which the observers were instructed to fixate. The initial adaptation interval was 1 min and the intertrial adaptation intervals were 15 sec.

The test stimuli were presented on a 10 x 8 deg bipartite field with a central fixation bar. Viewing distance was 2 m. During the test interval, two gratings were presented simultaneously, one in each hemifield. They were presented for 225 msec to reduce the likelihood that the observer would inadvertently make a large saccade during the test interval. The displays appeared juxtaposed, as in the pattern-adaptation experiment, and the trials were timed so that the observers could saccade from the adapting field to the test field and fixate the central bar before the test stimuli

were presented. The duration of this interval between presentation of the adapting and test stimuli was 1.2 sec. The contrasts of the test gratings in the two hemifields were varied randomly and independently in the range 40 to 60%, to prevent perceived contrast from being used as a cue to frequency. The phases of the gratings were also varied randomly and independently in the two hemifields (over the range 0 to 180 deg). The spatial frequencies of the two test gratings differed by 2, 4, 6, 8, 10, 12, or 14 %. The average spatial frequency of the two test gratings was 2.6 c/deg. The observers' task was to report whether the upper or lower hemifield appeared to have the grating of higher spatial frequency. No feedback was given. Experiments were conducted with adaptation to a uniform field (unadapted condition) and with adaptation to a stimulus in which the upper hemifield contained a flickering grating and the lower hemifield was uniform (adapted condition). The mean luminance of both hemifields was constant throughout the experiment, and the central fixation bar was always present.

One could determine whether the PSFS is tied to the retinal or perceived spatial frequencies by conducting a complete PSFS study with the test and adapting gratings at different viewing distances. However, a judicious choice of test and adapting frequencies made the complete study unnecessary. By using an adapting/test pair in which the adapting grating had a lower retinal spatial frequency but a higher perceived frequency than the test grating, we could distinguish between the two possibilities in a single experiment.

The rationale for the choice of stimuli can be explained most easily by reference to a typical PSFS curve. Figure 4 shows the PSFS data obtained by Blakemore *et al.*, (1970). [The figure is based on Klein *et al.* (1974, their Fig. 8).] If the adapting frequency is lower than the test (negative value on the abscissa), then the frequency of the test appears higher following adaptation (frequency ratio >1). On the other hand, if the adapting frequency is higher than that of the test, then the frequency of the test appears lower following adaptation. The peak effects occur when the

adapting and test gratings differ by about 0.5 octave. By making the retinal frequency of the adapting grating lower than that of the test and its perceived frequency higher (by the same amount), opposite predictions are achieved. If the PSFS is tied to retinal spatial frequency, then the test grating should appear to have a higher spatial frequency following adaptation. On the other hand, if the PSFS is tied to perceived spatial frequency, then the test grating should appear to have a lower spatial frequency following adaptation.

In the experiment reported here, the retinal spatial frequency of the adapting grating was 1.88 c/deg, presented at 1 meter, whereas that of the average test was 2.62 c/deg, presented at 2 meters. The object spatial frequency of the adapting grating was 1.08 c/cm and that of the average test was 0.76 c/cm. Thus, the perceived frequency of the adapting grating was higher than that of the test, but its retinal frequency was lower than that of the test.

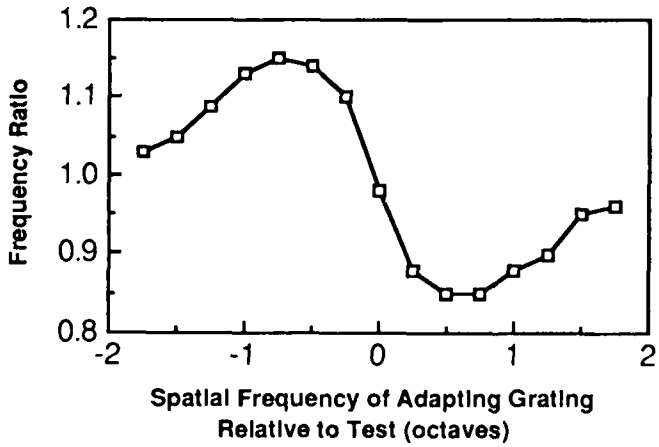

Figure 4. PSFS curve. Data by Blakemore *et al.*, (1970) as reported by Klein *et al.* (1974).

Results

Results of the adapted and unadapted conditions for two observers are shown in Fig. 5. The PSFS effect is clearly replicated: The perceived frequency of the test grating is shifted following adaptation to the high-contrast grating. Furthermore, this result was obtained with much briefer adapting durations than were used in the frequency discrimination experiments, where no adaptation effects were found. The magnitude of the effect obtained here is similar to that obtained by Klein *et al* and considerably smaller than that obtained by Blakemore. The points of subjective equality (PSE) for the frequencies of the two gratings are shown in Table 1.

Pattern adaptation raises the perceived spatial frequency of the grating seen in the (upper) adapting hemifield. This is what one would expect on the basis of the retinal spatial frequencies of the adapting and test gratings. It contradicts the prediction based on the perceived spatial frequencies of the gratings. Thus, the perceived spatial frequency shift that results from prior adaptation, like the contrast-threshold elevation effect, must occur at a stage of processing in which the spatial properties of the retinal image itself are represented, a stage that presumably precedes estimates of object properties.

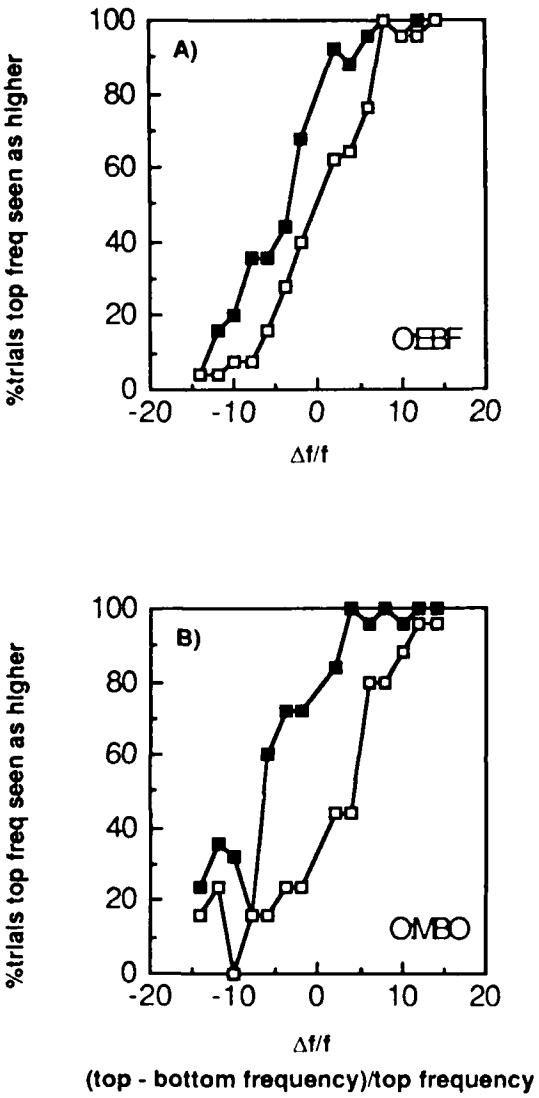

Figure 5. Effect of pattern adaptation on perceived spatial frequency of grating. Adapted data are shown by the filled symbols, unadapted by the open symbols. The effect of pattern adaptation is to raise the perceived frequency of the subsequently viewed test grating. Two observers.

Table 1
Δf/f at Point of Subjective Equality

Observer	Unadapted	Adapted
MBO	+.126	-6.92
EBF	-.20	-4.61

Negative values indicate that the grating in the top (adapted) hemifield appeared to have a higher spatial frequency than the grating in the bottom hemifield.

PERCEIVED SPATIAL FREQUENCY SHIFT WITH SIMULTANEOUS SURROUND

Although Klein *et al.* (1974) give evidence that the prior-adaptation-PSFS and the simultaneous-surround-PSFS have the same origin, some interesting issues remain. Specifically, we explored two basic questions:

- Is the effect of the surround tied to the relationship between the retinal spatial frequencies of the test and surround or to the relationship between their preceived spatial frequencies?

- Does the surround PSFS still occur if the test gratings being compared have the same perceived spatial frequencies but different retinal frequencies?

These questions had to be answered with more informal experimental techniques than were used in

previous experiments because of the difficulty of generating the stimuli on CRT's. Although one can easily display a test grating with a surrounding grating on a single screen, it is more difficult if the surrounding grating has to appear at a different distance than the test. Therefore, we resorted to paper, scissors, and square wave gratings (i.e., bars) using a MacIntosh computer and laser printer to generate the stimuli. This approach turned out to be satisfactory.

Square wave gratings of three fundamental spatial frequencies were printed on paper - the test frequency, twice the test frequency, and half the test frequency. The test gratings were presented against the two surrounds as shown in Fig. 6. Viewing in all cases was binocular in a room with normal illumination. The white surrounds between the test and surround gratings were used so that good depth cues could be achieved in the nonequidistant condition. In the equidistant condition, the stimuli appeared as shown in Fig. 6 and were presented at a viewing distance of 1 meter. In the nonequidistant condition, the surround gratings were presented at one meter, and the test gratings were presented at two meters. The test plus white surround was cut out of the Fig. 6 stimulus so that the test gratings could be viewed through the resulting holes. In the nonequidistant condition the object spatial frequency of the test gratings was half that used in the equidistant condition, and the test patches were twice the size. Therefore the test patches had the same retinal dimensions when viewed through the holes in the surround gratings as they had when presented in a single plane. Under these conditions, the observers perceived the test gratings as lying behind the surround gratings.

In both the equidistant and nonequidistant conditions, the normal PSFS was seen as predicted on the basis of the retinal spatial frequencies. Changing the viewing distance, while keeping the retinal frequencies the same, had no effect. In addition, we found that placing the test gratings in front of the surround gratings also resulted in the predicted effect. Therefore, the influence of the surround must occur at a stage of processing in which the retinal spatial frequencies

are represented, independent of their perceived spatial frequencies.

However, the whole phenomenon cannot be accounted for at that stage. The test gratings are still compared on the basis of their object spatial frequencies. Although this conclusions seems to follow directly from the results of our previous experiments (Burbeck, 1987), it seemed prudent to check that the PSFS and the comparison of object spatial frequencies were consistent. Toward this end, we conducted the following experiment. We presented the two halves of the stimulus shown in Fig. 6 at different viewing distances, so that the test patches differed in retinal spatial frequency. (This can be done by the reader by photocopying the figure and cutting the copy in half.) Over the range of distances in which size constancy holds well (an arms length and three-quarters of that are good), the test patches appear essentially the same as in the equidistant case, complete with the perceived spatial frequency shift. Thus, although the bias caused by the surrounding grating occurs at a stage of processing in which retinal spatial frequencies are represented, the comparison between the two test patches occurs at a stage in which the object spatial frequencies are estimated. Thus, one can begin to see evidence for at least two serial stages of processing.

This result is particularly interesting because when the stimuli are presented at a single viewing distance the surround-PSFS is accompanied by a shift in the perceived distances to the tests. The high-frequency surround appears closer than the test and the low-frequency surround appears farther. The robustness of the PSFS across changes in the distances to the test and surrounds suggests that the difference in perceived distances induced by the surrounds does not cause the effect, but is instead a result of the perceived frequency shift itself. This is also consistent with our finding that the PSFS occurs before depth information is incorporated into the analysis of the scene.

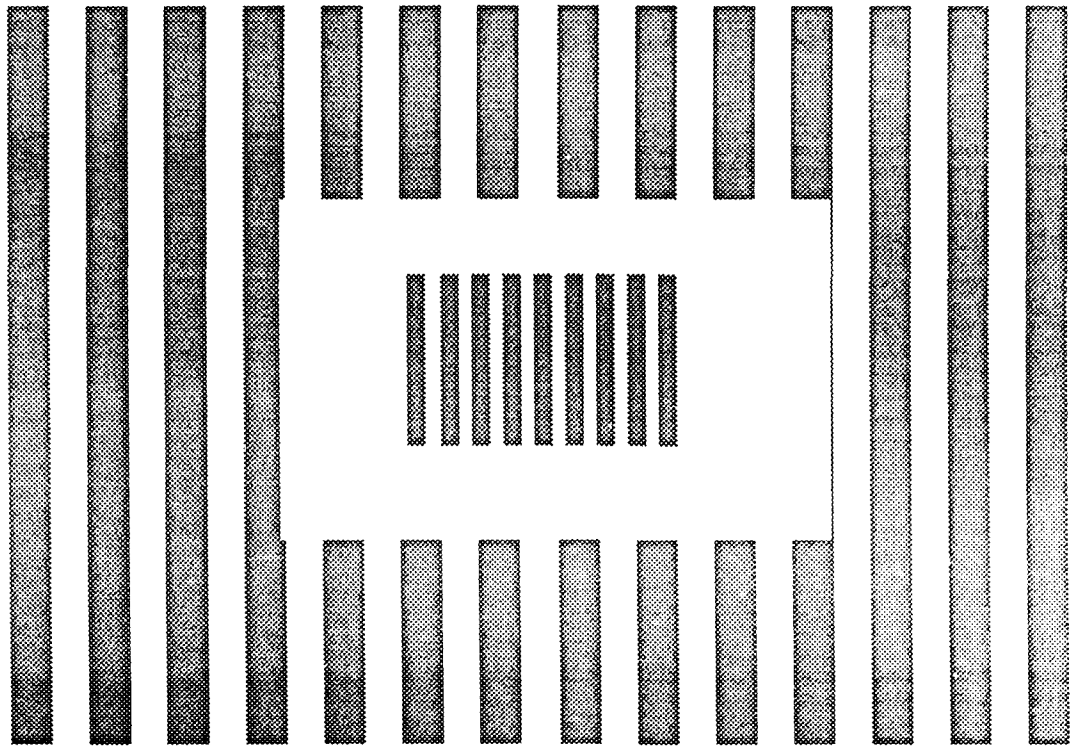

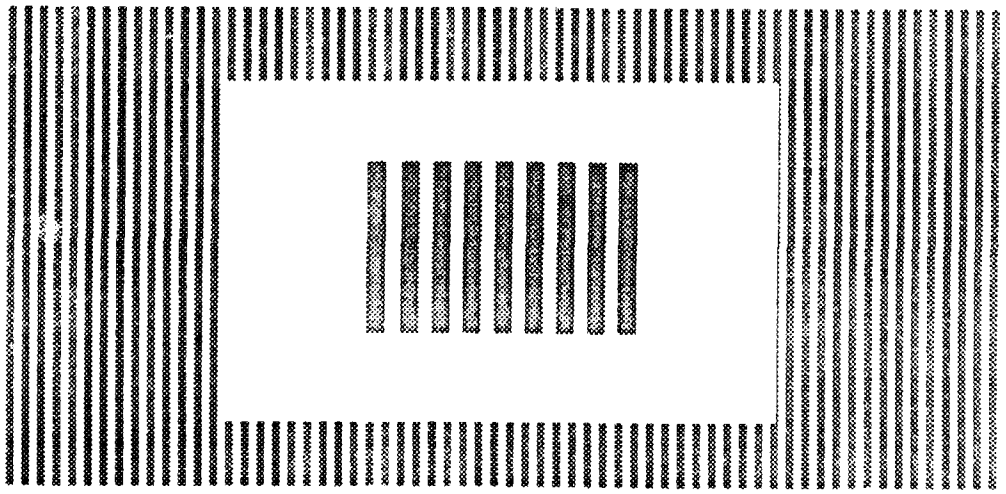

Figure 6. Stimulus for informal experiments on the effects of depth on the surround-PSFS.

RELATIONSHIP BETWEEN PSFS AND FREQUENCY DISCRIMINATION THRESHOLDS

Although the frequency-discrimination-threshold elevation effect is apparently not very robust, the PSFS is more so, and it predicts that there should be a change in frequency-discrimination thresholds following pattern adaptation. Consider, once again, the standard PSFS effect, as shown in Fig. 4. If the frequencies of the two gratings in a frequency-discrimination test pair flank the adapting frequency, then the test frequency that is higher than the adapting frequency should appear higher still, whereas the test frequency that is lower than the adapting frequency should appear lower still. Thus, the perceived difference between these two frequencies should be greater following adaptation, resulting in a lower frequency-discrimination threshold. On the other hand, if the test frequencies are both higher or both lower than the adapting frequency, and within the range of the PSFS effect, then their perceived difference may be smaller following adaptation -- the perceived frequencies being bunched together at frequencies about 0.5 octave higher or 0.5 octave lower than the adapting frequency.

The exact changes in frequency-discrimination thresholds that this analysis predicts are readily calculated. I assume that the frequency discrimination threshold is a 3% difference in the perceived frequencies. The actual frequencies that would result in a 3% difference in the perceived frequencies following adaptation can then be rdetermined from PSFS data.

Let $\mathbf{a}_i$ represent the perceived frequency of spatial frequency $\mathbf{f}_i$, following adaptation to

frequency **f**. Then $a_i = R_i f_i$, where R_i is the frequency ratio measured in PSFS experiments. We're assuming that at threshold $\Delta f/f = .03$. Therefore, it follows that at threshold,

$$\frac{2(R_2 f_2 - R_1 f_1)}{R_2 f_2 + R_1 f_1} = .03 \qquad (1)$$

Equation (1) can be rearranged to yield:

$$f_2 = \frac{2.03\ R_1}{1.97\ R_2}\ f.$$

and, by definition,

$$\frac{\Delta f}{f} = \frac{2(f_2 - f_1)}{f_2 + f_1}.$$

Substituting, we find that

$$\frac{\Delta f}{f} = \frac{4.06\ R_1 - 3.94\ R_2}{2.03\ R_1 + 1.97\ R_2} \qquad (2)$$

In our calculations the exact values of R_i that were required were obtained by interpolating linerarly between the data points. The resulting predictions are shown in Fig. 7. This figure shows predictions based on the data of Blakemore *et al.* (1970) and on the data of Klein *et al.* (1974). The original data from these two laboratories differed significantly, so that predictions based on their data also differ significantly. The data of Blakemore *et al.* (open diamonds) predict a large decrease in the frequency discrimination threshold at the adapting frequency and small frequency discrimination threshold elevations above and below the adapting frequency. The data of Klein *et al.* (filled diamonds) make much more modest predictions. Their data predict a small decrease in frequency discrimination thresholds, at the adapting frequency and negligible effects above and

below the adapting frequency. Our data, which are also shown in Fig. 7 (filled squares), are roughly consistent with the predictions of Klein *et al.* By contrast, Regan and Beverley found large threshold elevations when the test frequency was higher than the adapting frequency (negative values on the abscissa). Representative data from their study are shown in Fig. 8 together with the predictions from the two sets of PSFS data for comparison. Neither of the PSFS functions predicts the large threshold elevations that Regan and Beverley found.

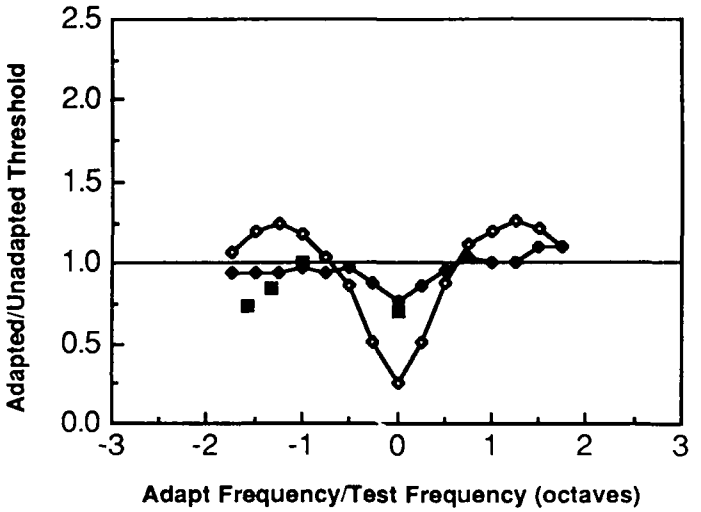

Figure 7. Effects of pattern adaptation on frequency discrimination predicted by PSFS data of Blakemore *et al.* (open diamonds,) and predictions based on data of Klein *et al.* (filled diamonds). Also shown for comparison are the data obtained in our lab (filled squares). Vertical and horizontal scales chosen to match those used in Fig. 8.

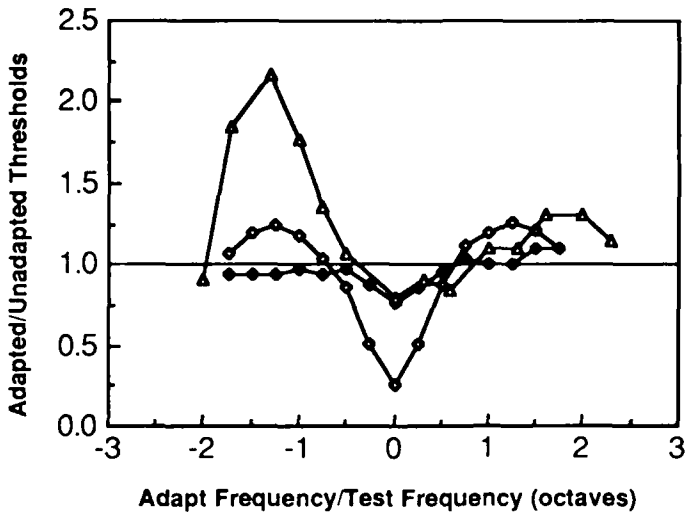

Figure 8. The triangles show typical result from Regan and Beverley (1983, their Fig. 1). Also shown for comparison are the predictions based on the PSFS data of Klein *et al.* (filled diamonds), and those based on the data of Blakemore *et al.* (open diamonds).

Relating the PSFS to the frequency-discrimination thresholds suggests a functional advantage for this form of pattern adaptation: Prolonged viewing (and hence intense interest in) a high-contrast stimulus enhances sensitivity to changes in the size (and hence distance to) the stimulus. Thus, prolonged viewing may result in slightly enhanced sensitivity to slow forward or backward motion of the object of interest.

SUMMARY AND DISCUSSION

The experiments reported above show that both the contrast-threshold elevation and the PSFS that result from pattern adaptation are tied to the retinal spatial frequencies of the test and

adapting gratings, independent of their perceived spatial frequencies. In short, all effects of pattern adaptation appear to be restricted to fairly distal representations of spatial information. Thus, the fact that pattern adapation effects appear in frequency discrimination tasks suggests that there is a serial relationship between the channels stage and the stage in which spatial frequency judgments are made. This supports the idea that the processing stage that is revealed by pattern adaption paradigms is fundamental to spatial vision in general.

ACKNOWLEDGEMENTS

This research was sponsored by the U.S. Air Force Office of Scientific Research, Air Force Systems Command, United States Air Force, under contract AFOSR F49620-85-0022. The United States Government is authorized to reproduce and distribute reprints for governmental purposes notwithstanding any copyright notation thereon.

REFERENCES

Blakemore C. and Campbell F. W. (1969) On the existence of neurones in the human visual system selectively sensitive to the orientation and size of retinal images. *J. Physiol., Lond.* **203**, 237-260.

Blakemore C. Garner E. T. and Sweet J. A. (1972) The site of size constancy. *Perception* **1**, 111-119.

Blakemore C. and Sutton P. (1969) Size adaptation: A new aftereffect. *Science* **166**, 245-247.

Burbeck C. (1987) Locus of spatial-frequency discrimination. *J. opt. Soc. Am. A* **4** (in press).

Burbeck C. (1986) Negative afterimages and photopic luminance adaptation in human vision. *J. opt. Soc. Am. A* **3**, 1159-1165.

Cornsweet T. N. (1962) The staircase method in psychophysics. *Amer. J. Psych.* **75**, 485-491.

De Valois R. L. and De Valois K. K. (1980) Spatial vision. *Ann. Rev. Psychol.* **31**, 309-341.

Kelly D. H. and Burbeck C. (1984) Critical problems in spatial vision. *CRC Critical Reviews in Biomedical Engineering* **10**, 125-177.

Klein S. Stromeyer C. F. III and Ganz L. (1974) The simultaneous spatial frequency shift: A dissociation between the detection and perception of gratings. *Vision Res.* **14**, 1421-1432.

Pantle A. and Sekuler R. (1968) Size-detecting mechanisms in human vision. *Science*, N. Y. **162**, 1146-1148.

Regan D. and Beverley K.I. (1983) Spatial-frequency discrimination and detection: comparison of postadaptation thresholds. *J. opt. Soc. Am.* **73**, 1684-1690.

Appendix G

Vision Res. Vol. 27, No 9, pp. 1527–1537, 1987
Printed in Great Britain

0042-6989/87 $3.00 + 0.00

FURTHER EVIDENCE FOR A BROADBAND, ISOTROPIC MECHANISM SENSITIVE TO HIGH-VELOCITY STIMULI

D. H. KELLY and CHRISTINA A. BURBECK
Visual Sciences Program, SRI International, Menlo Park, CA 94025, U.S.A.

(*Received* 18 *February* 1986; *in revised form* 23 *March* 1987)

Abstract—Spatial frequency and orientation selectivity, the most prominent properties of image processing in the striate cortex, are not uniform throughout the spatiotemporal frequency domain. Some current models include one "transient" mechanism at very high velocities (i.e. low spatial and high temporal frequencies), and multiple "sustained" mechanisms elsewhere in the spatiotemporal frequency domain, but they do not consider the parameter of orientation. On the basis of earlier, orthogonal masking experiments, we concluded that the high-velocity mechanism is sensitive to a broad band of spatial frequencies, and has little or no orientation selectivity. In the present study we use pattern adaptation to measure the spatiotemporal properties of this mechanism. In other experiments, we attempt to relate it to the direction-selective motion detectors that also respond at high velocities. Finally we compare the pattern-adaptation results to the results of orthogonal subthreshold summation experiments in the same region of high temporal and low spatial frequencies.

Pattern adaptation Spatiotemporal mechanisms High velocity Pattern/flicker
Transient/sustained Orientation selectivity Motion detectors Subthreshold summation

INTRODUCTION

Recent research in spatial vision has been dominated by the theory that there are multiple parallel channels, each sensitive to a different range of spatial frequencies (Blakemore and Campbell, 1969; Kelly and Burbeck, 1984). Developing concurrently with that theory was the idea that there are two types of mechanisms, often called sustained and transient, that have different temporal as well as spatial properties (Tulunay-Keesey, 1972; Tolhurst, 1973; Kulikowski and Tolhurst, 1973; Pantle, 1973). More recently these two approaches have been reconciled by the suggestion that there is a single mechanism that is most sensitive to high temporal and low spatial frequencies—the so-called transient mechanism—and multiple sustained mechanisms handling the rest of the spatiotemporal frequency domain (Legge, 1978). In this model, each sustained mechanism has narrower tuning for spatial frequency than does the transient mechanism; orientation tuning is not considered.

Although the terms "sustained" and "transient" are generally used to describe electrophysiological responses, numerous attempts have been made to link particular visual percepts to one or the other of these mechanisms. For example, percepts of pattern and flicker (or form and motion) were thought to arise specifically from the responses of sustained and transient mechanisms, respectively (Tulunay-Keesey, 1972; Tolhurst, 1973). Now, however, there is ample evidence that, although there may be parallels between some higher order percepts and more peripheral detection mechanisms, there are no identities between them (Green, 1984). Thus psychophysically determined thresholds may be more successful than subjective percepts in determining the properties of these two subsystems (Lennie, 1980; Burbeck, 1981).

The present study is mainly concerned with what has been called the "transient" mechanism. However, the terms "sustained" and "transient" properly indicate only the presence or absence of a steady-state response, so we prefer to identify these mechanisms in terms of the spatiotemporal frequency regions where they are most sensitive. We regard the "transient" mechanism, for example, as the low-spatial, high-temporal frequency mechanism.

In order to avoid using such cumbersome terms throughout the paper, we take advantage of the fact that, when the stimuli are moving or flickering sinusoidal gratings, the stimulus velocity always equals the ratio of its temporal to its spatial frequency ($V = f_t / f_s$). Thus we call

our stimuli "high-velocity" or "low-velocity" gratings, if they occur in the appropriate regions of the spatiotemporal frequency domain.

We use these terms for convenience only; they are not intended to imply any type of velocity tuning other than that described above. Where both spatial and temporal frequencies are high, or both are low, we state this explicitly. With these conventions, it becomes natural to refer to the mechanism that is optimally stimulated by (relatively) low spatial and high temporal frequencies as the "high-velocity" mechanism. This has the advantage of brevity, without implying that this mechanism has no steady-state response.

In a previous study, we found that masking by an orthogonal grating of the same spatial and temporal frequency as the test grating produced substantial contrast threshold elevation when both the test and mask were of high velocities, but not in any other frequency region (Burbeck and Kelly, 1981). In that paper, we interpreted this to mean that there were two types of mechanism, one type in the high-velocity region, and one type elsewhere in the spatio-temporal frequency domain. The fact that orthogonal masking had a profound effect in the high-velocity region suggested that the underlying mechanism in that region is not as narrowly tuned for orientation as are the mechanisms responsible for thresholds in the rest of the spatiotemporal frequency domain. We also found that the mechanism in the high-velocity region is more broadly tuned for spatial frequency than are the other mechanisms that have been revealed in masking studies. This result was confirmed and extended by Ferrara and Wilson (1985).

In the present study, we measure the orientation selectivity of this high-velocity mechanism, using a pattern-adaptation paradigm. We did not do this during the previous study because the masking paradigm was unsuitable for determining orientation selectivity. (When the mask and test are aligned, the task becomes contrast discrimination rather than contrast detection.) With the present pattern-adaptation paradigm, we find that thresholds are elevated at high velocities when the test and adapting gratings are orthogonal, just as we found using orthogonal masking. Moreover, we find that the high-velocity mechanism actually behaves isotropically when the spatial frequency is sufficiently low and the temporal frequency is sufficiently high.

METHODS

(*a*) *Equipment*

The apparatus used in these experiments has been described elsewhere (Kelly, 1982). The experimental procedures were controlled by a computer that also generated the stimulus functions, and collected and processed the subject's responses. The stimuli were displayed at a 60-Hz frame rate on a 30-cm, high-resolution monitor, subtending 8 deg at the 2-m viewing distance. Mean luminance of the screen was 90 cd m^{-2}. All observations were made monocularly, with the right eye, using a 3-mm artificial pupil. Fixation was controlled by stabilizing the retinal image with the SRI eyetracker (Crane and Steel, 1978; Crane and Clark, 1978).

(*b*) *Procedure*

The question of whether to use drifting or flickering stimuli required some consideration. In our masking study (Burbeck and Kelly, 1981), we used counterphase gratings throughout, but here prolonged viewing of high-contrast, counterphase gratings could produce second-harmonic afterimages (Virsu and Laurinen, 1977), which are particularly strong with stabilized, high-velocity gratings. These afterimages can be avoided by adapting with moving gratings instead of counterphase gratings, but then we must consider direction-selective motion aftereffects (Sekuler and Ganz, 1963; Levinson and Sekuler, 1975). In our main experiments, we drifted the adapting stimulus (to avoid afterimages) and flickered the test stimulus (to avoid motion aftereffects). To confirm that these test thresholds were, in fact, unaffected by adaptation of motion detectors, we also conducted a few motion-adaptation experiments at appropriate spatial and temporal frequencies [see Results (e)].

The adapting stimulus was usually a vertical grating, drifting horizontally at the appropriate velocity, while the test stimulus was a counterphase-flickering grating, usually horizontal, but sometimes vertical or at ± 45 deg. In a few cases, the adapting stimulus was oriented at 45 deg and the test at other orientations.

Pattern-adaptation experiments have traditionally used the method of adjustment, but we adopted a computer-controlled, yes/no staircase technique for all the adaptation experiments reported here. Each trial consisted of an 18-sec adapting interval followed by a 3-sec test interval. In addition, the contrasts of both the adapt-

ing and the test stimulus were faded in and out by a 1-sec, raised-cosine waveform at the beginning and end of each interval, making their total durations 20 and 5 sec, respectively. However, the test interval could be terminated by the subject at any time after the test reached full contrast, if he signalled "yes" or "no." (When we measured the unadapted threshold, the adapting interval was blank, but the timing remained the same.) In preliminary tests, the subject's (adapted or unadapted) threshold was estimated by the method of adjustment, and the staircase was started at this contrast. The adapting stimulus was always displayed at 95% contrast (after fading in).

A tone sounded near the beginning of the test interval, to cue the subject. At any time after this tone, he could indicate by pushing a button whether or not he detected the test stimulus. For each yes response, the test contrast in the next trial was decremented by 10%; for each no response, it was incremented by 10%. The staircase was terminated after six pairs of reversals of test contrast. Threshold was defined as the average of these (12) reversal contrasts. No preadapting period was used, but there was rarely any significant increase of threshold after the first reversal. (If the threshold did increase during reversals, data from that run were not used.)

(*c*) *Subjects*

The data reported here were all obtained from two subjects. The most complete set was from one, young, emmetropic, naive subject (A.E.M.). However, his results were spot-checked and all the important ones replicated by a more experienced subject (D.H.K.).

RESULTS

(*a*) *Orthogonal adaptation*

We define orthogonal pattern adaptation as an increase of threshold for a test grating following adaptation to a high-contrast grating whose orientation is orthogonal to that of the test. In our first experiments, the test and adapting stimuli had the same temporal and spatial frequencies (thus, this paradigm could be called "orthogonal self-adaptation"). To quantify the adaptation effect, we used the ratio (R) of the adapted threshold to the unadapted one. Because each adapted threshold was measured shortly after its unadapted control, this ratio showed very little of the long-term variation in sensitivity that often afflicts raw data. (Ideally $R = 1$ would represent no effect, allowing for residual noise, we treated any value of R less than 1.1 as representing no significant effect.)

Our first orthogonal adaptation tests were conducted under two conditions chosen on the basis of our previous masking study. In one condition (a low velocity) we had found no orthogonal masking, and in the other condition (a high velocity) we had found a large orthogonal masking effect. In the low-velocity condition, we also found no significant orthogonal adaptation effect, confirming previous pattern-adaptation studies of orientation selectivity. In the high-velocity condition, we obtained large effects of orthogonal adaptation: The threshold for a horizontal grating was roughly tripled by adaptation to a vertical one.

This form of pattern adaptation was previously unknown, and it seemed important to map the extent of its occurrence in the spatio-temporal frequency domain. We were also interested to see if it occurred in the same region as the orthogonal masking effects we reported previously. We therefore extended our orthogonal adaptation tests to a number of different spatial and temporal frequency combinations within the high-velocity region, paying special attention to the boundary zone in which the effect tapered off to insignificance. The results of these experiments are shown as spot values for subject A.E.M. in Fig. 1. When these threshold-elevation data are plotted versus log frequency, the functions obtained are almost linear. Thus, points not measured can be readily interpolated to obtain a plausible approximation to the complete surface. Figure 1 also shows this surface plotted as a contour map. Contours are given for threshold-elevation ratios from 1.2 to 2.6, at contour intervals of 0.2. The fit of the interpolated surface to the data can be judged by comparing the contours in Fig. 1 to the spot values.

These contours are approximately constant-velocity diagonals for much of their range, but they curve inward away from the diagonal at both ends, interacting with spatial and temporal frequency in these regions. Thus, although the data are not consistent with a mechanism that is simply tuned to velocity, they are not consistent with a mechanism that is simply tuned to temporal frequency either, contrary to previous suggestions.

However, the delineated region is essentially coincident with the orthogonal masking region.

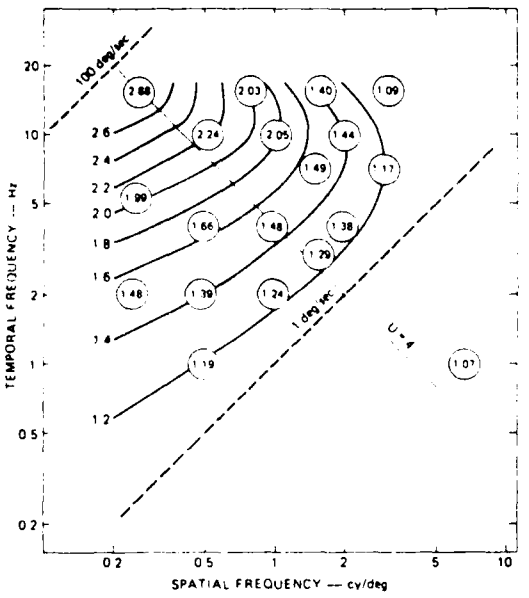

Fig. 1. Contour map of the threshold-elevation surface produced by orthogonal self-adaptation, as described in the text. Contours represent elevation ratios from 1.2–2.6. Encircled numbers represent the data from which this surface was constructed. The dashed diagonal lines represent constant velocities. Thus velocity changes most rapidly in the orthogonal direction typified by the solid diagonal line labelled $U = 4$ (see text). Subject, A.E.M.

reported by Burbeck and Kelly (1981), as shown in Fig. 2. All adaptation ratios in the region of large masking effects are greater than 1.9; in the region of small masking effects, they fall between 1.2 and 1.7; and where there are no significant masking effects, they are less than 1.2.

In the previous masking study, we conducted a few orthogonal adaptation tests, with negative results. However, only the highest velocity we tested (8 deg/sec) was great enough to permit a measurable threshold elevation according to the present results, and it did show a 20% elevation. [In the following section, we compare that datum with present data for the same subject (Fig. 4).] The results of the two studies are not inconsistent; we infer that they could be probing the same mechanism.

We would have liked to determine the boundaries of this mechanism at higher temporal and lower spatial frequencies than those used here, but we were unable to do so because of equipment limitations. (We did lower the spatial frequency still further in some tests by decreasing the viewing distance, as reported below.) The data of Figs 1 and 2 suggest that orthogonal adaptation occurs at even higher velocities (i.e. lower spatial and/or higher temporal frequencies) than we measured, but we did not establish the outer bounds of this effect.

(*b*) *Orientation selectivity*

The threefold elevation in threshold produced by orthogonal adaptation in the high-velocity region indicates that its underlying mechanism is not as orientation-selective as the mechanism that is measured in the traditional pattern-adaptation experiments at high spatial and low temporal frequencies (Blakemore and Nachmias, 1971; Kulikowski *et al.*, 1973). We therefore sought to determine the orientation selectivity of this high-velocity mechanism. We repeated the threshold elevation tests using a very high velocity (0.25 c/deg, 15 Hz, at a viewing distance of 2 m) with the test grating oriented at several angles relative to the adapting grating (0, 45, 90 and −45 deg). Results for the same subject used in Fig. 1 are given in Table 1, and are plotted in polar coordinates in Fig. 3(a). Results for another observer (obtained at 0.089 c/deg, 10 Hz, with a viewing distance of 1 m) are also given in Table 1 and are plotted in Fig. 3(b).

At the extreme spatial and temporal frequencies used, the threshold-elevation ratio for both subjects is essentially independent of

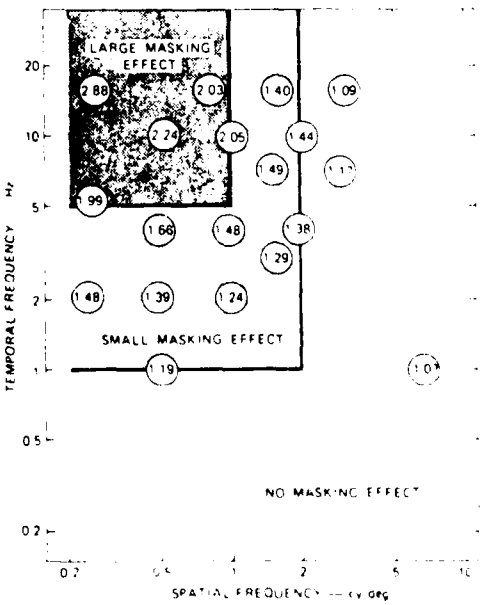

Fig. 2. Spatiotemporal map of the various degrees of masking obtained by Burbeck and Kelly (1981) in orthogonal masking experiments (shaded areas), superimposed on the orthogonal adaptation data of Fig. 2.

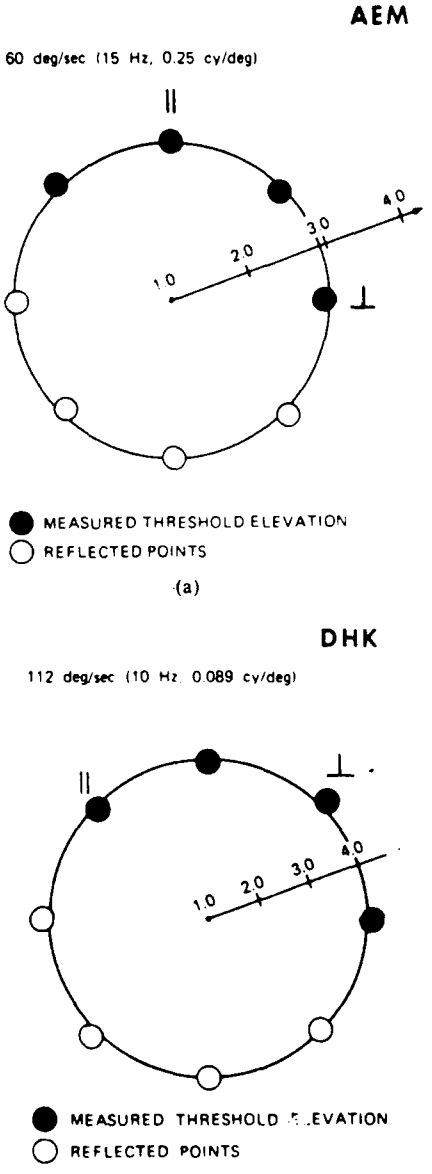

Fig. 3. Polar plots of threshold elevation as a function of test-grating orientation (a) subject A.E.M., at a velocity of 60 deg/sec, (15 Hz, 0.25 c/deg), (b) subject D.H.K. at a velocity of 112 deg/sec (10 Hz, 0.089 c/deg). This condition was obtained by halving the viewing distance (approximately doubling the field size), so the actual ratios may not be comparable to those in the other figures. Only four points were measured in each figure but their reflections are also shown, to indicate that 180-deg rotation of a flickering grating does not change the stimulus.

the orientation of the test grating: it shows no significant orientation selectivity. The circle drawn through the points in each figure is the theoretical locus for a perfectly isotropic mechanism. The data conform well to this theoretical form.

Table 1

Test orientation	Contrast thresholds: Adapted	Unadapted	R
(a) Fig. 3(a, A.E.M.) Adaptation at 0.25 c/deg, 15 Hz, vertical (0°)			
−45°	0.0337	0.0112	3.01
0°	0.0361	0.0122	2.96
45°	0.0297	0.0103	2.88
90°	0.0340	0.0118	2.88
(b) Fig. 3(b, D.H.K.) Adaptation at 0.089 c/deg, 10 Hz, oblique (−45°)			
−45°	0.0590	0.0147	4.01
0°	0.0508	0.0127	4.00
45°	0.0559	0.0137	4.08
90°	0.0624	0.0154	4.05
(c) Fig. 5(D.H.K.) Adaptation at 0.5 c/deg, 10 Hz, vertical (0°)			
−45°	0.0194	0.0071	2.73
0°	0.0271	0.0066	4.11
45°	0.0215	0.0065	3.31
90°	0.0192	0.0078	2.46

To quantify the shift from the strongly-oriented response at low velocities (which appears as a lemniscate form in polar coordinates), to the isotropic response at high velocities shown in Fig. 3, we measured both parallel and orthogonal adaptation for spatialtemporal frequency pairs lying along a diagonal path, running from the low-velocity corner to the high-velocity corner of the spatiotemporal frequency domain, as shown in Fig. 1. (The equation of such a path, at right angles to all constant-velocity profiles, is $f_S f_T = U$, where U is a constant. Here we followed the line $U = 4$.)

Figure 4 shows the threshold elevation ratios for both parallel and orthogonal adaptation plotted in linear units as a function of log velocity along this path. The orthogonal adaptation ratios for subject A.E.M. [Fig. 4(a)] were obtained by interpolation of the constant threshold-elevation contours, as shown in Fig. 1. They are indicated by the solid curve without data points. The orthogonal adaptation ratios for subject D.H.K. [Fig. 4(b)] were measured at two points in this study, and at another point in a previous study (discussed above). These data are shown by the open symbols, the solid curve through those points was drawn by eye. The solid symbols in both parts of the figure represent parallel adaptation ratios measured at velocities of 0.25, 4 and 60 deg/sec [also 20 deg/sec in Fig. 4(b)], spanning the constant-U line. The solid arrow in Fig. 4(a) indicates the velocity used for Fig. 3(a). [The velocity used for Fig.

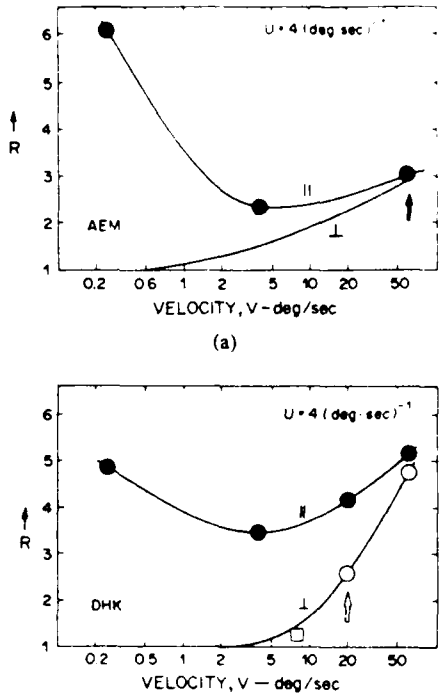

Fig. 4. Threshold elevation for parallel and orthogonal adaptation as a function of velocity. (a) subject A.E.M. The orthogonal adaptation curve (no plotting symbols) was interpolated from the contours in Fig. 2, along the path shown by the solid diagonal in that figure. Threshold elevation ratios produced by parallel adaptation at three velocities along the same path are shown by the solid circles. (b) Same as (a), but for subject D.H.K. Here data points are shown for both orthogonal and parallel adaptation results. Square symbol is a datum for Burbeck and Kelly (1981), under comparable conditions.

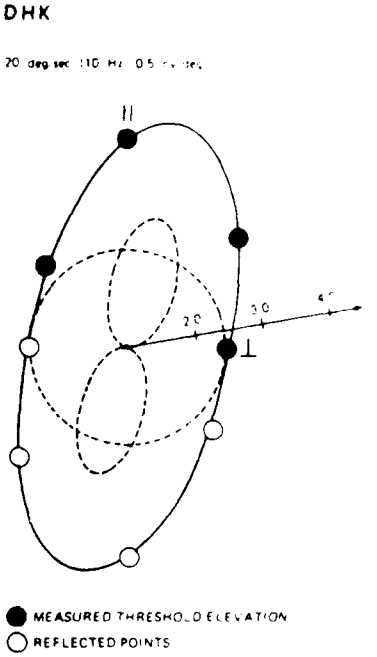

Fig. 5. Similar to Fig. 3, but at a velocity of 20 deg sec (10 Hz, 0.5 c/deg), as indicated by the open arrow in Fig. 4(b), subject D.H.K. The dashed lemniscate represents the putative response of purely orientation-tuned mechanisms at this velocity (see text).

3(b) is not included on this graph because those data were obtained at a different viewing distance and field size.] The open arrow in Fig. 4(b) indicates the velocity used subsequently in Fig. 5.

Clearly the two types of pattern adaptation shown in Fig. 4 behave quite differently as functions of velocity. For both subjects, orthogonal adaptation increases steadily with increasing velocity, but parallel adaptation decreases to a minimum at velocities of a few degrees per second and then increases, approaching the orthogonal result at high velocities. However, there are important quantitative differences between the data of the two subjects. (These differences are emphasized by the log-linear coordinate system chosen for Fig. 4.)

Subject D.H.K. [Fig. 4(b)] shows larger adaptation effects at high velocities than A.E.M. [Fig. 4(a)] does, and smaller effects at low velocities. Thus, the effect of orthogonal adaptation for D.H.K. falls off more rapidly with decreasing velocity. At 20 deg/sec, the orthogonal adaptation effect for this subject is about half the parallel one [as indicated by the arrow in Fig. 4(b)]; to obtain that ratio for A.E.M., the velocity must be reduced by another factor of three. These individual differences are consistent with the hypothesis that the data are governed by two separate mechanisms, an orientation-tuned one at low velocities, and an isotropic one at high velocities.

The results of Fig. 4 suggest the changing shape of orientation-tuning curves across the spatiotemporal frequency domain. To make this more explicit, we conducted another variable-orientation experiment with subject D.H.K. at a velocity of 20 deg/sec (0.5 c/deg, 10 Hz). The results, given in Table 1 and plotted in Fig. 5, are as would be expected. At this velocity, the orientation-tuning curve is elliptical, departing significantly from perfect isotropism, but still far from the lemniscate shape of the usual (low-velocity) orientation-tuning curves. (The 10-deg tilt of the best-fitting ellipse in Fig. 5 is caused by the measured ratios for ±45 deg not

being exactly equal. We have no explanation for this asymmetry.)

The dashed curves in Fig. 5 suggest that these medium-velocity data may be generated by a mixture of two mechanisms, one orientation-tuned and the other isotropic. (The lemniscate curve was formed merely by subtracting the dashed circle from the solid ellipse, to illustrate the point. It seems more likely that two such responses would combine by a nonlinear rule, but our data provide no basis for selecting one.)

(c) *Spatial and temporal bandwidths*

The results presented so far suggest the existence of a broadband, spatiotemporal channel at high velocities. But from the orthogonal self-adaptation paradigm described above (where the orthogonal test and adapting gratings have the same spatial and temporal frequencies), we cannot infer that the broadband results of Fig. 1 actually represent one mechanism that covers this large region in the spatiotemporal frequency domain. Alternatively, these data could represent the envelope of several sub-channels, each more narrowly tuned in spatial or temporal frequency. To test this possibility we conducted some experiments with cross-adaptation paradigms (in which the orthogonal test and adapting gratings are of different spatial or temporal frequencies).

To infer the bandwidths of underlying mechanisms from these adaptation experiments requires detailed theoretical assumptions (Swift and Smith, 1982), but such quantitative bandwidth calculations are not necessary here. For the present purpose, we need only invoke the following general principle. If we are dealing with an array of narrow-band mechanisms, each tuned to a different region of the spatiotemporal frequency domain, then for a given path across this domain, the self-adaptation (or self-test) paradigm should yield a broader threshold-elevation curve than does the standard cross-adaptation (or cross-test) paradigm in which the test frequency is fixed and the adapting frequency varied, or vice versa. (The best-known case of this relationship in spatial vision is the classic spatial-frequency tuning result.) On the other hand, if we are dealing with a single, monolithic mechanism, then the self-adaptation curve should not be significantly broader than the cross-adaptation curve, as measured across the same profile of Fig. 1.

Figure 6 shows two sets of cross-adaptation data in which the horizontal test stimulus was held constant at 0.25 c deg and 15 Hz, while the adapting stimulus was varied in temporal frequency [Fig. 6(a)] or spatial frequency [Fig. 6(b)]. These cross-adaptation data are shown by the open circles. The arrow above each graph indicates the frequency of the fixed test stimulus. The comparable self-adaptation results (from Fig. 1) are shown by the solid symbols. The curve was obtained by interpolation of the contours in Fig. 1 over the same range of adapting frequencies. There is no suggestion in these data that the self-adaptation curve (solid symbols and interpolated curve) is broader than the corresponding cross-adaptation result (open symbols). The implication of this result is that, at these spatial and temporal frequencies, we are dealing with a single, monolithic mechanism.

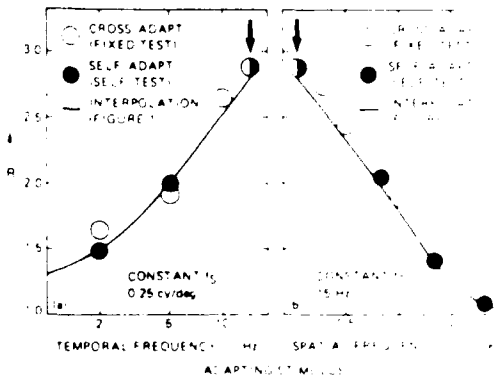

Fig. 6. Threshold elevation ratios obtained in cross-adaptation with a 15 Hz, 0.25 c deg test stimulus (60 deg sec). (a) Effect of varying the temporal frequency of the adapting stimulus, with a constant spatial frequency of 0.25 c deg and (b) effect of varying the spatial frequency of the adapting stimulus, with a constant temporal frequency of 15 Hz. The smooth curves represent self-adaptation profiles interpolated from the contours in Fig. 1 over the same frequency ranges as the cross-adaptation data. Subject, A.E.M.

(d) *Adaptation to patternless flicker*

The results of Fig. 1 suggest that the broadband, isotropic response may peak at still higher velocities (i.e. higher temporal and/or lower spatial frequencies) than those we used. Although the temporal frequency was limited by the frame rate of the display, the dominant spatial frequency of the stimulus could be lowered by uniformly flickering the 18-deg field (thereby changing its frequency distribution from bandpass to lowpass). The effect of adapting to this uniformly flickering field was measured with horizontal test gratings of 0.25, 1 and 3 c deg, in a cross-test paradigm (adapting fre-

quency held constant while the test frequency is varied). All stimuli were flickering at 15 Hz.

The resulting threshold-elevation curve is shown in Fig. 7 together with the comparable results from the orthogonal self-adaptation paradigm and the curve that was interpolated from the data of Fig. 1. The uniform flickering field does produce larger adaptation effects than does self-adaptation, but these effects decay more rapidly with increasing spatial frequency than do the effects produced by self-adaptation.

Can these two results be attributed to the same mechanism? The answer depends on the convention we adopt for quantifying their bandwidths. If we take the usual definition in terms of the frequency at half the peak height, the two bandwidths are equal. Indeed, if we normalize the two curves to the same peak value (at 0.25 c/deg), they are essentially identical.

This normalization (of threshold elevation on a linear scale can be justified if we assume that the high-velocity mechanism is more strongly adapted by patternless flicker than by moving gratings. Since none of our other results contradict that view, we prefer it to interpretations that would require more than one mechanism to account for these data.

(e) *Motion detectors*

In addition to the mechanisms we have considered so far, there is extensive evidence for a third type of mechanism, one that detects the direction of motion of a drifting grating or other moving stimulus (Sekuler and Ganz, 1963, Levinson and Sekuler, 1975, Stromeyer *et al.*, 1984). Such motion-selective mechanisms can be found in the same high-velocity region where we obtain isotropic masking and adaptation effects (Watson *et al.*, 1980; Burr, 1981, Hess and Plant, 1985). Now a direction-selective mechanism cannot be isotropic. So how can our isotropic results be obtained in the presence of such a mechanism?

In Fig. 8(a), we plot two pairs of adapted and unadapted thresholds obtained with our standard adaptation paradigm, where the adapting stimulus is a moving grating and the test stimulus is a counterphase flickering grating of the same spatial and temporal frequencies (Subject D.H.K.) When these patterns are orthogonal, the threshold elevation ratio at 60 deg/sec is 2.7, when they are parallel, it is 3.7 (still lower spatial frequencies are required to make the two ratios equal for this subject, as described above.).

Now if we change the paradigm slightly, changing the test stimulus from a flickering into a moving grating, we can make a comparison with the classic motion-adaptation paradigm. Here we must consider at least three geometries of the test and adapting stimuli: parallel (same

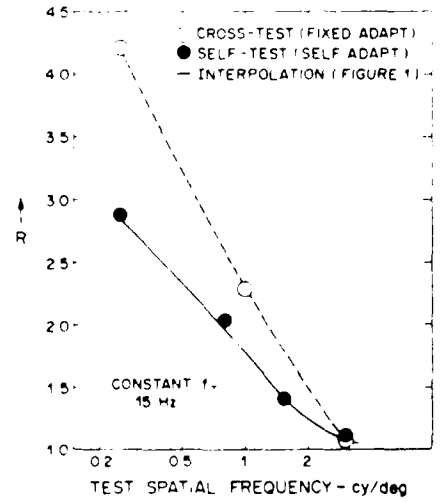

Fig. 7. Threshold elevation ratios produced by a constant adapting stimulus consisting of a uniform field flickering at 15 Hz, and 15-Hz test stimuli at three spatial frequencies. The solid curve is the same 15-Hz self-adaptation profile shown in Fig. 6(b). Subject, A.E.M.

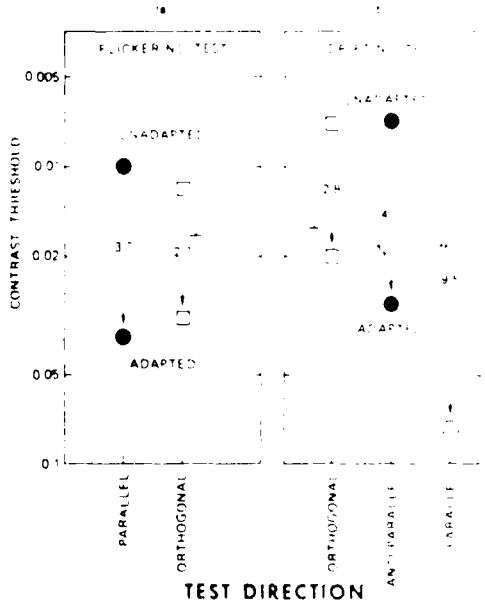

Fig. 8. Comparison of flickering and moving test gratings at 15 Hz, 0.25 c/deg (60 deg/sec), adapting grating is always moving. (a) Counterphase-flickering test, as used throughout this study. (b) Moving test, oriented parallel, and anti-parallel as well as orthogonal to the adapting grating. Subject, D.H.K.

direction), anti-parallel (opposite direction), and orthogonal. Figure 8(b) shows the adapted and unadapted thresholds for those three cases. The orthogonal and anti-parallel ratios are essentially the same as with the flickering test (2.8 and 4.1). But when the test is moving in the same direction as the adapting grating, then the ratio is much greater (9.5) than we can obtain with any of our other stimulus configurations. This is of course a well-known result: direction-selective motion adaptation.

The standard explanation for the difference between the parallel and antiparallel results is that there are two responding mechanisms that are sensitive to opposite directions of motion. But the orthogonal adaptation effect, which has about the same magnitude as the anti-parallel effect, doesn't fit into that scheme. An isotropic mechanism (or any mechanism that is not narrowly tuned for orientation) should respond equally well to gratings drifting in either direction. Thus, the critical question posed by these results, is: If there is an isotropic mechanism, why doesn't it detect the drifting grating in the case of parallel, same-direction adaptation [Fig. 8(b)], instead of leaving detection to the (now quite insensitive) motion detector? The only plausible explanation that occurs to us is that the isotropic mechanism is not capable of detection on its own; instead, it is a distal component of the motion-sensitive mechanism. (The detection site clearly follows the locus of motion sensitivity, as demonstrated by motion-selective adaptation effects.) We suggest that the isotropic mechanism feeds into the motion detecting mechanisms and that adaptation occurs at both sites—the isotropic stage and the motion-detecting stage.

Under this line of reasoning, thresholds for flickering test stimuli (used in most of the experiments reported here) should have been unaffected by adaptation of the motion-sensitive stage, because they can be detected by the unadapted motion-channel that is sensitive to the direction-of-motion opposite to that of the adapting grating. The quantitative similarity of the results for orthogonal adaptation and for opposite-direction parallel adaptation is consistent with this interpretation. Finally, small residual differences between the orthogonal and anti-parallel results are likely to be the result of oriented, nonmotion-specific adaptation (as seen in Figs 4 and 5). Thus, our data collectively suggest the existence of three sites of spatial adaptation, that may overlap in a sizable region of the spatiotemporal domain: isotropic, oriented, and direction-selective.

(f) *Subthreshold summation*

Previous studies of subthreshold summation between horizontal and vertical gratings having a limited range of spatial and temporal frequencies (e.g. Kulikowski *et al.*, 1973) showed the independence that would be expected of strongly orientation-selective mechanisms. To determine whether this independence breaks down at high velocities, as suggested by our orthogonal adaptation (and masking) results, we conducted subthreshold-summation experiments with stabilized, counterphase-flickering gratings at spatio-temporal frequency pairs of 6 c/deg, 1 Hz; 0.5 c/deg, 10 Hz; and 0.25 c/deg, 15 Hz. Complete horizontal vertical independence was obtained with the lowest velocity stimulus, as expected.

Figure 9 shows the more interesting results with higher velocity stimuli. At the highest velocity obtainable at our standard viewing distance (0.25 c/deg, 15 Hz), we did obtain a significant interaction between horizontal and vertical thresholds (summation exponent < 2

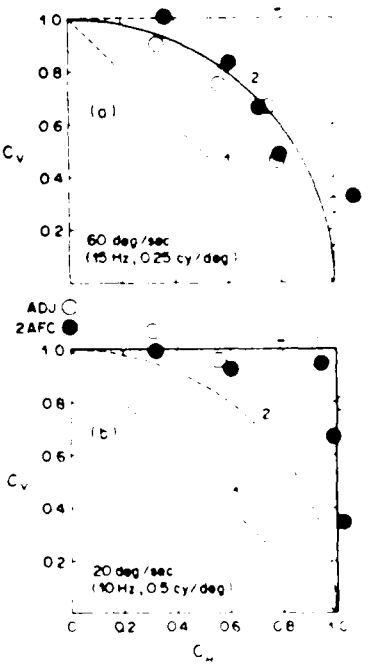

Fig. 9. Subthreshold summation between horizontal and vertical, high-velocity gratings under two conditions also used for pattern adaptation. All thresholds normalized to the horizontal and vertical component thresholds. Subjects D.H.K., open symbols, method of adjustment, solid symbols, two-alternative forced-choice. (a) 60 deg/sec, (b) 20 deg/sec, as in Fig. 5.

shown in Fig. 9(a). Thus the expected trend is present.

However, at lower velocities, we found complete threshold independence. Figure 9(b) shows data for 0.5 c deg, 10 Hz. The same subject shows considerable orthogonal adaptation with this frequency pair, see Figs 4(b) and 5. We emphasize that there is no such conflict between masking and pattern adaptation, only between the threshold and suprathreshold techniques. Subthreshold summation yields narrower estimates of orientation tuning than do techniques involving suprathreshold stimuli, as has previously been found in other spatiotemporal frequency regions as well (Blakemore and Nachmias, 1971; Kulikowski *et al.*, 1973; Thomas and Gille, 1979).

DISCUSSION

Taken together, the present adaptation study and our previous masking results (Burbeck and Kelly, 1981) provide strong support for the notion that an isotropic, adaptable mechanism is involved in the detection of high-velocity gratings. New mechanisms should always be accepted with caution but in this case, there is a well-known body of earlier work that seems closely related to our results. The isotropic mechanism found in our experiments appears to be the same as the so-called "transient" mechanism of numerous other studies.

If our inference is correct that a single mechanism is being adapted, both by patternless flicker and by high-velocity gratings, then the identity of the two mechanisms seems clear. Our isotropic mechanism is broadband in its temporal frequency response, peaking at a high flicker frequency, and is low-pass in its spatial response, cutting off at a few cycles per degree. This description closely matches one suggested earlier by Kulikowski and Tolhurst (1973), and confirmed experimentally many times (Kelly and Burbeck, 1984).

This suggests that the present study could be regarded as an attempt to measure the orientation tuning of the transient mechanism. If the characteristics of this mechanism are most clearly revealed at the highest velocities, as suggested by the larger adaptation effects obtained with the lowest spatial, highest temporal frequency combinations, then the "transient" mechanism has no orientation tuning at all, but is completely isotropic. That conclusion is supported by the fact that the largest adaptation effect was obtained with a patternless (hence non-oriented) adapting field, and is also consistent with the flicker-masking results in the literature (Breitmeyer *et al.*, 1981; Green, 1984).

What else is known about the "high-velocity corner" of the spatiotemporal frequency domain? In several experiments with sinewave stimuli, this region has revealed other visual properties not found elsewhere. Historically, the earliest of these properties to be discovered was the linearity of the flicker threshold. It was found that the threshold modulation for various periodic waveforms could be predicted from a knowledge of the sinewave modulation thresholds at high temporal frequencies (Ives, 1922; De Lange, 1952; Kelly, 1961). Measured in terms of retinal illuminance, the threshold for these Fourier-equivalent waveforms is also independent of the d.c. component of the stimulus (Kelly, 1964), a generalization of Talbot's law.

This linear independence of the background level is found only with low spatial and high temporal frequencies. In other parts of the spatiotemporal domain, sinewave amplitude thresholds vary with the d.c. component, following well-known adaptation laws: Weber's law when both temporal and spatial frequencies are low, and the De Vries–Rose law when the spatial frequency is high (Kelly, 1972).

Another property found only in the high-velocity corner of the spatiotemporal domain has been called spatial-frequency doubling (Kelly, 1966, 1981). In this phenomenon, amplitude distortion at an early stage of the visual process results in the appearance of a second harmonic of the spatial frequency of a low-frequency grating when it flickers at a high temporal frequency, if the contrast of the stimulus is well above threshold.

Drawing on the available results, we suggest that the mechanism previously identified as "transient" is isotropic, low-pass in the spatial-frequency domain, tuned to high temporal frequencies, linear at threshold and highly nonlinear above threshold. This mechanism probably constitutes a stage in the input to direction-selective motion detectors. In other respects, however, its functional significance remains an intriguing question.

Acknowledgements—This work was partly supported by NIH Grants EY 01128 (D.H.K.) and EY 04120 (C.A.B.) and by the Air Force Office of Scientific Research, Air Force Systems Command, U.S. Air Force, under contract AFOSR F49620-85-K-0022 (to C.A.B.). Some of the data were presented at the *Annual Meeting of the Association for Research in Vision and Ophthalmology*, Sarasota, FL, 1985.

REFERENCES

Blakemore C. and Nachmias J. (1971) The orientation specificity of two visual after-effects. *J. Physiol., Lond.* **213**, 157–174.

Blakemore C. and Campbell F. (1969) On the existence of neurones in the human visual system selectively sensitive to the orientation and size of retinal images. *J. Physiol., Lond.* **203**, 237–260.

Breitmeyer B., Levi D. M. and Harwerth R. S. (1981) Flicker masking in spatial vision. *Vision Res.* **21**, 1377–1385.

Burbeck C. A. (1981) Criterion-free pattern and flicker thresholds. *J. opt. Soc. Am.* **71**, 1343–1350.

Burbeck C. A. and Kelly D. H. (1981) Contrast gain measurements and the transient/sustained dichotomy. *J. opt. Soc. Am.* **71**, 1335–1342.

Burr D. C. (1981) Temporal summation of moving images by the human visual system. *Proc. R. Soc., Lond.* **211**, 321–339.

Crane H. D. and Clark M. R. (1978) Three-dimensional visual stimulus deflector. *Appl. Opt.* **17**, 706–714.

Crane H. D. and Steele C. (1978) Accurate three-dimensional eyetracker. *Appl. Opt.* **17**, 691–705.

De Lange H. (1952) Experiments on flicker and some calculations on an electrical analog of the foveal systems. *Physica* **18**, 935–950.

Ferrara V. P. and Wilson H. R. (1985) Spatial frequency tuning of transient non-oriented units. *Vision Res.* **25**, 67–72.

Green M. (1984) Masking by light and the sustained-transient dichotomy. *Percept. Psychophys.* **35**, 519–535.

Hess R. F. and Plant G. T. (1985) Temporal frequency discrimination in human vision: Evidence for an additional mechanism in the low spatial and high temporal frequency region. *Vision Res.* **25**, 1493–1500.

Ives H. E. (1922) Critical frequency relations in scotopic vision. *J. opt. Soc. Am. Rev. Sci. Instr.* **6**, 254–268.

Kelly D. H. (1961) Visual responses to time-dependent stimuli. I. Amplitude sensitivity measurements. *J. opt. Soc. Am.* **51**, 422–429.

Kelly D. H. (1964) Sine waves and flicker fusion. *Documenta ophth.* **18**, 16–35.

Kelly D. H. (1966) Frequency doubling in visual responses. *J. opt. Soc. Am.* **56**, 1628–1633.

Kelly D. H. (1972) Adaptation effects on spatio-temporal sine-wave thresholds. *Vision Res.* **12**, 89–101.

Kelly D. H. (1981) Nonlinear visual responses to flickering sinusoidal gratings. *J. opt. Soc. Am.* **71**, 1051–1055.

Kelly D. H. (1982) Motion and vision IV. Isotropic and anisotropic responses. *J. opt. Soc. Am.* **72**, 432–439.

Kelly D. H. and Burbeck C. A. (1984) Critical problems in spatial vision. *CRC Cr. Rev. Biomed. Engng.* **10**, 125–177.

Kulikowski J. J., Abadi R. and King-Smith P. E. (1973) Orientational selectivity of grating and line detectors in human vision. *Vision Res.* **13**, 1479–1486.

Kulikowski J. J. and Tolhurst D. J. (1973) Psychophysical evidence for sustained and transient detectors in human vision. *J. Physiol., Lond.* **232**, 149–162.

Legge G. E. (1978) Sustained and transient mechanisms in human vision: temporal and spatial properties. *Vision Res.* **18**, 69–81.

Lennie P. (1980) Perceptual signs of parallel pathways. *Phil. Trans. R. Soc.* **290**, 23–37.

Levinson E. and Sekuler R. (1975) The independence of channels in human vision selective for direction of motion. *J. Physiol., Lond.* **250**, 347–366.

Pantle A. (1973) Visual effects of sinusoidal components of complex gratings: independent or additive? *Vision Res.* **13**, 2195–2204.

Sekuler R. and Ganz L. (1963) Aftereffect of seen motion with a stabilized retinal image. *Science, N.Y.* **139**, 419–420.

Stromeyer C. F., Kronauer R. E., Madsen J. C. and Klein S. A. (1984) Opponent-movement mechanisms in human vision. *J. opt. Soc. Am.* **A1**, 876–884.

Swift D. and Smith R. A. (1982) An action spectrum for spatial-frequency adaptation. *Vision Res.* **22**, 235–246.

Thomas J. P. and Gille J. (1979) Bandwidths of orientation channels in human vision. *J. opt. Soc. Am.* **69**, 652–660.

Tolhurst D. J. (1975) Sustained and transient channels in human vision. *Vision Res.* **15**, 1151–1155.

Tolhurst D. J. (1973) Separate channels for the analysis of the shape and the movement of a moving visual stimulus. *J. Physiol., Lond.* **231**, 385–402.

Tulunay-Keesey U. (1972) Flicker and pattern detection: a comparison of thresholds. *J. opt. Soc. Am.* **62**, 446–448.

Virsu V. and Laurinen P. (1977) Long-lasting afterimages caused by neural adaptation. *Vision Res.* **17**, 853–860.

Watson A. B., Thompson P., Murphy B. and Nachmias J. (1980) Summation and discrimination of gratings moving in opposite directions. *Vision Res.* **20**, 341–347.

END

FILMED

FEB. 1988

DTIC